AD NUMBER	
AD352807	
CLASSIFICATION CHANGES	
TO:	**UNCLASSIFIED**
FROM:	**CONFIDENTIAL**
LIMITATION CHANGES	
TO:	**Approved for public release; distribution is unlimited.**
FROM:	**Distribution authorized to U.S. Gov't. agencies and their contractors; Administrative/Operational Use; 18 MAY 1964. Other requests shall be referred to Bureau of Naval Weapons, Washington, DC.**
AUTHORITY	
NOL ltr 29 Aug 1974; NOL ltr 29 Aug 1974	

~~CONFIDENTIAL~~

NOLTR 63-47

3 5 2 8 0 7

STATIC AND DYNAMIC STABILITY STUDIES ON SEVERAL LAZY DOG CONFIGURATIONS AT SUBSONIC AND TRANSONIC SPEEDS (U)

RELEASED TO DDC
BY THE N[illegible] [illegible] LABORATORY
[x] Without [illegible]
[ ] For R[illegible] [illegible] and Government
[illegible]
[ ] A[illegible] for release
to [illegible]
[ ] Approv[illegible] required for all
subsequent release.

18 MAY 1964

DDC

DDC IRA D

NOL

UNITED STATES NAVAL ORDNANCE LABORATORY, WHITE OAK, MARYLAND

NOTICE: This material contains information affecting the national defense of the United States within the meaning of the Espionage Laws, Title 18, U.S.C. Sections 793 and 794, the transmission or revelation of which in any manner to an unauthorized person is prohibited by law.

NOLTR 63-47

Downgraded at 3 Year Intervals
Declassified after 12 Years. DOD Dir 5200.10

~~CONFIDENTIAL~~

Aerodynamics Research Report 191

STATIC AND DYNAMIC STABILITY STUDIES ON SEVERAL LAZY DOG CONFIGURATIONS AT SUBSONIC AND TRANSONIC SPEEDS

Prepared by:
J. B. Eades, Jr.
C. Powers

ABSTRACT: A summary is presented of the investigations conducted in the Naval Ordnance Laboratory's Supersonic Tunnel No. 1 on several of the Navy's Lazy Dog weapon configurations. Lazy Dog is a free-fall missile employing a 50 caliber bullet or its core as the basic aerodynamic body.

Static stability tests were conducted on six configurations over a Mach number range from 0.3 to 1.3. Dynamic stability tests were made using the more promising configurations. In addition to these tests, ballistics range firings were conducted.

As a consequence of the information obtained in this investigation, two alternate configurations have been proposed.

U. S. NAVAL ORDNANCE LABORATORY
WHITE OAK, MARYLAND

NOLTR 63-47 18 May 1964

STATIC AND DYNAMIC STABILITY STUDIES ON SEVERAL LAZY DOG CONFIGURATIONS AT SUBSONIC AND TRANSONIC SPEEDS

The purpose of this investigation was to determine the aerodynamic characteristics of several Lazy Dog configurations. This work was performed at the request of the Bureau of Naval Weapons under Task Number RMMO-42-005/212-1/F008-09-01.

The contributions of W. D. Piper, V. L. Schermerhorn, F. J. Regan, I. Shantz and P. A. Cerreta are gratefully acknowledged.

R. E. ODENING
Captain, USN
Commander

K R Enkenhus

K. R. ENKENHUS
By direction

CONTENTS

TABLES

ILLUSTRATIONS

INTRODUCTION

Lazy Dog is the name of a project established by the Bureau of Naval Weapons to develop an antipersonnel weapon from the existing surplus of 50 caliber bullets. The modified bullets are to be dropped, in quantity, from high speed, low flying aircraft. Concentrations of ground troops will be the principal targets. In order to accomplish its mission, Lazy Dog must have a concentrated mass and possess a relatively high kinetic energy at impact.

This report describes and summarizes the testing program, and the subsequent evaluation, for several Lazy Dog configurations. In those cases where the 50 caliber bullet served as the basic body, the unloaded shell casing was retained attached to the projectile. Various stabilizing afterbodies were produced by cutting and forming the shell casing. Other configurations were formed by attaching a finned afterbody to the bullet core.

The principal result is the recommendation that the steel core of the 50 caliber bullet be utilized as the basic missile body. An afterbody with stabilizing fins is added to form a low drag, fin stabilized weapon. The fins provide the stabilization which is normally realized by spin in the conventional application of the bullet.

This report represents a significant contribution to the aerodynamics of the 50 caliber bullet. It appears that prior to these tests very little aerodynamic data had been gathered on the bullet. A literature search led to the belief that no systematic studies of this sort had been conducted. Therefore, it is presumed that this report contains the majority of the aerodynamic data on this ballistic shape.

AERODYNAMIC SYMBOLS

A	reference area (based on maximum bullet or core diameter) (in^2)
b	span (in)
c	chord (in)
C_A	axial force coefficient (F_A/qA)
C_D	drag force coefficient (F_D/qA)
C_m	pitching moment coefficient (M_y/qAd)

C_{m_α}	slope of the curve of pitching moment coefficient versus angle of attack; the stability derivative $(dC_m/d\alpha)$
C_N	normal force coefficient (F_N/qA)
C_{N_α}	slope of the normal force coefficient-angle of attack curve; the stability derivative $(dC_N/d\alpha)$
$C_{m_{\dot\theta}} + C_{m_{\dot\alpha}}$	the pitch damping coefficient, $\dfrac{\partial C_m}{\partial(\frac{\dot\theta d}{2V})} + \dfrac{\partial C_m}{\partial(\frac{\dot\alpha d}{2V})}$
C_ℓ	rolling moment coefficient (M_x/qAd)
C_{ℓ_p}	roll damping derivative, $\dfrac{\partial C_\ell}{\partial(\frac{pd}{2V})}$
d	reference length (bullet or core maximum diameter) (in)
F_A	axial force (lbs)
F_D	drag force (lbs)
F_N	normal force (lbs)
I_{xx}	mass moment of inertia about the longitudinal axis (slug-in^2)
I_{yy}	mass moment of inertia about the transverse axis (slug-in^2)
L	rolling moment (in-lbs)
L_p	roll damping moment derivative (in-lbs-sec/rad)
L_δ	induced rolling moment derivative (in-lbs/rad)
m	mass (slugs)
M	Mach number
M_α	slope of the pitching moment-angle of attack curve (in-lbs/rad)
M_x	(rolling) moment about the body x-axis (in-lbs)
M_y	(pitching) moment about the body y-axis (in-lbs)
p	body spin rate (rad/sec)

q	windstream dynamic pressure (psia)
t	time (sec)
V	velocity (ft/sec)
W	model weight (lbs)
X_{CG}	distance to the center of gravity from the nose measured along the x-axis (calibers)
X_{CP}	distance to the center of pressure from the nose measured along the x-axis (calibers)
X_{RC}	distance to the moment reference center from the nose measured along the x-axis (calibers)
α	angle of attack (deg, rad)
$\dot{\alpha}$	angle of attack angular velocity, $d\alpha/dt$ (rad/sec)
$\ddot{\alpha}$	angle of attack angular acceleration, $d^2\alpha/dt^2$ (rad/sec^2)
$\bar{\alpha}$	$\alpha_o e^{\lambda t}$ which is the envelope of the pitch damping trace (deg) (see Appendix A)
$\Delta\alpha$	angle (of attack) difference $(\alpha_p - \alpha_j)$ (rad)
Δt	time difference $(t_j - t_i)$ (sec)
θ	pitch angle (deg, rad)

Subscripts

C	refers to the 50 caliber bullet core
F	refers to an afterbody fin
in	initial conditions
im	impact conditions
j	refers to a general point or position
o	zero angle of attack conditions
p	peak angle of attack conditions
t	terminal condition

MODELS, TEST TECHNIQUES AND DATA REDUCTION

The 50 caliber bullet, the bullet core, and the six flared or finned configurations tested in this program are shown in

Figures 1 through 8, and are listed in Table 1. Figure 1 is a sketch of the 50 caliber bullet, while Figure 2 depicts the core alone. It should be noted that the dimensions on Figure 1 are given in inches, while those on the other model drawings are expressed in calibers.

Configurations 1, 2 and 3 (see Figures 3-6) are flared tail models which were formed by simply cutting and shaping the cartridge case of the 50 caliber round. These three shapes were initially chosen on the basis of their performance as observed during drop tests conducted at the Naval Ordnance Laboratory. Configuration 1 (Figure 3) is the most elementary design, wherein the case has been clipped and the powder charge removed. This design represents a relatively simple aerodynamic shape which, incidentally, was later discarded due to its poor performance. Configurations 2 and 3 (Figures 4 and 5) are more sophisticated split skirt designs.

After the above-mentioned configurations utilizing the bullet and cartridge core were found to have rather poor aerodynamic qualities, several finned designs employing the bullet core were devised, tested and evaluated. Those considered have been designated as Configurations 4, 5 and 6 and are sketched in Figures 6, 7 and 8. Configurations 4 and 6, which were designed by the Naval Ordnance Test Station, are quite similar; they differ only in the planform shape of the uncanted stabilizing fins attached to the basic body. Configuration 5 is comprised of the bullet core fitted with four canted fins, serving to both fin-stabilize the body and provide for an aerodynamically induced spin which produces a degree of gyrodynamic stability. This design, which was suggested by the Bureau of Naval Weapons, was subsequently discarded after testing due to certain undesirable characteristics.

Figures 11 through 14 are photographs of the wind tunnel models tested. Figure 11 shows the 50 caliber core, Figure 12 the three flared configurations, and Figures 13 and 14 the three finned shapes. Once again it is recalled that the configurations employ two different forebodies. Each is fitted with differing aerodynamic stabilizing afterbodies to form the various shapes tested. Configuration 4 in Figure 13 does not have the nose section attached; the nose is in place on Configuration 5. The nose is employed whenever these bodies are being tested.

The initial part of the testing program was concerned with the measuring of static forces and moments on the several configurations, just discussed above, and the 50 caliber bullet core alone. These data were gathered from tests conducted in NOL Supersonic Tunnel No. 1 (reference (1)) with the models

mounted on a six-component, internal strain gage balance (see reference (2)). The data were collected and reduced to to aerodynamic coefficients, with corrections applied to account for sting deflection due to aerodynamic loads.

A brief analysis of the data indicated the overall superior qualities of Configurations 4 and 6, the finned models with zero fin cant angle. As a consequence, Configuration 6 was chosen as the model for further study and evaluation. This configuration was dynamically tested to ascertain its damping capabilities in pitch and in roll. A photograph of the pitch damping apparatus is shown as Figure 15. High-speed motion pictures were used to obtain the time to damp to half amplitude, which determines the total pitch damping coefficient, $C_{m_{\dot\theta}} + C_{m_{\dot\alpha}}$. This technique is described in reference (3).

An estimate of the pitching moment coefficient for the model can also be made from these photographic records. This scheme requires that the oscillatory mode be viewed in regard to how the motion, in the vicinity of the peak oscillation, is related to the aerodynamically induced pitching moment. The photographic records are utilized to provide an approximate expression for the angular acceleration; the approximation (see Appendix B) is

$$\frac{d^2\alpha}{dt^2} \approx - \frac{2\Delta\alpha}{(\Delta t)^2} \qquad (1)$$

where $\Delta\alpha$ is the difference in (pitch) angle of attack occurring during the time increment Δt. Using equation (1) in the single-degree-of-freedom relationship specialized for peak displacement equation (B-8) gives

$$C_m\Big|_{\alpha_p} = - \frac{2\Delta\alpha I_{yy}}{(\Delta t)^2 qAd} \qquad (2)$$

where $C_m\Big|_{\alpha_p}$ is the pitching moment coefficient at the peak angle of attack, α_p. A more complete description of this method of analysis is available in Appendix B. Incidentally, this model had three tail fins and was tested in two modes; one with a tail fin placed vertically and the other with a fin horizontally located. This procedure was adopted to see if a difference in damping would be noted.

Roll damping derivatives were obtained for Configuration 6 using the apparatus described in reference (4). Briefly, the

model is driven at a predetermined roll rate, and then the rolling motion allowed to decay with time. The roll rate-time history is recorded and then analyzed to determine the time for the motion to decay to a desired level, etc. This information is then utilized, analogous to the scheme set down above, to calculate values of the roll damping derivatives. See Appendix C for a more complete description of the method employed.

The last phase of testing on Configuration 6 was conducted in the NOL Pressurized Ballistics Range No. 3 and the NOL Aerodynamics Range No. 1. Here full scale models were test-fired down these ranges to ascertain their free-flight behavior. Several shots were made, at high subsonic and transonic Mach numbers, and at initial launch angles of 15, 45 and 90 degrees. No quantitative data were collected from the range firings; the purpose of these shots was to verify the stability evaluations made from the aerodynamic data gathered during the wind tunnel testing program.

A compendium of the wind tunnel and range testing conditions is given in Table 1.

The overall results of this investigation indicate that none of the configurations tested is entirely satisfactory for the purposes intended. As a consequence, two designs have been proposed which should better meet the requirements of the Lazy Dog weapon; these are presented herein as Configurations 7 and 8, and are shown in Figures 9 and 10. These designs were analytically determined employing data gathered during this testing program and other experimental data. It is suggested that models of the configurations be constructed and tested to prove their effectiveness.

DISCUSSION OF RESULTS AND CONCLUSIONS

The data collected, reduced and calculated during this program are set down in Figures 18 through 69. All of the wind tunnel data have been corrected for aeroelastic deformations of the balance sting. It should be recalled that these results have been collected essentially for a family of three body types. These include the basic 50 caliber shell, cut and formed to provide a stabilized configuration; the 50 caliber bullet core with stabilizing fins added; and the bullet core alone.

As mentioned in the preceding section, wind tunnel tests were conducted to ascertain the static and certain dynamic (stability) characteristics of the several configurations. In Figures 18 through 32, normal force data are presented as a

function of angle of attack for several free-stream Mach numbers. The free-stream Mach numbers for these tests varied from approximately 0.3 to 1.26. The corresponding static pitching moment data, for the several bodies, are presented on Figures 35 through 49. The angle of attack range for the stabilized bodies (formed and finned afterbodies) was $-4° \leq \alpha \leq +16°$, while for the bullet core alone the range was $-5° \leq \alpha \leq +90°$. Figures 33 and 34 show the normal force coefficient slope ($C_{N_{\alpha_o}}$) determined in the neighborhood of $\alpha = 0$. The moment coefficient slope ($C_{m_{\alpha_o}}$) is presented on Figures 50 and 51. From these results the static stability margin ($X_{RC} - X_{CP}$) is readily determined; this quantity also serves as a measure of a configuration's static longitudinal stability. For those cases where the margin of stability is positive ($X_{RC} - X_{CP}$) > 0, the body is statically stable; that is, the center of pressure lies aft of the moment reference center. In this regard, when the moment reference center coincides with the center of the mass then the constrained margin of stability (as determined here from wind tunnel data) would ideally be the same as that experienced by a prototype in free flight under similar aerodynamic flight conditions.

Figure 54 presents the drag data (C_{A_o}, axial force or drag coefficient at $\alpha = 0$) for Configurations 1-6, inclusive, over the Mach number range from 0.49 to 1.26. Generally speaking, then, Figures 33, 34, and 50 through 54 summarize the basic (static) aerodynamic characteristics of the bodies tested in the Lazy Dog program.

A study of Figures 18 through 29 indicates that the configurations fitted with stabilizing afterbodies develop a decided nonlinearity of the normal force coefficient in the transonic speed range. This nonlinear influence is most pronounced at the higher angles of attack and after the typical onset of transonic compressible influence. Apparently, these diversities are brought on by local sonic conditions, since they appear at near the drag divergence Mach number and diminish at approximately the upper (Mach number) limit for transonics. It is rather interesting to note that Configurations 2 and 3 (see Figures 4 and 5) show almost identical normal force variations throughout the transonic speed range. This would imply that these body types are essentially equivalent in transverse force capabilities. Configuration 5, with its canted fins, generates the largest normal force. Configuration 1 generates the least.

Special attention is called to the data presented for Configurations 4 and 6, because these are the configurations on which the dynamic stability tests were performed. Configuration 4 is better than 6, with regard to normal forces produced over the entire transonic speed range.

From Figure 33, it is evident that the fin stabilized bodies are more susceptible to transonic influences than are the skirted afterbodies. Configurations 4, 5 and 6 show the typical transonic "hump" in the normal force curve slope ($C_{N_{\alpha_o}}$). Though the other configurations (1, 2 and 3) show a similar influence, it is not nearly so severe.

The bullet core data, C_N vs. α, for the several Mach numbers, is presented on Figures 30 through 32. Here, a decided nonlinearity, at angles of attack not near zero, is quite apparent. These results, up to approximately 60 degrees angle of attack, are typical for bodies of revolution having an ogival type nose. The rather abrupt rise in slope (C_{N_α}) at approximately 30 degrees angle of attack, and the subsequent reduction in slope at about 60 degrees, is indicative of the influence of body shape and flow separation on C_N.

Figures 35 through 59 present pitching moment coefficients versus angle of attack for the speed range of the tests. Analogous to those cases just discussed, the nonlinear influence of transonics is quite evident. It should be noted that Configuration 1 is statically unstable over the entire range of angle of attack. The other configurations (2 through 6) are statically stable about their trim angle of attack. A study of these graphs indicates that in general the stable configurations have an increased stability index ($C_{m_{\alpha_o}}$) at transonic speeds. They also experience an increased nonlinearity in C_m at these (same) speeds. These effects are most apparent for Configurations 1, 4 and 6 and least evident for the shapes designated as "2" and "3." Actually, near sonic speeds the trend is for the more largely influenced bodies to develop a trim angle outside of the test range; that is, for $\alpha > 16°$. This is somewhat disturbing in view of the many launch conditions possible for the Lazy Dog weapon. A second trim angle means that the bomblet might not properly trail.

In terms of the static stability index ($C_{m_{\alpha_o}}$), Configuration 5, with its canted fins, is clearly superior to all others.

Configurations 4 and 6 have the next best stability characteristics, and, as mentioned previously, Configuration 1 is statically unstable (see Figure 50).

On Figures 47 through 49 the static instability of the bullet core alone is described. Once again the phenomena of flow separation and/or compressibility are quite apparent. At least two changes in slope (C_{N_α}) are indicated, and a sharp slope reversal is noted at approximately 60 or 70 degrees angle of attack. The need for some sort of stabilizing augmentation is clear. Further, it is apparent that the core possesses a second trim orientation in the vicinity of 100 degrees angle of attack. These conditions imply a need for, say, the spin stabilization of a bullet, and point up the sometimes noted "instability" of nonspinning, projectile-like bodies.

Analogous to the normal force coefficient, the basic stability derivatives ($C_{m_{\alpha_o}}$) for the core alone are only slightly influenced by Mach number, at least in the speed range of the tests as reported (see Figure 51).

Figures 52 and 53 summarize and give an aerodynamic representation to the data collected and described above. These figures describe the static margin of stability for the various configurations as a function of free-stream Mach number. As mentioned before, a positive value for the term implies a body which exhibits static stability. Also, the larger the magnitudes of this term the more stable is the configuration. This is apparent when one considers that for a wind tunnel model the measured moment is obtained about a moment center, which in turn is produced by the aerodynamically generated normal force. The ratio of the moment to the force is then proportional to the moment arm. This would be the same as the ratio of the linear slopes, M_α to N_α. Having measured the slopes (see Figures 33 and 50, for example) it is a simple matter to calculate the static margin, which is given here in calibers. The similarity to the curves of $C_{N_{\alpha_o}}$ and $C_{m_{\alpha_o}}$ is immediately seen; once again it is evident that Configuration 5 is superior to all others, with Configurations 6, 2 and 4 following on a next-best basis. Typically, Configuration 1 is indicative of the unstable situation where the center of gravity lies aft of the force center, or center of pressure, on the body. It is of interest to note that in the main the stable configurations show an increase in static margin over the transonic speed region, while the unstable Configuration 1 is at best only slightly affected by Mach number.

Figure 54, prepared for the bullet core, also shows the unstable character of this body type but shows a more marked dependence on free-stream Mach number.

In Figure 55 the last of the usual aerodynamic wind tunnel data is presented. This graph is a plot of the zero angle of attack axial force, or the drag coefficient at $\alpha = 0$, as a function of free-stream Mach number. Recalling that one requisite for Lazy Dog is low drag, then it is evident that the least values of C_{A_o} describe the best configurations. A cursory glance at this figure indicates a choice of either Configuration 4 or 6 in terms of a least basic drag for the speed range considered.

Having the basic data from the wind tunnel measurements, it is now possible to select a configuration which would seem best suited to serve as the Lazy Dog weapon. From an overall consideration it would appear that either Configuration 4 or 6 should be selected. As a consequence, Configuration 6 was chosen and used in the dynamic stability studies conducted as a part of the weapon's evaluation program. Even though Configuration 5 showed some superior capabilities it was not selected for further evaluation primarily because of the need for a least drag configuration. It should be noted that the canted fins on Configuration 5 would probably introduce an added drag component, when the bomblet was free to rotate, arising from the fin lift increment needed to provide the rotation. Of course, it is likewise apparent that body rotation is a necessary evil for fin stabilized bodies since it would be virtually impossible to mass produce a finned afterbody unit without some fin misalignment. Fin misalignments will produce some trim. Roll produced by fin cant eliminates dispersion due to such asymmetries. However, the phenomenon of pitch-roll resonance may be incurred. When the roll rate equals the natural pitching frequency, there is a large amplification of trim. The trim at resonance depends on the aerodynamic damping. If the damping is low, or if the asymmetry is sufficiently large, very erratic behavior (such as a flat spin) could result. In practice, it is difficult to manufacture fins with the small differential deflection required to keep the terminal roll rate below resonance. Hence, it is common to increase the fin cant to produce a roll rate above resonance. This incurs a penalty in the form of induced drag.

On Figures 55 through 59 the total pitch damping capacity $(C_{m_{\dot{\theta}}} + C_{m_{\dot{\alpha}}})$ of Configuration 6 is presented. This damping term is measured as the sum indicated since the technique of experimentation used does not permit separation of the derivatives. Figures 56 through 59 are graphs of pitch damping as a function

of the angle $\bar{\alpha}$. Each graph represents a particular free-stream Mach number. The Mach number range is $0.3 \leq M \leq 0.9$. Figure 55 summarizes these data by showing the range of pitch damping as a function of free-stream Mach number. The range of the damping term, at a given Mach number, has been arbitrarily selected to correspond to an $\bar{\alpha}$ variation of $0° \leq \bar{\alpha} \leq 10°$. Values of the pitch damping derivatives were taken from Figures 56 through 59 for this purpose.

It should be pointed out that on these figures (56 through 59) there is a region of uncertainty connected with each graph. For this reason all curves have been extrapolated to the $\bar{\alpha} = 0$ value shown, and the curve plotted as a dashed line in the region of uncertainty.

The damping in pitch of Configuration 6 was expected to depend on its roll orientation because of the triform tail. This expectation was studied by performing two damping tests, one with a fin vertically aligned in the wind tunnel and one with a fin parallel to the tunnel horizontal plane. The experimental results showed no effect of model roll orientation.

Figure 55, representing somewhat of a summary, shows that for the configuration tested there was a continual increase in pitch damping derivative with free-stream Mach number. Generally such results are expected. The damping derivatives arise from the pitching rate and from the heave. In most cases, the pitch rate damping $C_{m_{\dot{\theta}}}$ is the more important trim. It can be enhanced by increasing the fin moment arm or the fin area.

It should be mentioned, in connection with tests of this type and those conducted to determine other damping derivatives for other modes of motion, that an "as yet unaccounted for" source of error is present. This error arises because of the uncertainty in the amount of bearing friction present in the experimental apparatus. It has been tacitly assumed that the magnitude of the moment created by the bearing friction is small compared to the aerodynamic moment.

A development carried out in Appendix B suggests that the pitch damping data can be utilized to determine the static

pitching moment. Two methods appear in the appendix; however, only the method suggested by equation (B-8) was actually utilized in this report. Having measured the time and angle increments, and knowing the characteristics of the body and the windstream, equation (B-8) is solved for a value of C_m. The calculated values are presented as graphs of C_m versus α for the free-stream Mach numbers of the pitch damping tests. These graphs appear as Figures 60, 61 and 62 in this report.

In view of the inevitability of finned configurations having some rolling motion, a series of tests was conducted on Configuration 6 to ascertain its damping in roll. This characteristic of the bomblet could arise from fin cant angle (intentionally or accidentally provided) and could have a decided influence on the free-fall trajectory of the weapon.

Under the controlled testing conditions present in the wind tunnel, and for a precisely constructed model, accurate data have been collected and analyzed. Figures 63 and 64 present the roll damping derivative as a function of free-stream Mach number and angle of attack.

From Figure 63 it is seen that the Mach number influence on C_{l_p} is mainly confined to the transonic and supersonic speed range. Too, it is evident that as the angle of attack is increased the influence of Mach number is reduced in comparison to, say, the $\alpha = 0$ case.

A cross plot of these results appears on Figure 64. Here it is apparent that the Mach number influence can be more pronounced as the angle of attack is reduced. Once again the tendency of the body to seek a common level of roll damping, without regard to Mach number or angle of attack, is demonstrated. A diverse occurrence is observed on Figure 64. The general trend is for the roll damping capacity to decrease as the angle of attack is increased; all cases except that for the lowest test Mach number show this characteristic. For a free-stream Mach number of 0.3 the trend is reversed in that the damping capacity increases with increasing angle of attack, reaching a maximum and hinting that at still larger angles the expected decrease in $|C_{l_p}|$ will occur.

The method used to calculate C_{l_p} from the roll motion time history records is described in Appendix C. The equation used in connection with this report is equation (C-8). This represents the case of no induced roll action. The calculation

requires a knowledge of the roll rate, p(t), and certain properties of the model and the wind tunnel operation conditions. For cases where induced rolling would occur, and a subsequent steady state rolling would follow, the applicable formulation is given by equation (C-6), rather than (C-8).

In addition to the information gathered here, it was decided that several range firings of full scale models should be conducted. These tests were suggested primarily for the purpose of gaining further information on the free-flight behavior of the weapon, especially to observe flight characteristics for launchings at large initial angles of pitch. These tests were carried out in the NOL Pressurized Ballistics Range and the Aerodynamics Range.

The range test shots indicated that pitch damping was not as large as expected; that generally the high angle motion was lightly damped; and that in all probability the models were unstable to varying degrees. This confirms the wind tunnel data which indicated instabilities at large angles of attack and the possibility of relatively large trim angles.

After having completed these last studies, and with a full evaluation of all available test results, it was concluded that no one of the several configurations tests was acceptable. It was felt that Configuration 6 (see Figure 8), though the best of the original designs, in the last analysis did not satisfy all requirements of the Lazy Dog concept. In an effort to find a more optimal configuration, some added criteria were established from which two new designs evolved. These designs were to have the low drag of Configurations 4 and 6, yet they would hopefully have better stability characteristics, both static and dynamic. The criteria on stability suggest that the new configurations must have adequate stability up through angles of attack of 90 degrees, and have adequate damping to reduce pitching (in particular) to a low level within a few oscillations. Such requirements are necessary if the weapon is to properly trail and have a reasonably predictable trajectory. Configurations without fairly large damping and with good lifting capacities have the undesirable tendency of "sailing" rather than "falling" along their free-flight trajectories.

The design analysis, using the bullet core as the basic body, incorporated empirical data from reference (5). Thus, the analysis included several stabilizer configurations. The final selection was made in favor of fins having a rectangular planform. Primarily this selection was made in order to keep the center of pressure aft and to achieve the required static margin, namely, $(X_{RC} - X_{CP}) = 0.75$ calibers.

The overall center of pressure for the configuration can be estimated from a weighted factor formulation which includes only the known center of pressure locations for the various body elements and neglects interference and interaction effects. The mathematical description for a composite configuration is

$$X_{CP_{(C+F)}} = \frac{C_{N_{\alpha(C)}} X_{CP_{(C)}} + C_{N_{\alpha(F)}} \dfrac{2A_{(F)}}{A_{(C)}} X_{CP_{(F)}}}{C_{N_{\alpha(C)}} + C_{N_{\alpha(F)}} \dfrac{2A_{(F)}}{A_{(C)}}} \qquad (3)$$

where subscripts (c) and (f) refer to the "core" and "fin", respectively; $A_{(F)}$ and $A_{(C)}$ are reference areas, and

$A_{(F)} = \frac{b}{2} \times c$. Incidentally, the factor "2" is introduced into the equation to signify that two of the fins influence the center of pressure location. In view of the fact that the proposed configuration is one having cruciform fins, then (it is assumed that) only two fins would be influenced by a pitching action. Coupled effects, like interference effects, are neglected here.

The particulars of these newest configurations are as follows: It was estimated that the mass center for the core body and cruciform fins would be located 2.8 calibers (1.20 inches) aft of the nose. With the static margin set at 0.75 calibers (0.32 inches), then the overall center of pressure would be located at 3.55 calibers (1.52 inches) aft of the vehicle nose. These specifications, coupled with the aerodynamic data for the core, taken at a free-stream Mach number of 0.50, and data contained in reference (5), account for the calculated fin dimensions. A plot of the required span, as a function of chord length for these conditions, is given on Figure 65. Two configurations, selected from the possible family of solutions and designated as Configurations 7 and 8, are shown as Figures 9 and 10, respectively. It is apparent that these two designs are distinctive by the difference of fin dimensions selected for them. To date, no tests have been made on these configurations. They have been proposed for subsequent evaluation.

In connection with the overall research program, several particle, free-flight trajectories were calculated. These

trajectories do not show the influence of vehicle aerodynamics, except for drag, and only represent the motion in a vertical plane. Also, these particular studies were carried out in terms of a selected fixed parameter (W/C_D) for each path. In this regard the variation of C_D with Reynolds number and Mach number has been neglected. Primarily, the altitudes (and, in general, the velocities) are so low as to neglect the influence of these various dimensionless quantities. The trajectory analyses were conducted and results are included here to illustrate the influence of drag, or specifically C_D, on impact conditions; and to ascertain what launch conditions would be required to have the weapon reach the ground with the required kinetic energy.

The trajectory analysis is summarized on Figures 66 through 69. Each graph will show two reference velocities; one, the lower reference value, corresponding to a selected kinetic energy (at impact) of 58 foot-pounds, and the larger value (marked V_t) corresponding to the sea level terminal velocity for the particle having a value of (W/C_D) prescribed for that figure. Most of the results are similar, and the data of Figure 68, for the case of $(W/C_D) = 0.75$, are typical. The bomblet, when released from an altitude of 100 feet with no initial velocity, will strike the ground at a speed of 80 fps. This corresponds to an impact kinetic energy of 13.12 foot-pounds (the bomblet has a mass of approximately 0.0041 g-pounds). Therefore, the weapon would have to be launched from a 100 foot altitude at a speed of 140 fps to have the desired 58 foot-pounds of kinetic energy at impact. In the extreme case of a launching at 800 fps from a 100 foot altitude, the bomblet reaches the ground with an impact speed of 710 fps, corresponding to a kinetic energy of 1033.4 foot-pounds. Apparently, up through altitudes of 1,000 feet, at a launch speed of approximately 425 fps, the bomblet will impact at nearly a fixed speed -- or at essentially a fixed kinetic energy. At an altitude of approximately 5,000 feet, and upward, the launching speed has only a small influence on the impact speed; that is, the bomblet has about the same level of kinetic energy at impact, regardless of the initial speed. Though it is not apparent from the graph, the trajectory data show that for the higher altitudes the weapon's velocity first decreases (due to drag deceleration), passes through a lowest speed, and then accelerates slowly (due to gravity) as it continues to fall along its trajectory.

The above comments are generally true for all graphs of impact speed versus initial speed; the numbers quoted above are necessarily true only for the one case considered. This is evidenced by the differences in drag coefficients for the graphs. For instance, $(W/C_D) = 0.75$ corresponds to a bomblet

with a $C_D \approx 0.176$, while for a $(W/C_D) = 0.25$ the $C_D \approx 0.528$. It is expected that the proposed designs would have a drag coefficient somewhere between these levels at subsonic speeds. The general picture of drag influence on a trajectory is available from these figures (66 through 69), and a changing drag can be interpreted from a visual interpolation of the graphs.

In conclusion, a final comment is offered on the proposed Lazy Dog designs (Configurations 7 and 8): No attempt has been made to predict any of the dynamic characteristics for these shapes. It is well known that dynamic predictions are mere guesses, particularly at transonic speeds. There is good reason to believe that the suggested designs will be an improvement over the configurations tested; however, the verification of this surmise awaits actual experimental results.

REFERENCES

(1) Meeks, P. P., "Aeroballistic Research Facilities," NOLR 1233, Unclassified

(2) Shantz, I., Gilbert, B. D., and White, C. E., "NOL Wind Tunnel Internal Strain-Gage Balance System," NAVORD Rpt 2972, 1953, Unclassified

(3) Shantz, I., and Groves, R. T., "Subsonic Damping in Pitch Measurements of the EX-10, EX-30 and 6" Test Vehicle," NAVORD Rpt 4025, 1958, Confidential

(4) Shantz, I., Schermerhorn, V. L., and Groves, R. T., "Roll-Damping Moment Measurements for the Basic Finner at Subsonic and Supersonic Speeds," NAVORD 6652, 1963, Unclassified

(5) DeJonge, Clark, "The Effect of Low Aspect Ratio Rectangular and Delta Cruciform Fins on the Stability of Bodies of Revolution with Tangent Ogives at Small Angles of Attack Through a Mach Number Range of 0 to 3.5," U. S. Army Ordnance Missile Command Rpt No. RF-TR-62-1, Rev, 1962, Unclassified

TABLE I CONFIGURATIONS AND TEST CONDITIONS

CONFIG.	BASIC BODY, 50 CALIBER BULLET	BASIC BODY, 50 CALIBER CORE	FULL SCALE LENGTH (IN.)	FULL SCALE DIA. (IN.)	WIND TUNNEL MODEL SCALE	CONFIG. ORIGINATOR	FREE-STREAM TEST MACH Nº 0.30	0.49	0.50	0.70	0.80	0.90	0.94	0.95	1.05	1.15	1.26	1.30	α TEST RANGE (DEG.)	NOTES
							REYNOLDS Nº/FOOT ×10⁻⁶ *													
1	x		3.57	0.511	2.50	NOL		3.1			4.2			4.5		4.6	4.7	4.7	-5 TO +15	C_N & C_M TESTS
2	x		2.80	0.511	2.50	NOL		3.1			4.2			4.5		4.6	4.6	4.7	-5 TO +15	C_N & C_M TESTS
3	x		2.85	0.511	2.50	NOL		3.1			4.2			4.5		4.7	4.8	4.8	-5 TO +15	C_N & C_M TESTS
4		x	2.00	0.428	2.92	NOTS		3.1			4.2			4.5		4.8	4.8	4.8	-5 TO +15	C_N & C_M TESTS
5		x	2.47	0.428	2.92	NOL		3.0			4.1			4.5		4.6	4.6	4.7	-5 TO +15	C_N & C_M TESTS
6		x	2.00	0.428	2.92	NOTS		3.0			4.0			4.5		4.7	4.6	4.7	-5 TO +15	C_N & C_M TESTS
6		x	2.00	0.428	2.92	NOTS	1.96		3.0	3.8		4.3							FREE TO PITCH	PITCH DAMPING
6		x	2.00	0.428	2.92	NOTS	1.96		3.0		4.1			4.5				4.5	9,5,10,15	ROLL DAMPING
CORE		x	1.87	0.428	2.92	—	2.0		3.1	3.9									-6 TO +86	C_N & C_M TESTS
7		x	2.50	0.428	~	NOL														PROPOSED
8		x	2.17	0.428	~	NOL														CONFIG'S
6	6 SHOTS FIRED IN PRESSURIZED RANGE Nº1 (FULL SCALE MODELS)						MACH Nº RANGE 0.70 TO 1.10												15,45,90	α = LAUNCH ANGLE
6	2 SHOTS FIRED IN AERODYNAMICS RANGE Nº1 (FULL SCALE MODELS)						MACH NOS: 0.62, 0.70												90	α = LAUNCH ANGLE

* WHERE REYNOLDS NUMBERS ARE SPECIFIED, A TEST WAS CONDUCTED ON THE MODEL NOTED AT LEFT AT THE MACH Nº FOR THAT COLUMN

TABLE 2

TABULATED DATA

Pages

TABULATED DATA

Normal Force and Pitching Moment Coefficients

M=0.485

WTR	RUN	CONFIG.
739	21	1

α(deg)	C_N	C_m
- 4.98	-0.4663	-0.1645
-04.07	-0.3826	-0.1464
-02.82	-0.3109	-0.0911
-01.07	-0.1435	-0.0549
00.03	-0.0478	-0.0183
01.08	0.0478	0.0183
01.99	0.1316	0.0364
03.09	0.2272	0.0730
04.03	0.2990	0.1005
05.05	0.3826	0.1464
06.08	0.4783	0.1830
07.15	0.5379	0.2478
08.28	0.6335	0.3123
09.08	0.6933	0.3491
10.03	0.7530	0.3859
11.00	0.8366	0.4598
12.10	0.9202	0.5337
13.07	0.9919	0.5611
14.02	1.0756	0.6071
15.01	1.1473	0.6346
15.83	1.2310	0.6806

M=0.485

WTR	RUN	CONFIG.
739	22	2

α (deg)	C_N	C_m
-05.02	-0.4660	0.1656
-04.00	-0.4062	0.1422
-03.20	-0.3465	0.1189
-02.11	-0.2389	0.0656
-01.01	-0.1434	0.0617
00.02	-0.0837	0.0383
01.04	0.0239	-0.0149
02.03	0.1434	-0.0617
03.11	0.2390	-0.0935
04.06	0.3107	-0.1104
05.03	0.3703	-0.1058
06.10	0.4779	-0.1591
07.06	0.5735	-0.1909
08.02	0.6452	-0.2358
09.13	0.7408	-0.2676
10.06	0.8364	-0.2994
11.03	0.8961	-0.3228
12.13	0.9798	-0.3612
13.11	1.0434	-0.3995
14.05	1.1352	-0.4443
15.06	1.2308	-0.4762

M=0.504

WTR	RUN	CONFIG.
739	33	3

α (deg)	C_N	C_m
-05.06	-0.4090	0.1567
-04.05	-0.3315	0.0921
-03.12	-0.2652	0.0737
-02.15	-0.1879	0.0608
-00.97	-0.1216	0.0424
00.00	-0.0553	0.0240
01.08	0.0442	-0.0037
02.03	0.1106	-0.0480
03.21	0.1878	-0.0349
04.08	0.2542	-0.0792
05.03	0.3205	-0.0977
06.08	0.3868	-0.1161
07.18	0.4753	-0.1751
08.28	0.5526	-0.1880
09.10	0.6189	-0.2064
10.17	0.6742	-0.2304
11.10	0.7627	-0.2895
12.04	0.8400	-0.3023
13.11	0.9064	-0.3207
14.09	0.9727	-0.3392
15.05	1.0279	-0.3373
15.42	1.0943	-0.4074

M=0.504

WTR	RUN	CONFIG.
739	07	4

α(deg)	C_N	C_m
-04.60	-0.5264	0.1390
-03.09	-0.3913	0.0847
-01.98	-0.2795	0.0684
-01.02	-0.1770	0.0230
00.10	-0.0606	0.0009
01.03	0.0419	-0.0241
02.05	0.1444	-0.0585
03.01	0.2609	-0.0823
04.14	0.3960	-0.1256
05.06	0.4705	-0.1364
06.33	0.6149	-0.1838
07.05	0.7313	-0.2409
08.12	0.8198	-0.2746
09.09	0.9829	-0.3413
10.05	1.1040	-0.3950
11.01	1.2064	-0.4516
12.12	1.3648	-0.5329
13.07	1.5091	-0.6135
14.05	1.6209	-0.6742
15.00	1.7699	-0.7625
15.84	1.8724	-0.8190

M=0.804

WTR	RUN	CONFIG.
739	09	5

α(deg)	C_N	C_m
-04.44	-0.7262	0.5027
-03.08	-0.5121	0.3502
-01.99	-0.3631	0.2402
-01.04	-0.2281	0.1489
00.02	-0.0792	0.0390
01.04	0.0558	-0.0523
02.03	0.2002	-0.1450
03.27	0.3677	-0.2575
04.04	0.5120	-0.3613
05.00	0.6703	-0.4614
06.23	0.8193	-0.5714
06.99	1.0008	-0.7248
08.05	1.1451	-0.8396
09.04	1.2800	-0.9642
10.10	1.4755	-1.1252
11.09	1.6477	-1.2884
12.17	1.8199	-1.4627
13.14	2.0200	-1.6632
14.08	2.1829	-1.8250
15.07	2.3597	-2.0167
15.46	2.4667	-2.1375

M-0.495

WTR	RUN	CONFIG.
739	01	6

α(deg)	C_N	C_m
-04.88	-0.5340	0.2345
-04.02	-0.4577	0.1962
-03.01	-0.3862	0.1673
-01.98	-0.2527	0.1058
-01.11	-0.1812	0.0769
00.05	-0.0620	0.0439
01.05	0.0382	-0.0078
02.07	0.1335	-0.0274
03.08	0.2623	-0.0794
04.07	0.3385	-0.1064
05.09	0.4434	-0.1450
06.07	0.5579	-0.1912
07.07	0.6389	-0.2163
08.08	0.7486	-0.2544
09.10	0.8487	-0.3048
10.10	0.9155	-0.3356
11.08	1.0156	-0.3873
12.07	1.1014	-0.4332
13.03	1.2110	-0.4927
14.01	1.3158	-0.5540
15.03	1.3970	-0.5792
15.[illegible]	1.[illegible]	-0.6041

M=0.80

WTR	RUN	CONFIG.
739	20	1

α(deg)	C_N	C_m
-05.09	-0.4284	-0.1573
-04.10	-0.3599	-0.1311
-02.89	-0.2628	-0.1006
-02.04	-0.1942	-0.0743
-01.10	-0.1142	-0.0437
00.13	-0.0114	-0.0177
01.09	0.0629	0.0174
02.05	0.1714	0.0523
03.05	0.2399	0.0735
04.04	0.3142	0.1003
05.05	0.3942	0.1442
06.00	0.4456	0.1572
07.02	0.5483	0.2232
08.11	0.6283	0.2671
09.10	0.7082	0.3111
10.06	0.7539	0.3419
11.00	0.8395	0.3947
12.08	0.9252	0.4341
13.02	1.0051	0.4781
14.10	1.1079	0.5174
15.09	1.1765	0.5436
15.65	1.2393	0.5610

M=0.80

WTR	RUN	CONFIG.
739	23	2

α(deg)	C_N	C_m
-04.79	-0.4568	0.2589
-04.09	-0.3997	0.2098
-03.00	-0.3083	0.1661
-02.15	-0.2341	0.1263
-01.08	-0.1256	0.0652
00.03	-0.0228	0.0009
01.17	0.0800	-0.0500
02.04	0.1428	-0.0959
03.05	0.2399	-0.1633
04.10	0.3141	-0.1897
05.05	0.4226	-0.2508
06.04	0.5025	-0.2875
07.05	0.5881	-0.3076
08.33	0.6908	-0.3452
09.05	0.7422	-0.3706
10.04	0.8279	-0.4175
11.15	0.9078	-0.4541
12.12	0.9991	-0.4979
13.23	1.0905	-0.5416
14.05	1.1533	-0.5742
15.02	1.2333	-0.6242
15.32	1.2789	-0.6528

M=0.80

WTR	RUN	CONFIG.
739	32	3

α(deg)	C_N	C_m
-04.52	-0.3880	0.1790
-04.11	-0.3594	0.1532
-03.10	-0.2795	0.1132
-02.11	-0.2054	0.0837
-01.13	-0.1312	0.0409
00.12	-0.0228	-0.0115
01.09	0.0514	-0.0410
01.89	0.1313	-0.0810
03.03	0.2055	-0.1105
04.02	0.2910	-0.1476
05.03	0.3709	-0.1876
06.01	0.4565	-0.2247
07.03	0.5421	-0.2752
08.03	0.6324	-0.3228
09.09	0.7133	-0.3494
10.13	0.7761	-0.3846
11.08	0.8560	-0.4246
12.05	0.9415	-0.4484
13.02	1.0100	-0.4808
14.11	1.1012	-0.5017
15.22	1.1583	-0.5264

M=0.80

WTR	RUN	CONFIG.
739	06	4

α(deg)	C_N	C_m
-04.47	-0.6254	0.2547
-04.03	-0.5567	0.2101
-03.04	-0.4264	0.1495
-02.04	-0.2914	0.1038
-00.91	-0.1587	0.0506
00.33	-0.0118	0.0024
01.08	0.0948	-0.0307
02.06	0.2132	-0.0719
03.05	0.3293	-0.1036
04.00	0.4643	-0.1607
05.00	0.5543	-0.1893
06.12	0.7131	-0.2512
07.11	0.8457	-0.3100
08.00	0.9381	-0.3538
09.17	1.1110	-0.4389
10.13	1.2271	-0.5045
11.01	1.3479	-0.5665
12.00	1.4758	-0.6401
13.00	1.6131	-0.7067
14.12	1.7671	-0.8003
15.11	1.8950	-0.8740
16.09	2.0276	-0.9554
16.15	2.0394	-0.3148

M=0.80

WTR	RUN	CONFIG.
739	10	5

α(deg)	C_N	C_m
-04.52	-0.7594	0.6581
-04.10	-0.6850	0.5701
-03.07	-0.5095	0.4392
-01.91	-0.3293	0.2789
-01.05	-0.2115	0.1733
00.02	-0.0889	0.0499
01.12	0.1370	-0.1026
02.10	0.3196	-0.2718
03.02	0.4278	-0.3645
03.99	0.6056	-0.5216
05.01	0.7787	-0.6608
06.00	0.9349	-0.8119
07.14	1.1271	-0.9940
08.30	1.3193	-1.1875
09.09	1.4876	-1.3432
10.06	1.6486	-1.4950
11.04	1.8528	-1.7046
12.15	2.0787	-1.9316
13.13	2.2421	-2.0866
14.10	2.4704	-2.3168
15.10	2.6602	-2.5071
15.67	2.6770	-2.5181

M=0.80

WTR	RUN	CONFIG.
739	02	6

α(deg)	C_N	C_m
-04.40	-0.5321	0.2438
-03.08	-0.3937	0.1705
-02.05	-0.2867	0.1312
-01.06	-0.1579	0.0657
-00.02	-0.0462	0.0283
01.01	0.0826	-0.0372
02.04	0.1920	-0.0872
03.07	0.3110	-0.1333
04.08	0.4082	-0.1706
05.09	0.5346	-0.2313
06.08	0.6269	-0.2647
07.07	0.7314	-0.3108
08.06	0.8408	-0.3549
09.07	0.9404	-0.3971
10.08	1.0352	-0.4353
11.07	1.1372	-0.4823
12.08	1.2393	-0.5235
13.07	1.3316	-0.5627
14.06	1.4410	-0.6069
15.02	1.5260	-0.6489
15.67	1.6038	-0.6707

M=0.95

WTR	RUN	CONFIG.
739	19	1

α(deg)	C_N	C_m
-05.07	-0.4529	-0.1621
-04.13	-0.3758	-0.1213
-03.03	-0.2843	-0.0919
-02.05	-0.2024	-0.0550
-01.10	-0.1205	-0.0405
00.11	-0.0193	-0.0074
01.05	0.0626	0.0184
02.01	0.1446	0.0441
03.07	0.2265	0.0698
04.00	0.3084	0.1068
05.10	0.3999	0.1362
06.02	0.4626	0.1545
07.10	0.5589	0.2027
08.06	0.6263	0.2285
09.02	0.7130	0.2954
10.11	0.8045	0.3360
11.03	0.8816	0.3655
12.00	0.9731	0.3949
13.07	1.0647	0.4244
14.06	1.1659	0.4575
15.03	1.2526	0.4692
15.31	1.3153	0.4753

M=0.95

WTR	RUN	CONFIG.
739	24	2

α(deg)	C_N	C_m
-05.04	-0.4765	0.2978
-04.10	-0.4050	0.2587
-03.09	-0.3240	0.2137
-02.08	-0.2383	0.1601
-01.15	-0.1430	0.1005
00.10	-0.0286	0.0179
01.05	0.0620	-0.0443
02.03	0.1525	-0.1065
03.02	0.2383	-0.1712
04.08	0.3336	-0.2308
05.06	0.4146	-0.2758
06.01	0.5098	-0.3243
07.13	0.6003	-0.3641
08.08	0.6718	-0.4032
09.03	0.7432	-0.4423
10.10	0.8432	-0.4882
11.06	0.9242	-0.5221
12.03	0.9756	-0.5612
13.25	1.0861	-0.6011
14.03	1.1624	-0.6487
15.11	1.2624	-0.6945
15.66	1.3005	-0.7184

M=0.95

WTR	RUN	CONFIG.
739	31	3

α(deg)	C_N	C_m
-05.09	-0.4770	0.3352
-04.06	-0.4000	0.3063
-03.07	-0.3132	0.2372
-02.04	-0.2409	0.1833
-01.09	-0.1446	0.1077
00.02	-0.0434	0.0346
01.09	0.0530	-0.0410
02.05	0.1494	-0.1053
03.16	0.2457	-0.1584
04.12	0.3324	-0.2275
05.10	0.4095	-0.2677
06.05	0.4721	-0.3038
07.25	0.5781	-0.3633
08.23	0.6648	-0.4099
09.03	0.7371	-0.4751
10.08	0.8141	-0.5040
11.03	0.8960	-0.5530
12.08	0.9827	-0.5996
13.00	1.0694	-0.6462
14.07	1.1560	-0.6928
15.01	1.2283	-0.7241
15.77	1.3053	-0.7530

M=0.95

WTR	RUN	CONFIG.
739	05	4

α(deg)	C_N	C_m
-04.47	-0.7803	0.4981
-04.02	-0.6485	0.4180
-03.13	-0.5533	0.3299
-02.08	-0.3648	0.2149
-01.00	-0.2088	0.1143
-00.00	-0.0183	0.0008
01.04	0.1257	-0.0654
02.09	0.2939	-0.1714
03.01	0.4358	-0.2343
04.03	0.5979	-0.3351
05.07	0.7013	-0.3641
06.07	0.8412	-0.4382
07.12	0.9932	-0.5225
08.11	1.1472	-0.6053
09.14	1.2770	-0.6773
10.03	1.3925	-0.7309
11.00	1.5192	-0.7963
12.01	1.6520	-0.8653
13.13	1.7898	-0.9360
14.11	1.9155	-1.0062
15.76	2.1020	-1.0792

M=0.95

WTR	RUN	CONFIG.
739	12	5

α(deg)	C_N	C_m
-04.47	-0.8749	0.9775
-03.02	-0.6034	0.6745
-02.13	-0.4575	0.4917
-01.13	-0.2615	0.3015
00.02	-0.0603	0.0447
00.96	0.1407	-0.1402
02.26	0.3570	-0.4052
03.01	0.4877	-0.5439
04.00	0.6733	-0.7686
05.04	0.8498	-0.9558
06.04	1.0458	-1.1461
07.04	1.2167	-1.3266
08.05	1.4078	-1.5221
09.08	1.6089	-1.7310
10.09	1.7898	-1.9249
11.11	1.9959	-2.1166
12.11	2.1819	-2.3054
13.12	2.4130	-2.5067
14.16	2.6141	-2.7037
15.84	3.0165	-3.2052

M=0.95

WTR	RUN	CONFIG.
739	09	6

α(deg)	C_N	C_m
-04.45	-0.7191	0.4808
-03.10	-0.5154	0.3366
-02.05	-0.3556	0.2324
-01.07	-0.2137	0.1402
00.05	-0.0559	0.0353
01.09	0.0899	-0.0458
02.11	0.2357	-0.1364
03.13	0.3576	-0.1983
04.12	0.4615	-0.2435
05.12	0.5934	-0.3062
06.12	0.7133	-0.3641
07.11	0.8052	-0.3997
08.08	0.9211	-0.4449
09.11	1.0210	-0.4868
10.10	1.1269	-0.5311
11.11	1.2208	-0.5611
12.08	1.3107	-0.5927
13.07	1.4067	-0.6124
14.06	1.4826	-0.6208
15.06	1.5666	-0.6167
15.66	1.6126	-0.6178

M=1.05

WTR	RUN	CONFIG.
739	18	1

α(deg)	C_N	C_m
-04.82	-0.4186	-0.1756
-04.04	-0.3569	-0.1520
-03.11	-0.2600	-0.1046
-02.03	-0.1630	-0.0675
-01.10	-0.0881	-0.0440
00.00	-0.0132	-0.0205
00.96	0.0838	0.0063
02.05	0.1764	0.0161
03.04	0.2645	0.0498
04.01	0.3439	0.0596
05.01	0.4364	0.0899
06.13	0.5290	0.1201
07.07	0.6128	0.1265
08.06	0.7009	0.1499
09.04	0.7979	0.1768
10.03	0.8861	0.1899
11.03	0.9832	0.1859
12.00	1.0846	0.1784
13.12	1.2170	0.1571
14.11	1.3362	0.1258
15.11	1.4465	0.1111
16.08	1.5877	0.0[illegible]1
16.33	1.6230	0.0860

M=1.05

WTR	RUN	CONFIG.
739	25	2

α(deg)	C_N	C_m
-05.13	-0.4855	0.2677
-04.11	-0.4155	0.2342
-02.98	-0.3193	0.1843
-02.00	-0.2362	0.1374
-01.09	-0.1356	0.0797
00.00	-0.0219	0.0086
00.91	0.0569	-0.0611
02.01	0.1619	-0.1268
03.09	0.2713	-0.1900
04.04	0.3413	-0.2338
05.03	0.4244	-0.2806
06.13	0.5163	-0.3329
07.08	0.5994	-0.3798
08.20	0.6781	-0.4035
09.03	0.7392	-0.4263
10.10	0.8310	-0.4582
11.08	0.9054	-0.4791
12.03	0.9840	-0.5079
13.09	1.0671	-0.5240
14.16	1.1545	-0.5685
15.09	1.2333	-0.6074
16.09	1.3295	-0.6574

M=1.05

WTR	RUN	CONFIG.
739	30	3

α(deg)	C_N	C_m
-04.57	-0.4066	0.1845
-04.03	-0.3541	0.1393
-03.06	-0.2710	0.0992
-02.08	-0.1923	0.0671
-01.15	-0.1093	0.0372
00.03	-0.0131	0.0036
01.02	0.0700	-0.0365
02.10	0.1618	-0.0722
02.92	0.2230	-0.1233
04.04	0.3018	-0.1759
05.03	0.3893	-0.2343
06.00	0.4724	-0.2846
07.26	0.5687	-0.3591
08.22	0.6562	-0.4175
09.06	0.7262	-0.4847
10.01	0.8137	-0.5329
11.11	0.9099	-0.5971
12.08	0.9930	-0.6372
13.02	1.0761	-0.6376
14.11	1.1592	-0.7277
15.04	1.2510	-0.7737
15.66	1.3035	-0.7882

M=1.05

WTR	RUN	CONFIG.
739	03	4

α(deg)	C_N	C_m
-04.58	-0.8972	0.6872
-04.01	-0.7741	0.5646
-03.09	-0.6380	0.4604
-02.01	-0.4027	0.2816
-01.02	-0.2151	0.1414
-00.01	-0.0588	0.0349
01.08	0.1305	-0.0995
02.22	0.3255	-0.2254
03.08	0.4615	-0.3077
04.06	0.6289	-0.4235
05.08	0.8017	-0.5352
06.06	0.9819	-0.6589
07.21	1.0996	-0.6936
08.10	1.2192	-0.7532
09.13	1.3442	-0.8174
10.12	1.4711	-0.8758
11.00	1.5723	-0.9185
12.00	1.6716	-0.9494
12.99	1.7875	-0.9898
14.00	1.8960	-1.0225
14.99	1.9917	-1.0430
15.88	2.0837	-1.0443

M=1.08

WTR	RUN	CONFIG.
739	13	5

α(deg)	C_N	C_m
-04.64	-0.9568	0.9872
-03.72	-0.7346	0.7550
-03.02	-0.6075	0.6070
-02.09	-0.4126	0.4004
-00.95	-0.2358	0.2288
00.03	-0.0317	0.0316
01.19	0.1768	-0.1716
02.07	0.3718	--0.3674
03.05	0.5441	-0.5545
04.02	0.7346	-0.7443
05.13	0.9341	-0.9569
06.07	1.1337	-1.1596
07.05	1.3378	-1.3991
08.03	1.5464	-1.6239
09.02	1.7505	-1.8642
10.02	1.9909	-2.1206
11.00	2.1995	-2.3670
11.99	2.4172	-2.5931
13.11	2.6803	-2.8778
14.12	2.8934	-3.1106
15.10	3.1292	-3.3610
16.08	3.3878	-3.6524

M=1.05

WTR	RUN	CONFIG.
739	08	6

α (deg)	C_N	C_m
-04.86	-0.7775	0.5985
-04.12	-0.6556	0.5141
-03.06	-0.5097	0.3994
-02.01	-0.3435	0.2707
-01.13	~~-0.2142~~	~~0.1760~~
00.01	-0.0406	0.0325
01.03	0.1127	-0.0880
02.04	0.2770	-0.2087
03.08	0.3971	-0.2762
04.08	0.5227	-0.3284
05.08	0.6539	-0.4004
06.08	0.7702	-0.4562
07.05	0.8755	-0.4987
08.05	0.9642	-0.5125
09.04	1.0530	-0.5176
10.03	1.1472	-0.5326
11.04	1.2359	-0.5342
12.01	1.3080	-0.5193
13.00	1.3857	-0.5023
14.12	[illegible]	-0.4934
15.09	[illegible]	-0.4644
15.64	[illegible]	[illegible]

M=1.15

WTR	**RUN**	**CONFIG.**
739	17	1

α (deg)	C_N	C_m
-05.04	-0.4534	-0.1062
-04.19	-0.3833	-0.1034
-03.11	-0.2802	-0.0880
-01.91	-0.1854	-0.0758
-01.00	-0.0988	-0.0571
00.03	-0.0041	-0.0160
01.10	0.0866	-0.0005
02.02	0.1773	0.0342
03.07	0.2638	0.0625
04.11	0.3628	0.0811
05.04	0.4411	0.0870
06.07	0.5442	0.1120
07.03	0.6349	0.1179
08.08	0.7255	0.1622
09.02	0.8162	0.1777
10.09	0.9275	0.2154
11.01	1.0142	0.1957
12.06	1.1297	0.1726
13.09	1.2617	0.1653
14.14	1.3855	0.1550
15.09	1.5092	0.1446
16.32	1.6908	0.1082

M=1.15

WTR	RUN	CONFIG.
739	26	2

α(deg)	C_N	C_m
-05.08	-0.4987	0.3166
-04.12	-0.4287	0.2872
-03.33	-0.3463	0.2357
-02.24	-0.2473	0.1739
-01.03	-0.1278	0.1040
00.03	-0.0083	0.0148
01.21	0.0660	-0.0509
02.10	0.1731	-0.1179
03.19	0.2762	-0.1871
04.13	0.3627	-0.2364
05.07	0.4534	-0.2930
06.10	0.5440	-0.3401
07.04	0.6306	-0.3727
08.11	0.7234	-0.4223
09.15	0.8077	-0.4664
10.08	0.8960	-0.5009
11.00	0.9560	-0.5206
12.05	1.0734	-0.5422
13.08	1.1531	-0.5734
14.13	1.2278	-0.5942
15.07	1.3134	-0.6220
16.05	1.4549	-0.6616

M=1.15

WTR	RUN	CONFIG.
739	29	3

α (deg)	C_N	C_m
-04.88	-0.4243	0.1917
-04.05	-0.3542	0.1498
-03.37	-0.2965	0.1209
-02.00	-0.1853	0.0708
-01.09	-0.1030	0.0447
00.03	-0.0165	0.0014
01.14	0.0783	-0.0474
02.22	0.1524	-0.0777
03.04	0.2184	-0.1120
04.04	0.2884	-0.1443
05.04	0.3873	-0.2007
06.07	0.4820	-0.2495
07.01	0.5645	-0.3045
08.04	0.6592	-0.3630
09.10	0.7540	-0.4214
10.14	0.8488	-0.4806
11.28	0.9477	-0.5170
12.05	1.0053	-0.5459
13.09	1.0877	-0.5719
14.00	1.1742	-0.[illegible]056
15.21	1.2978	-0.6765
15.69	1.3554	-0.6977

M=1.15

WTR	RUN	CONFIG.
739	02	4

α(deg)	C_N	C_m
-04.62	-0.8507	0.6561
-04.07	-0.7433	0.5547
-03.05	-0.5822	0.4315
-02.00	-0.3621	0.2700
-00.91	-0.1698	0.1207
00.02	-0.0295	0.0151
01.03	0.1334	-0.0860
02.10	0.3154	-0.2224
03.06	0.4627	-0.3105
04.14	0.6221	-0.4101
05.06	0.7711	-0.5092
06.00	0.9184	-0.6014
07.10	1.0969	-0.7156
08.03	1.2371	-0.8045
09.01	1.3880	-0.9066
10.02	1.5578	-1.0150
11.03	1.7069	-1.1059
12.11	1.8767	-1.2142
13.05	2.0257	-1.3092
14.02	2.1678	-1.4218
15.08	2.2255	-1.4979
15.83	2.3845	-1.4992

M=1.15

WTR	RUN	CONFIG.
739	14	5

α(deg)	C_N	C_m
-04.87	-1.0200	1.1068
-04.08	-0.8521	0.9133
-03.02	-0.6455	0.6884
-02.18	-0.4949	0.5282
-01.01	-0.2411	0.2913
00.02	-0.0560	0.0645
01.12	0.1635	-0.1673
01.94	0.3400	-0.3621
03.02	0.5337	-0.5901
04.08	0.7790	-0.8462
05.03	0.9511	-1.0455
06.05	1.1750	-1.3036
07.00	1.3859	-1.5341
08.04	1.6054	-1.7864
09.12	1.8421	-2.0412
10.05	2.0487	-2.2967
11.12	2.2812	-2.5663
12.02	2.5007	-2.3084
13.09	2.7374	-3.0734
14.04	2.9741	-3.3[illegible]
15.29	3.24[illegible]2	-[illegible]
15.72	3.3873	-3.7778

M=1.15

WTR	RUN	CONFIG.
739	06	6

α(deg)	C_N	C_m
-04.78	-0.7408	0.5995
-04.04	-0.6165	0.4917
-03.04	-0.48[illegible]5	0.3831
-02.04	-0.3367	0.2635
-01.03	-0.1848	0.1500
-00.02	-0.0276	0.0262
01.00	0.1123	-0.0796
02.00	0.2487	-0.1745
03.02	0.3920	-0.2749
04.02	0.5250	-0.3629
05.02	0.6373	-0.4260
06.01	0.7755	-0.5038
07.00	0.8912	-0.5738
07.99	1.01[illegible]0	-0.[illegible]515
09.01	1.1468	-0.72[illegible]1
10.16	1.2902	-0.8172
11.12	1.4007	-0.8687
12.10	1.5147	-0.9106
13.10	1.[illegible]374	-0.[illegible]656
14.08	1.[illegible]47[illegible]	-1.0130
15.06	1.[illegible]	-1.[illegible]7
1[illegible]	1.[illegible]	-1.[illegible]

M=1.26

WTR	RUN	CONFIG.
739	16	1

α(deg)	C_N	C_m
-04.57	-0.4287	-0.1177
-04.05	-0.3771	-0.1026
-03.53	-0.3295	-0.0937
-03.04	-0.2977	-0.0815
-02.52	-0.2461	-0.0664
-02.00	-0.1945	-0.0605
-01.50	-0.1588	-0.0422
-01.01	-0.1111	-0.0333
-00.47	-0.0675	-0.0212
-00.02	-0.0278	-0.0153
00.57	0.0238	0.0091
01.08	0.0794	0.0211
01.60	0.1151	0.0302
02.00	0.1429	0.0362
02.49	0.1985	0.0482
03.03	0.2501	0.0633
03.53	0.2898	0.0785
04.07	0.3414	0.0843
04.46	0.3732	0.0872
05.00	0.4248	0.1023

M-1.26

WTR	RUN	CONFIG.
739	16	1

α(deg)	C_N	C_m
05.50	0.4645	0.1083
06.03	0.5200	0.1295
06.67	0.5677	0.1446
07.09	0.6193	0.1536
07.46	0.6511	0.1565
08.54	0.7543	0.1775
09.06	0.8059	0.1926
09.59	0.8575	0.1984
10.10	0.9091	0.2136
10.48	0.9528	0.2164
11.04	1.0005	0.2161
11.53	1.0640	0.2219
12.07	1.1236	0.2215
12.57	1.1632	0.2212
13.12	1.2467	0.2269
13.51	1.2904	0.2298
14.01	1.3540	0.2170
14.55	1.4175	0.2321
15.24	1.5049	0.2284
15.61	1.5645	0.2372

M-1.26

WTR	RUN	CONFIG.
739	27	2

α(deg)	C_N	C_m
-04.54	-0.4405	0.2800
-03.33	-0.3413	0.2226
-02.04	-0.2143	0.1525
-01.65	-0.1826	0.1234
-00.99	-0.1231	0.1001
00.11	-0.0159	0.0192
01.14	0.0794	-0.0496
02.08	0.1667	-0.1135
03.21	0.2461	-0.1631
04.05	0.3413	-0.2226
05.00	0.4127	-0.2580
06.00	0.5119	-0.3061
07.08	0.6111	-0.3542
08.23	0.7261	-0.4029
09.00	0.7855	-0.4169
10.01	0.8648	-0.4387
11.05	0.9520	-0.4561
12.09	1.0392	-0.4643
12.98	1.1105	-0.4718
14.03	1.2016	-0.4592
15.07	1.3008	-0.4887
15.66	1.3800	-0.5012

M=1.26

WTR	RUN	CONFIG.
739	28	3

α(deg)	C_N	C_m
-04.51	-0.3846	0.1501
-03.99	-0.3410	0.1164
-03.07	-0.2736	0.0946
-02.00	-0.1784	0.0588
-01.08	-0.0872	0.0211
-00.02	-0.0119	0.0033
01.01	0.0555	-0.0278
02.06	0.1428	-0.0675
03.01	0.2142	-0.0966
04.02	0.3054	-0.1250
05.01	0.4164	-0.1713
06.00	0.4838	-0.1931
07.08	0.5750	-0.2401
08.10	0.6583	-0.2818
09.00	0.7416	-0.3235
10.01	0.8288	-0.3447
11.07	0.9082	-0.3791
12.09	0.9953	-0.3909
13.00	1.0786	-0.4048
14.15	1.1777	-0.4473
15.07	1.27[illegible]	-0.4415
15.70	1.348[illegible]	-0.5013

M=1.26

WTR	RUN	CONFIG.
739	01	4

α(deg)	C_N	C_m
-04.61	-0.7834	0.5659
-04.21	-0.6950	0.4850
-03.96	-0.6567	0.4581
-03.53	-0.5867	0.4072
-03.04	-0.5034	0.3464
-02.63	-0.4334	0.2955
-02.08	-0.3484	0.2359
-01.59	-0.2600	0.1749
-01.04	-0.1784	0.1129
-00.51	-0.1033	0.0657
00.02	-0.0217	0.0036
00.55	0.0717	-0.0497
01.24	0.1717	-0.1139
02.04	0.2984	-0.1939
02.89	[illegible]	-0.2495
04.03	0.6051	-0.3895
05.00	0.7234	-0.4598
06.04	[illegible]	-0.5630
06.57	[illegible]	-0.6075
07.12	[illegible]	[illegible]
[illegible]	[illegible]	-0.7418
[illegible]	[illegible]	[illegible]
[illegible]	[illegible]	[illegible]
[illegible]	[illegible]	[illegible]
12.04	[illegible]	[illegible]
13.11	[illegible]	[illegible]
[illegible]	[illegible]	[illegible]
[illegible]	[illegible]	[illegible]
[illegible]	[illegible]	[illegible]

M=1.26

WTR	RUN	CONFIG.
739	15	5

α(deg)	C_N	C_m
-04.62	-0.8953	0.9496
-03.97	-0.7544	0.7910
-03.43	-0.5632	0.6[illegible]8
-03.06	-0.6051	0.6212
-02.39	-0.4808	0.5044
-02.01	-0.4187	0.4509
-01.31	-0.3192	0.3476
-00.99	-0.2280	0.2553
-00.45	-0.1327	0.1975
00.03	-0.0374	0.0696
00.59	0.0562	-0.0393
00.98	0.1492	-0.1304
01.51	0.2[illegible]	-0.2171
02.03	0.3108	-0.3247
02.42	0.4061	-0.3948
03.11	0.5263	-0.5259
03.49	0.6251	-0.6015
04.03	0.7[illegible]4	-0.7092
04.55	0.7958	-0.8168
05.12	0.9201	-0.9337
05.62	1.0272	-1.0303

M=1.26

WTR	RUN	CONFIG.
739	15	5

α(deg)	C_N	C_m
06.02	1.0983	-1.1225
06.54	1.2020	-1.2413
07.09	1.3097	-1.3458
07.59	1.4051	-1.4634
08.03	1.5005	-1.5612
08.55	1.6165	-1.6965
09.08	1.7078	-1.7986
09.59	1.8279	-1.9198
10.14	1.9398	-2.0299
10.52	2.0269	-2.1265
11.59	2.2549	-2.3621
11.97	2.3460	-2.4445
12.52	2.4496	-2.5533
13.04	2.5782	-2.6954
13.46	2.6652	-2.7723
13.99	2.7895	-2.9089
14.51	2.9180	-3.0411
15.06	3.0133	-3.1857
15.48	3.1377	-3.2656
16.08	3.2366	-3.4624

M=1.26

WTR	RUN	CONFIG.
739	07	6

α(deg)	C_N	C_m
-04.96	-0.6934	0.5119
-04.06	-0.5789	0.4182
-03.07	-0.4296	0.3184
-02.09	-0.3085	0.2392
-01.09	-0.1808	0.1349
00.02	-0.0265	0.0371
01.02	0.1045	-0.0580
02.02	0.2372	-0.1445
03.02	0.3633	-0.2218
03.99	0.4927	-0.2978
05.11	0.6255	-0.3685
06.07	0.7366	-0.4358
07.05	0.8528	-0.5011
08.01	0.9788	-0.5704
08.99	1.0900	-0.6259
10.13	1.2277	-0.6907
11.09	1.3389	-0.7422
12.07	1.4567	-0.7792
13.03	1.5679	-0.8228
14.14	1.6957	-0.8559
15.06	1.8052	-0.8804
15.81	1.8516	-0.8980

M=0.30

50 CALIBER CORE

α(deg)	C_N	C_M
-05.35	-0.0539	-0.4997
-04.15	-0.0558	-0.2736
-02.31	-0.0373	-0.1730
-01.10	-0.0380	-0.0882
00.13	-0.0192	0.0159
01.99	0.0377	0.1165
03.23	0.0565	0.1989
04.99	0.0746	0.3460
06.19	0.0933	0.4184
08.55	0.1501	0.5790
10.34	0.1683	0.7079
12.07	0.2445	0.8561
14.38	0.2621	0.9567
15.54	0.3011	1.0450
16.69	0.3006	1.1015
17.84	0.3583	1.1490
19.52	0.3965	1.2090
20.04	0.4542	1.2566

M=0.30

50 CALIBER CORE

α(deg)	C_N	C_m
22.22		1.4063
24.06	0.8207	1.4166
25.90	0.8979	1.4518
28.33	1.1493	1.4885
30.18	1.3038	1.5306
32.02	1.5360	1.5513
35.13	1.9422	1.6018
38.22	2.3668	1.7529
40.04	2.5401	1.8674
42.53	2.7908	1.9888
45.53	3.0987	2.2143
47.95	3.4076	2.3268
50.36	3.6006	2.4006
52.76	3.7936	2.4744
55.14	4.0058	2.5641

M=0.30

50 CALIBER CONE

α(deg)	C_N	C_m
58.51	4.0047	2.5350
61.94	4.1587	2.6335
64.82	4.1964	2.7500
67.15	4.1577	2.7465
70.11	4.2159	2.7376
72.97	4.1395	2.6177
75.83	4.0633	2.4695
77.54	4.0061	2.3655
78.10	3.7379	2.0305
79.23	3.4517	1.5385
82.03	3.4918	1.3725
84.34	3.4156	1.2243
87.71	3.4180	0.9418
89.42	3.4583	0.7476
90.13	3.4011	0.6435

M=0.50

50 CALIBER CONE

α(deg)	C_N	C_m
-05.57	-0.0596	-0.3959
-03.71	-0.0293	-0.2553
-02.46	-0.0144	-0.1621
-00.58	0.0158	-0.0101
00.01	0.0233	0.0308
01.93	0.0613	0.1893
03.17	0.0684	0.2876
04.98	0.0909	0.4217
07.47	0.1288	0.5916
09.90	0.1823	0.7745
12.94	0.2356	0.9803
15.33	0.2973	1.1236
19.45	0.4055	1.3631

M=0.50

50 CALIBER CONE

α(deg)	C_N	C_m
22.21	0.5129	1.5183
24.59	0.6299	1.6032
27.60	0.8252	1.7066
30.00	1.0998	1.7025
33.60	1.6175	1.7145
36.03	2.0403	1.8096
37.81	2.2980	1.9530
40.16	2.6020	2.1922
42.55	2.8984	2.4020
45.53	3.2497	2.6110
47.86	3.4946	2.7644
50.18	3.6320	2.8572
52.50	3.8894	3.0464
54.82	4.0612	3.1305

M=0.50

50 CALIBER CORE

α(deg)	C_N	C_m
56.34	4.2430	3.0958
58.00	4.2979	3.0950
59.66	4.3606	3.1006
62.48	4.4542	3.1779
65.31	4.5243	3.2356
66.99	4.5242	3.2471
69.25	4.4547	3.1091
71.47	4.3694	2.9925
72.58	4.2224	2.7444
73.12	3.8200	2.0666
74.22	3.7355	1.8256
76.42	3.7369	1.6753
78.65	3.7459	1.5443
81.41	3.7472	1.3839
84.15	3.7409	1.2057
86.36	3.7577	1.0697
87.47	3.7432	0.9309
88.58	3.7598	0.8177
90.22	3.7062	0.6582

M=0.70

50 CALIBER CORE

α(deg)	C_N	C_m
-05.46	-0.0628	-0.4135
-04.24	-0.0587	-0.3336
-03.02	-0.0406	-0.2421
-01.17	-0.0134	-0.1014
-00.53	0.0050	-0.0376
00.06	0.0048	-0.0030
01.90	0.0319	0.1446
03.09	0.0500	0.2430
04.30	0.0681	0.3483
05.49	0.0864	0.4259
07.21	0.1089	0.5627
08.37	0.1366	0.6482
10.12	0.1733	0.7828
12.43	0.2147	0.9213
14.16	0.2705	1.0507
16.45	0.3356	1.1810
18.74	0.4100	1.3190
20.33	0.4710	1.4100

M=0.70

50 CALIBER CORE

α(deg)	C_N	C_m
22.19	0.5537	1.5250
23.88	0.6333	1.6045
25.04	0.7130	1.6772
27.84	0.9006	1.8250
30.07	1.1215	1.9447
32.38	1.4414	2.0767
34.65	1.8605	2.2004
36.36	2.1618	2.2963
38.03	2.4678	2.4020
39.14	2.6790	2.5425
40.22	2.8197	2.6596
42.47	3.1384	2.9284
44.10	3.3258	3.1037
45.73	3.5274	3.2769
47.37	3.7289	3.4501
48.97	3.8698	3.5395
50.02	3.9449	3.6004
52.70	4.1514	3.7292
54.27	4.2592	3.8250

M=0.70

50 CALIBER CORE

α(deg)	C_N	C_m
56.73	4.6594	3.9539
58.95	4.8151	3.9713
60.04	4.8575	3.9785
61.17	4.9048	3.9690
62.80	4.8258	3.8205
63.88	4.7655	3.6876
64.95	4.6630	3.5198
66.05	4.5048	3.2437
67.67	4.1892	2.6018
68.69	4.0971	2.3247
70.32	4.0609	2.1422
74.03	4.0912	1.[illegible]036
75.54	4.0919	1.8140
78.75	4.0935	1.[illegible]280
80.84	4.0804	1.4993
83.44	4.1288	1.[illegible]519
86.51	4.0975	1.1526
89.07	4.0430	0.8857
90.38	4.0488	0.7[illegible]37

TABULATED DATA

Normal Force and Pitching
Moment Coefficient Slopes and
Center of Pressure Locations

	$C_{m_{\alpha_o}}$ (per deg)	$C_{N_{\alpha_o}}$ (per deg)	$X_{RC}-X_{CP}$ (calibers)	M
CONFIG. 1				
	0.0303	0.0909	0.3333	0.4850
	0.0305	0.0836	0.3648	0.8080
	0.0274	0.0833	0.3289	0.9350
	0.02174	0.0830	0.2619	1.0500
	0.0294	0.0909	0.3234	1.1500
	0.0253	0.08888	0.2846	1.2600
CONFIG. 2				
	-0.0315	0.0909	-0.3465	0.4850
	-0.05195	0.0907	-0.57277	0.8080
	-0.0650	0.0926	-0.7019	0.9350
	-0.0666	0.0961	-0.6930	1.0500
	-0.0672	0.0952	-0.7059	1.1500
	-0.06211	0.0926	-0.6707	1.2600
CONFIG. 3				
	-0.0222	0.0714	-0.3109	0.4850
	-0.0370	0.0843	-0.4394	0.8080
	-0.0578	0.0930	-0.6215	0.9350
	-0.0433	0.0843	-0.5136	1.0500
	-0.0370	0.0814	-0.4545	1.1500
	-0.03053	0.0778	-0.3924	1.2600
CONFIG. 4				
	-0.0280	0.1062	-0.2636	0.4850
	-0.0437	0.1263	-0.3460	0.8080
	-0.0908	0.1568	-0.5791	0.9350
	-0.1136	0.1732	-0.6560	1.0500
	-0.1126	0.1600	-0.7040	1.1500
	-0.1042	0.1541	-0.6762	1.2600

	$C_{m_{\alpha_o}}$ (per deg)	$C_{N_{\alpha_o}}$ (per deg)	$X_{RC}-X_{CP}$ (calibers)	M
CONFIG. 5				
	-0.0930	0.1385	-0.6715	0.4850
	-0.1351	0.1449	-0.9317	0.8080
	-0.2024	0.1938	-1.0444	0.9350
	-0.1887	0.1894	-0.9963	1.0500
	-0.2112	0.1976	-1.0688	1.1500
	-0.1894	0.1779	-1.0646	1.2600
CONFIG. 6				
	-0.03883	0.1000	-0.3883	0.4850
	-0.0505	0.1152	-0.4387	0.8080
	-0.0822	0.1464	-0.5615	0.9350
	-0.1160	0.1506	-0.7702	1.0500
	-0.1111	0.1416	-0.7846	1.1500
	-0.09153	0.13441	-0.6810	1.2600
50 CALIBER BULLET CORE				
			4.267	0.3000
			5.314	0.5000
			5.396	0.7000

TABULATED DATA

Drag
Coefficients

	C_{A_o}	M
CONFIG. 1		
	0.4145	0.4850
	0.4543	0.7980
	0.5836	0.9350
	0.7316	1.0370
	0.8807	1.1490
	1.1132	1.2540
CONFIG. 2		
	1.3362	0.4850
	1.5403	0.7980
	1.9375	0.9460
	2.3543	1.0470
	2.4425	1.1490
	1.9962	1.2540
CONFIG. 3		
	0.7099	0.5040
	0.8460	0.7980
	1.1215	0.9350
	1.5256	1.0470
	1.7326	1.1490
	1.6084	1.2540
CONFIG. 4		
	0.2307	0.5040
	0.2804	0.3080
	0.3617	0.9350
	0.6136	1.0470
	0.8000	1.1490
	0.7608	1.2540

C_{A_o}	M
CONFIG. 5	
0.4445	0.5040
0.5173	0.7980
0.6529	0.9350
0.9201	1.0470
1.1277	1.1490
1.0259	1.2540
CONFIG. 6	
0.2483	0.4950
0.2778	0.7880
0.3154	0.8960
0.3791	0.9460
0.6001	1.0370
0.7911	1.1490
0.7650	1.2540

TABULATED DATA

Pitch Damping Coefficients

CONFIG. 6

M	$\overline{\alpha}$	$C_{m_q} + C_{m_{\dot{\alpha}}}$
0.300	31.4	-39.7
0.300	24.2	-35.4
0.300	19.1	-33.1
0.300	15.2	-31.4
0.300	12.4	-29.3
0.300	10.1	-27.9
0.300	08.4	-26.8
0.300	07.0	-27.1
0.300	05.8	-26.3
0.300	04.8	-23.9
0.300	04.2	-20.9
0.300	03.6	-22.3
0.300	03.2	-11.4
0.500	32.8	-39.2
0.500	22.2	-36.2
0.500	15.4	-34.0
0.500	11.1	-29.0
0.500	08.3	-27.0
0.500	06.4	-22.0
0.500	05.2	-19.7
0.500	39.8	-45.9
0.500	25.0	-42.0
0.500	16.6	-34.[illegible]
0.500	11.8	-31.2
0.500	08.6	-29.7
0.500	05.5	-30.[illegible]
0.500	04.5	-36.0
0.700	22.1	-42.2
0.700	13.1	-39.3
0.700	03.1	-35.3

CONFIG. 6

M	$\bar{\alpha}$	$C_{m_q} + C_{m_{\dot{\alpha}}}$
0.700	05.1	-39.1
0.700	03.0	-48.1
0.700	01.6	-49.6
0.700	23.4	-43.5
0.700	13.8	-38.3
0.700	08.8	-31.4
0.700	05.8	-34.4
0.700	03.8	-36.6
0.700	02.4	-29.5
0.700	01.7	-25.5
0.900	11.3	-53.2
0.900	07.0	-49.2
0.900	04.5	-48.2
0.900	03.0	-43.1
0.900	02.1	-34.8

TABULATED DATA

Roll Damping Coefficients

M	α	C_{ℓ_p}
0.299	0.0	03.3
0.299	05.0	03.37
0.299	10.0	03.48
0.299	15.0	03.50
0.504	0.0	03.16
0.504	05.0	03.24
0.524	10.0	03.19
0.524	15.0	03.20
0.798	00.0	03.49
0.798	05.0	03.42
0.798	10.0	03.27
0.946	0.0	03.87
0.946	05.0	03.59
0.946	15.0	03.35
1.297	00.0	04.20
1.297	05.0	03.90
1.297	10.0	03.65
1.297	15.0	03.52

APPENDIX A

THE METHOD EMPLOYED FOR DETERMINING THE DAMPING IN PITCH

A free oscillation technique is used for the measurement of the damping in pitch coefficient, $C_{m_{\dot\theta}} + C_{m_{\dot\alpha}}$. In this technique the model is attached to a transverse rod by means of ball bearings. Because of the constraints imposed by the support rod the model has one degree of freedom, that being in pitch. A mathematical expression relating the inertial to aerodynamic moments is postulated to have the form:

$$I_{yy}\ddot\theta = \Sigma M_{EXTERNAL} = M_\alpha \alpha + M_{\dot\alpha}\dot\alpha + M_{\dot\theta}\dot\theta \tag{A-1}$$

Making use of the fact that the support constraints imply that $\alpha = \theta$, it is possible to rearrange equation (A-1) as:

$$\ddot\alpha - \frac{(M_{\dot\alpha} + M_{\dot\theta})}{I_{yy}}\dot\alpha - \frac{(M_\alpha)}{I_{yy}}\alpha = 0$$

or:

$$\ddot\alpha - \frac{\left(C_{m_{\dot\theta}} + C_{m_{\dot\alpha}}\right) qAd^2}{2VI_{yy}}\dot\alpha - \left(\frac{C_{m_\alpha} qAd}{I_{yy}}\right)\alpha = 0 \tag{A-2}$$

where use has been made of the following coefficient definitions:

$$C_{m_\alpha} = \frac{M_\alpha}{qAd}$$

$$C_{m_{\dot\theta}} + C_{m_{\dot\alpha}} = \frac{M_{\dot\theta} + M_{\dot\alpha}}{(qAd)\left(\frac{d}{2V}\right)}$$

The solution to equation (A-2) may be expressed in the following form:

$$\alpha = \alpha_o e^{\lambda t} \mathrm{Cos}(\omega t + \psi) \tag{A-3}$$

where the constants α_o and ψ depend solely upon the initial conditions. Of importance in the data reduction is the log decrement λ and the frequency ω. These quantities are given, respectively, as:

$$\lambda = \frac{\left(C_{m_{\dot\theta}} + C_{m_{\dot\alpha}}\right) qAd^2}{4VI_{yy}} \tag{A-4}$$

$$\omega = \sqrt{-\frac{C_{m_\alpha} qAd}{I_{yy}}}\sqrt{1 - \frac{\left(C_{m_{\dot\theta}} + C_{m_{\dot\alpha}}\right)^3 qAd^3}{16V^2 I_{yy}}} \tag{A-5}$$

Since wind tunnel models are lightly damped (by making I_{yy} as large as possible), the second term in the radicand of equation (A-5) may be neglected to give:

$$\omega = \sqrt{-\frac{C_{m_\alpha} qAd}{I_{yy}}} \tag{A-6}$$

Figure (A-1), below, represents a typical damped pitch oscillation of a wind tunnel model:

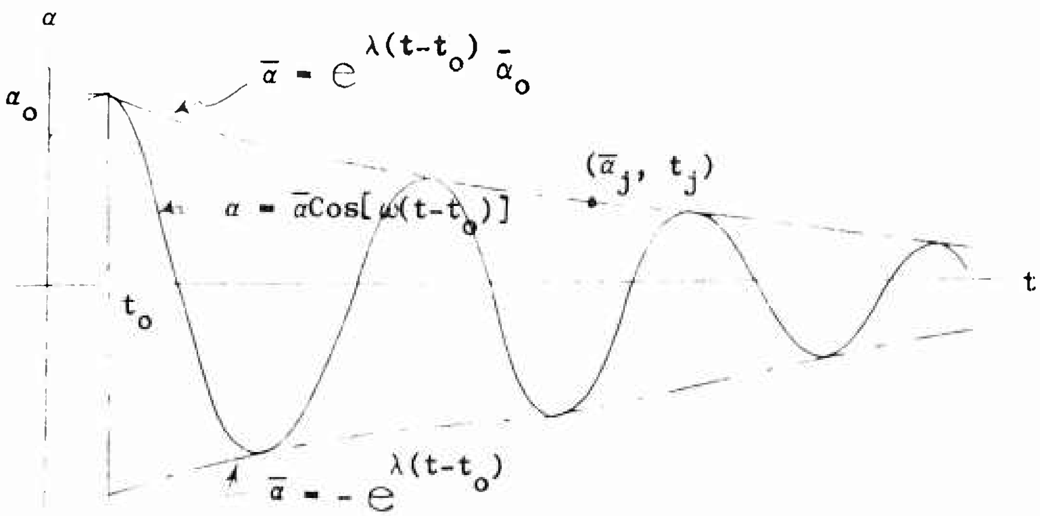

FIGURE (A-1)
Typical Pitch Damping Trace

It should be noted in the above figure that the envelope of the damped sinusoid is given as:

$$\bar{\alpha} = \alpha_o e^{\lambda(t - t_o)} \tag{A-7}$$

Using the amplitude record (obtained photographically) one may obtain the envelope, $\bar{\alpha}(t)$. From this envelope, the log decrement, λ, may be obtained. If this is done, and λ is in turn replaced by its equivalent from equation (A-4), one has an expression for the pitch damping coefficient in terms of measurable quantities.

$$C_{m_{\dot{\theta}}} + C_{m_{\dot{\alpha}}} = \frac{4VI_{yy}}{qAd^2(t_j - t_o)} \ln\left(\frac{\bar{\alpha}_j}{\alpha_o}\right) \tag{A-8}$$

Equation (A-8) is based upon the supposition that aerodynamic damping is a linear phenomenon, i.e., that the coefficients of equation (A-2) are constant. For cases where the amplitude envelope does not support this hypothesis ($\bar{\alpha}(t)$ not exactly exponential), a method of "piecewise" linearization is used. In this approach the amplitude envelope is divided into small time intervals over which intervals the pitch damping is assumed linear. This is accomplished as illustrated in Figure (A-2).

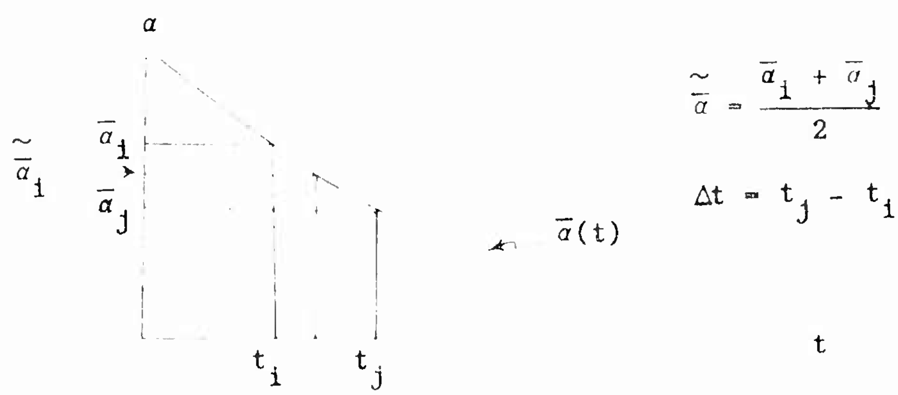

FIGURE (A-2)
Pitch Damping Envelope

Since equation (A-2) is assumed linear over the interval Δt, equation (A-8) may be rewritten as:

$$C_{m_{\dot{\theta}}}(\tilde{\bar{\alpha}}_i) + C_{m_{\dot{\alpha}}}(\tilde{\bar{\alpha}}_i) = \frac{4VI_{yy}}{qAd^2\,\Delta t}\,\ln\left(\frac{\bar{\alpha}_i}{\bar{\alpha}_j}\right) \tag{A-9}$$

APPENDIX B

METHODS FOR DETERMINING THE STATIC MOMENT COEFFICIENT FROM PITCH DAMPING RECORDS

In addition to the damping coefficient, $C_{m_{\dot{\theta}}} + C_{m_{\dot{\alpha}}}$, it is also possible to use the pitch damping record to obtain static data. The equation describing the single-degree-of-freedom pitch oscillation (equation (A-2)) has been stated as:

$$\ddot{\alpha} - \left(\frac{(C_{m_{\dot{\theta}}} + C_{m_{\dot{\alpha}}}) qAd^2}{2VI_{yy}} \right) \dot{\alpha} - \left(\frac{C_{m_\alpha} qAd}{I_{yy}} \right) \alpha = 0 \qquad \text{(B-1)}$$

In the vicinity of the oscillation peak, $\alpha = \alpha_p$, equation (B-1) may be simplified as:

$$\ddot{\alpha}_p - \left(\frac{C_m\big|_{\alpha_p} qAd}{I_{yy}} \right) \alpha_p = 0 \qquad \text{(B-2)}$$

where the following statements have been assumed valid in the vicinity of the local maximum of the function $\alpha(t)$:

$$\alpha\big|_{t=t_p} = \alpha_p$$

$$\dot{\alpha}\big|_{t=t_p} \cong 0$$

$$\ddot{\alpha}\big|_{t=t_p} \cong \ddot{\alpha}_p$$

Equation (B-2) may be rewritten as a solution for $C_m|_{\alpha_p}$ as:

$$C_m|_{\alpha_p} = \frac{\ddot{\alpha}_p I_{yy}}{qAd} \tag{B-3}$$

It now becomes necessary to obtain some approximation to $\ddot{\alpha}_p$. In Figure (B-1), below, a typical pitch oscillation is shown.

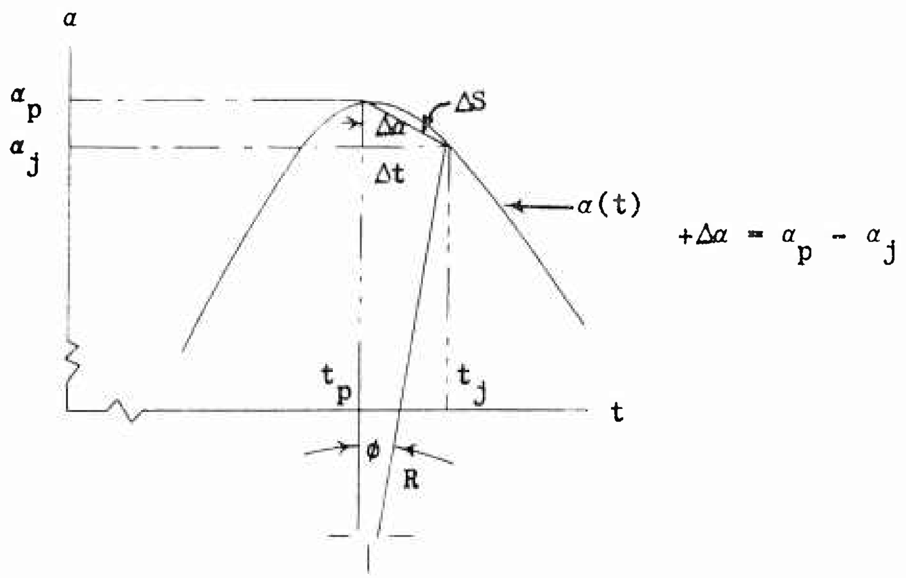

FIGURE (B-1)
A Representative Curve of $\alpha(t)$

The curvature of $\alpha(t)$ in the vicinity of t_p is

$$R = \frac{[1 + (\dot{\alpha})^2]^{3/2}}{\ddot{\alpha}}\Big|_{t=t_p} \simeq \frac{1}{\ddot{\alpha}_p} \tag{B-4}$$

where $(\dot{\alpha})^2$ has been assumed negligible compared with unity over the interval, Δt. Over this interval, Δt, the following relationships are held to be valid:

$$-\Delta\alpha = R(1 - \cos\phi) \simeq \frac{R\phi^2}{2} \tag{B-5}$$

but

$$\phi \cong \frac{\Delta S}{R} \cong \frac{\sqrt{1 + (\dot{\alpha})^2}}{R} \Delta t \cong \frac{\Delta t}{R} \tag{B-6}$$

Combining (B-4), (B-5), and (B-6), one readily obtains:

$$\ddot{\alpha}_p = -\frac{2\Delta\alpha}{(\Delta t)^2} \tag{B-7}$$

Finally, inserting equation (B-7) into equation (B-3), one obtains:

$$C_m\Big|_{\alpha_p} = -\frac{2\Delta\alpha I_{yy}}{(\Delta t)^2 qAd} \tag{B-8}$$

An alternate method exists for obtaining essentially the same information. It can readily be shown (equation (A-6)) that the period of oscillation can be expressed as:

$$T = 2\pi \sqrt{-\frac{I_{yy}}{C_{m_\alpha} qAd}} \tag{B-9}$$

Equation (B-9) may now be solved for the slope of the static pitching moment coefficient, C_{m_α}, to give:

$$C_{m_\alpha} = -\frac{4\pi^2 I_{yy}}{T^2 qAd} \tag{B-10}$$

Equation (B-10) is easier to use than equation (B-9); however, since equation (B-10) gives only the slope through the origin, it cannot be used to evaluate nonlinearities in the static pitching moment coefficient, C_m. For evaluation of $C_m(\alpha)$ where it varies nonlinearly it would be necessary to make use of equation (B-8).

APPENDIX C

THE METHOD EMPLOYED FOR THE DETERMINATION OF DAMPING IN ROLL

A free decay technique is used for the measurement of the damping in roll coefficient, C_{l_p}, and the induced rolling moment coefficient (due to fin cant, δ_f, or control deflection, δ_c), C_{l_δ}. In this procedure the model is axially mounted to a rotating sting. The model-sting combination is spun to a high spin rate, decoupled from the drive system, and permitted to decay to either zero spin rate or a steady state spin rate, if any. An analog record of the spin history is obtained from a magnetic tachometer. An identical run is made in a vacuum to provide a tare for the removal of the damping contribution of bearing friction.

Because of the nature of the support and drive system, a first order homogeneous differential equation relating the inertial to aerodynamic moments is presumed to describe the spin decay. This equation may be written as:

$$I_{xx}\dot{p} = \Sigma L_{EXTERNAL} = L_p p + L_\delta \delta \qquad \text{(C-1)}$$

where p is the spin rate, I_{xx} the axial moment of inertia, $L_\delta \delta$ the induced roll moment, and $L_p p$ the roll damping moment. The solution of equation (C-1) is:

$$\left(p + \frac{L_\delta \delta}{L_p}\right) = \left(p_o + \frac{L_\delta \delta}{L_p}\right) e^{\frac{L_p}{I_{xx}}(t-t_o)} \qquad \text{(C-2)}$$

In equation (C-2) the initial conditions are chosen as $p=p_o$ when $t=t_o$. The definition of steady state roll follows from equation (C-1) and may be expressed as:

$$\dot{p} = 0, \; p = p_{ss} = -\left(\frac{L_\delta}{L_p}\right)\delta$$

Using the above definition, equation (C-2) may be rewritten as:

$$(p-p_{ss}) = (p_o-p_{ss}) \quad e^{\frac{L_p}{I_{xx}}(t-t_o)} \qquad \text{(C-3)}$$

The roll damping moment derivative, L_p, and the induced rolling moment derivative, L_δ, have the following definition in terms of nondimensional quantities:

$$L_p = C_{\ell_p} \frac{qAd^2}{2V} \qquad \text{(C-4)}$$

$$L_\delta = C_{\ell_\delta} \; qAd \qquad \text{(C-5)}$$

If equation (C-3) is solved for the roll damping moment derivative, L_p, and then rewritten in terms of the roll damping coefficient, C_{ℓ_p}, from equation (C-4), the result is:

$$C_{\ell_p} = - \frac{I_{xx}}{(t-t_o)} \left(\frac{2V}{qAd^2}\right) \ln \left(\frac{p_o-p_{ss}}{p-p_{ss}}\right) \qquad \text{(C-6)}$$

Definition of the steady state roll and the definition of C_{ℓ_δ} from equation (C-5) results in the following expression:

$$C_{\ell_\delta} = - \frac{p_{ss}}{\delta} \left(\frac{b}{2V}\right) C_{\ell_p} \qquad \text{(C-7)}$$

Thus it should be noted that both coefficients C_{ℓ_p} and C_{ℓ_δ} may be calculated from measurable quantities.

Where there is no induced roll ($C_{\ell_\delta}\,\delta = 0$) equation (C-6) becomes:

$$C_{\ell_p} = - \frac{I_{xx}}{(t-t_o)} \left(\frac{2V}{qAd^2}\right) \ln \left(\frac{p_o}{p} \right) \qquad \text{(C-8)}$$

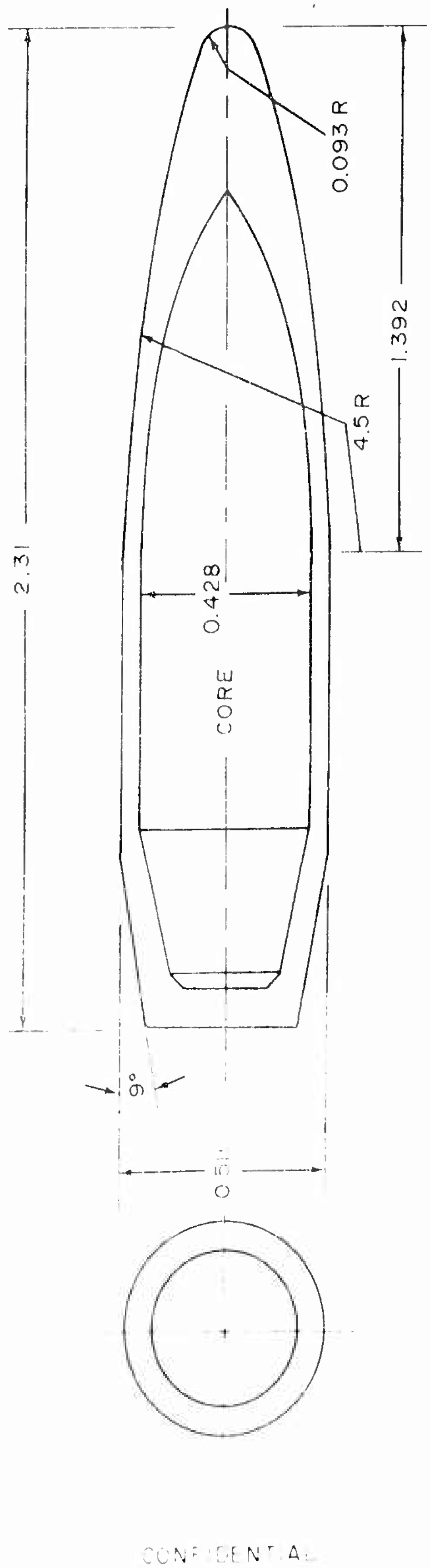

DIMENSIONS IN INCHES

FIG. 1 50 CALIBER BULLET

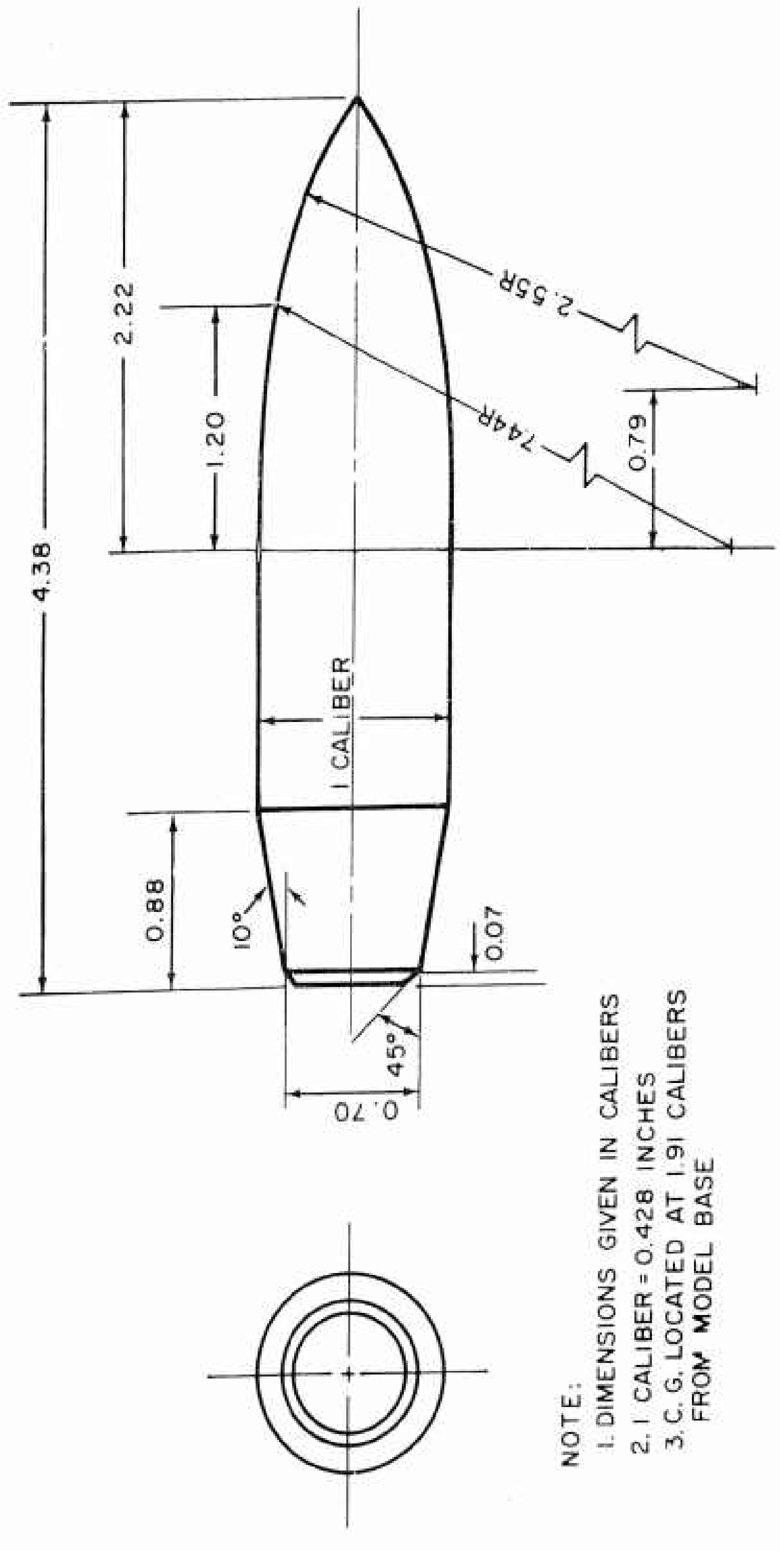

NOTE:
1. DIMENSIONS GIVEN IN CALIBERS
2. 1 CALIBER = 0.428 INCHES
3. C.G. LOCATED AT 1.91 CALIBERS FROM MODEL BASE

FIG.2 50 CALIBER STEEL CORE

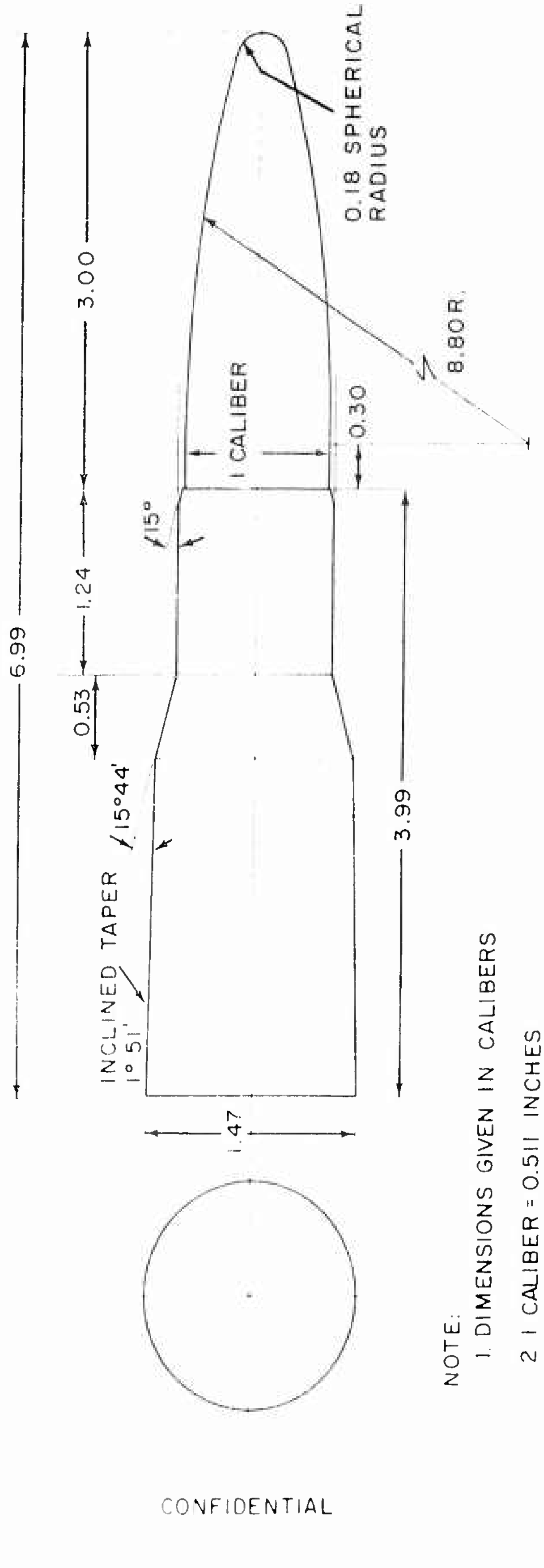

NOTE:
1. DIMENSIONS GIVEN IN CALIBERS
2. 1 CALIBER = 0.511 INCHES
3. C.G. LOCATED AT 4.05 CALIBERS FROM MODEL BASE

FIG.3 LAZY DOG CONFIGURATION I

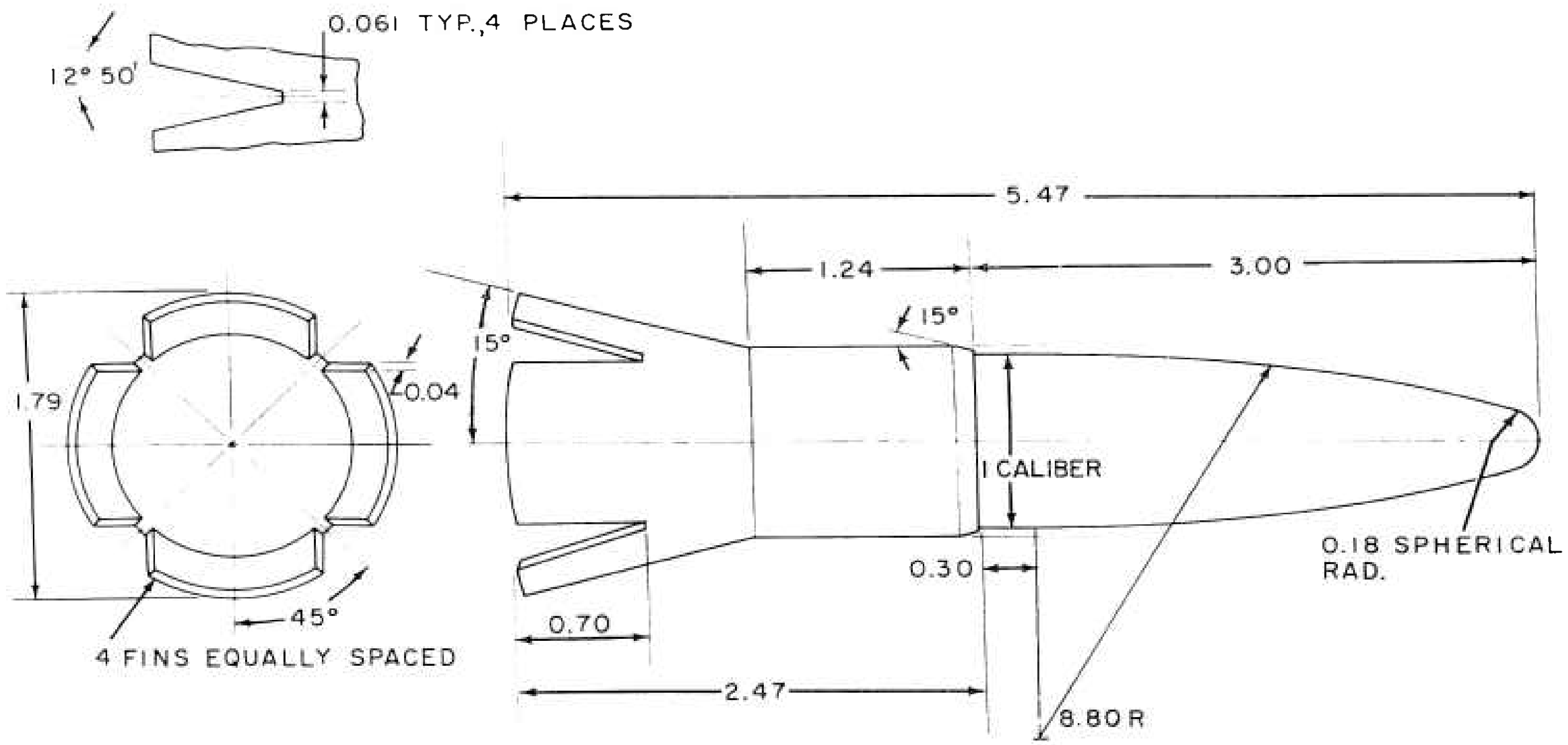

NOTE:

1. DIMENSIONS GIVEN IN CALIBERS
2. I CALIBER = 0.511 IN.
3. C.G. LOCATED 2.89 CALIBERS FROM MODEL BASE

FIG.4 LAZY DOG CONFIGURATION 2

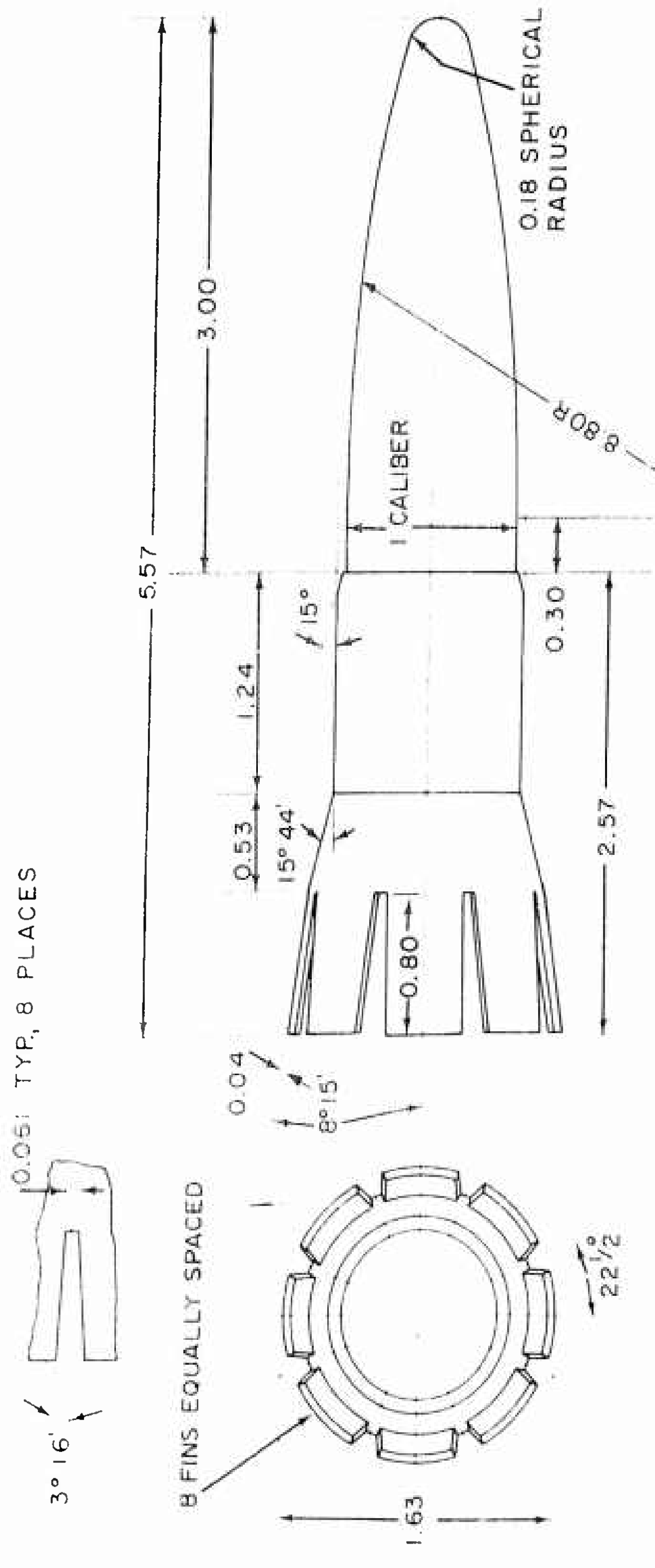

NOTE:

1. DIMENSIONS GIVEN IN CALIBERS
2. 1 CALIBER = 0.511 INCHES
3. C.G. LOCATED 2.89 CALIBERS FROM MODEL BASE

FIG.5 LAZY DOG CONFIGURATION 3

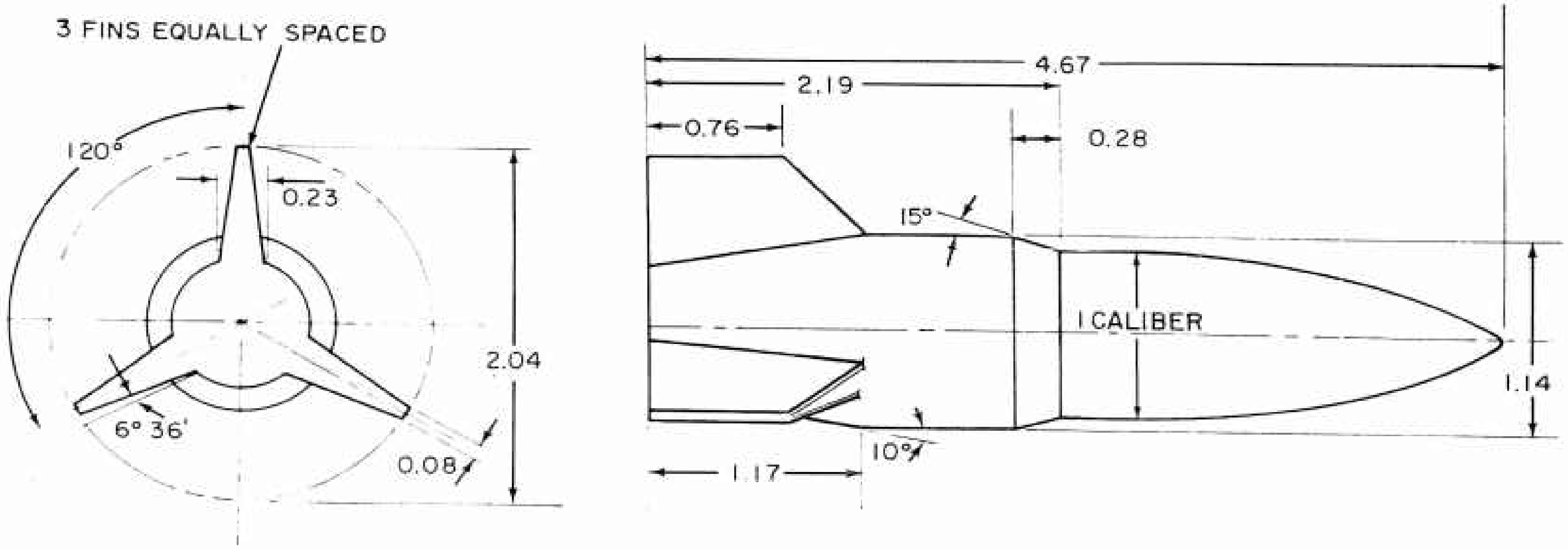

NOTE:
1. DIMENSIONS GIVEN IN CALIBERS
2. 1 CALIBER = 0.428 INCHES
3. C. G. LOCATED 2.18 CALIBERS FROM MODEL BASE

FIG. 6 LAZY DOG CONFIGURATION 4

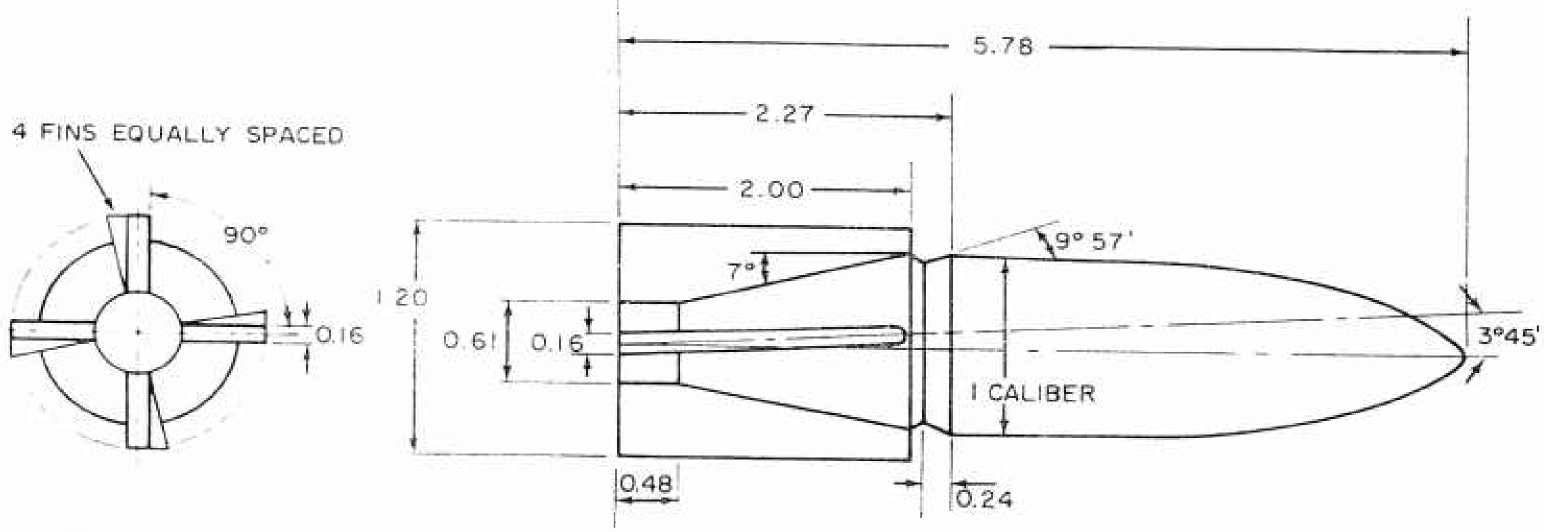

NOTE.
1. DIMENSIONS GIVEN IN CALIBERS
2. 1 CALIBER = 0.428 IN.
3. C.G. LOCATED 2.96 CALIBERS FROM MODEL BASE

FIG.7 LAZY DOG CONFIGURATION 5

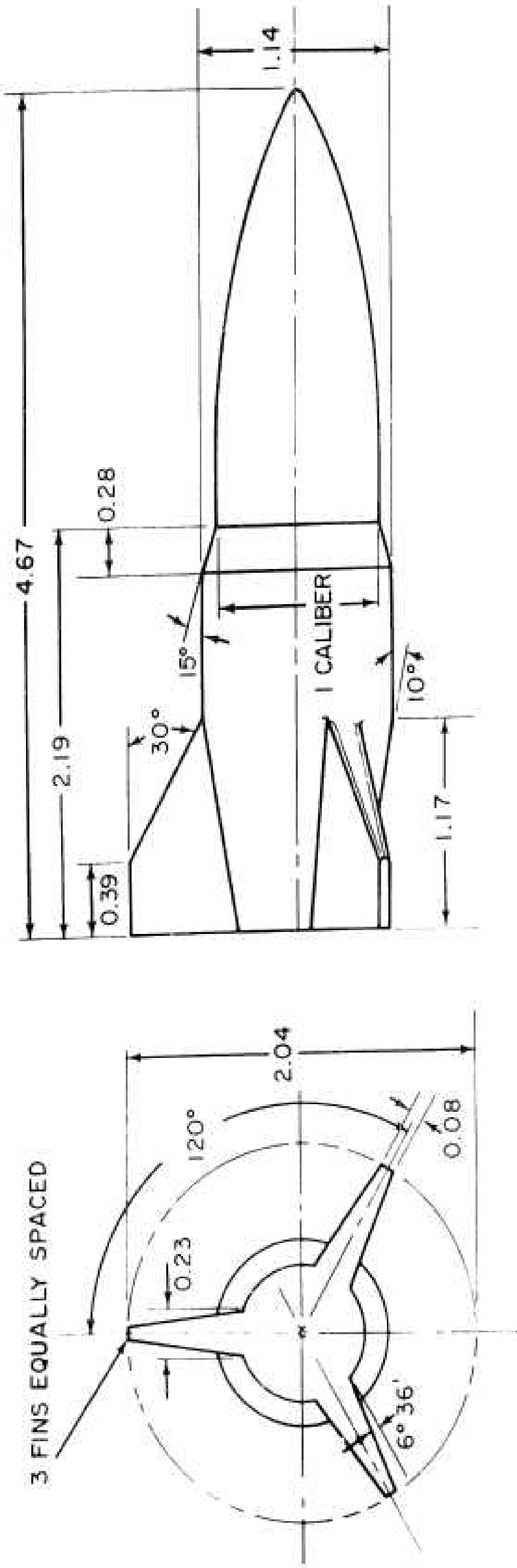

NOTE:

1. DIMENSIONS GIVEN IN CALIBERS
2. 1 CALIBER = 0.428 IN.
3. C.G. LOCATED 2.18 CALIBERS FROM MODEL BASE

FIG.8 LAZY DOG CONFIGURATION 6

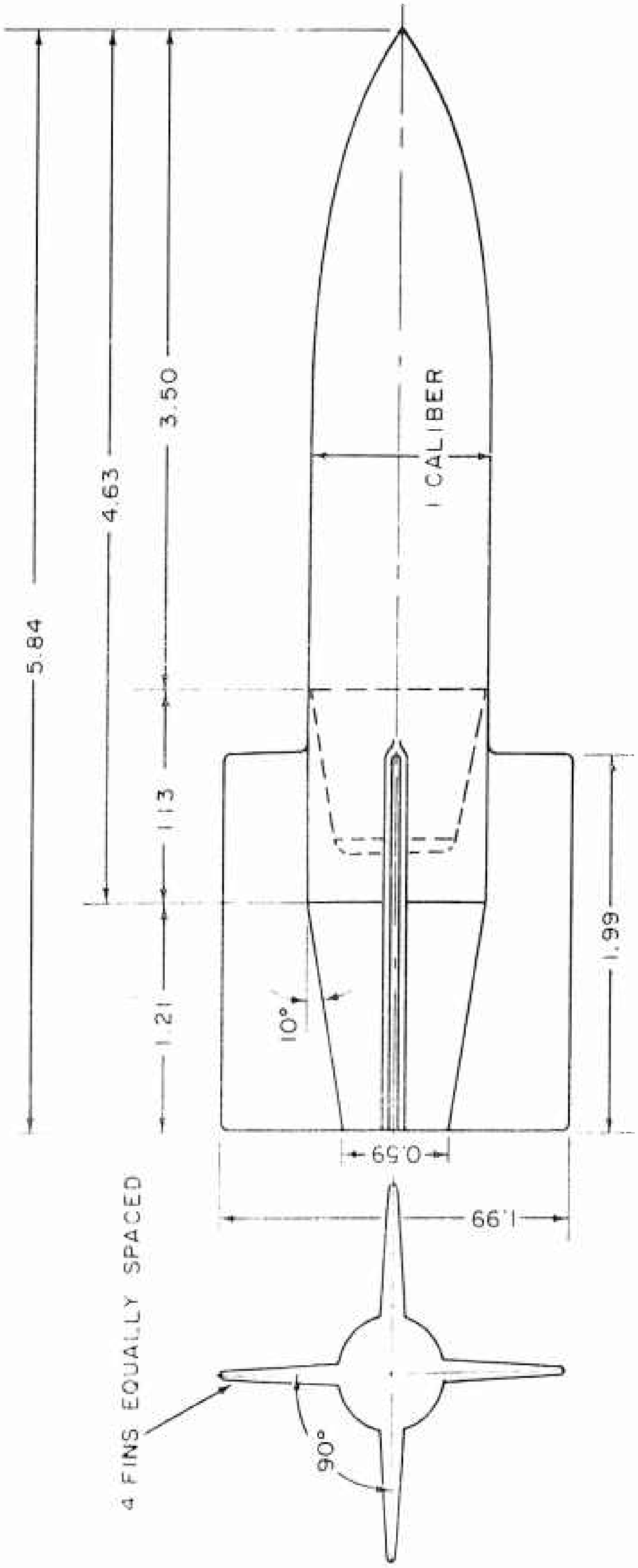

1. DIMENSIONS GIVEN IN CALIBERS
2. 1 CALIBER = 0.428 INCHES
3. C.G. LOCATED AT 3.04 CALIBERS FROM MODEL BASE

FIG. 9 LAZY DOG CONFIGURATION 7

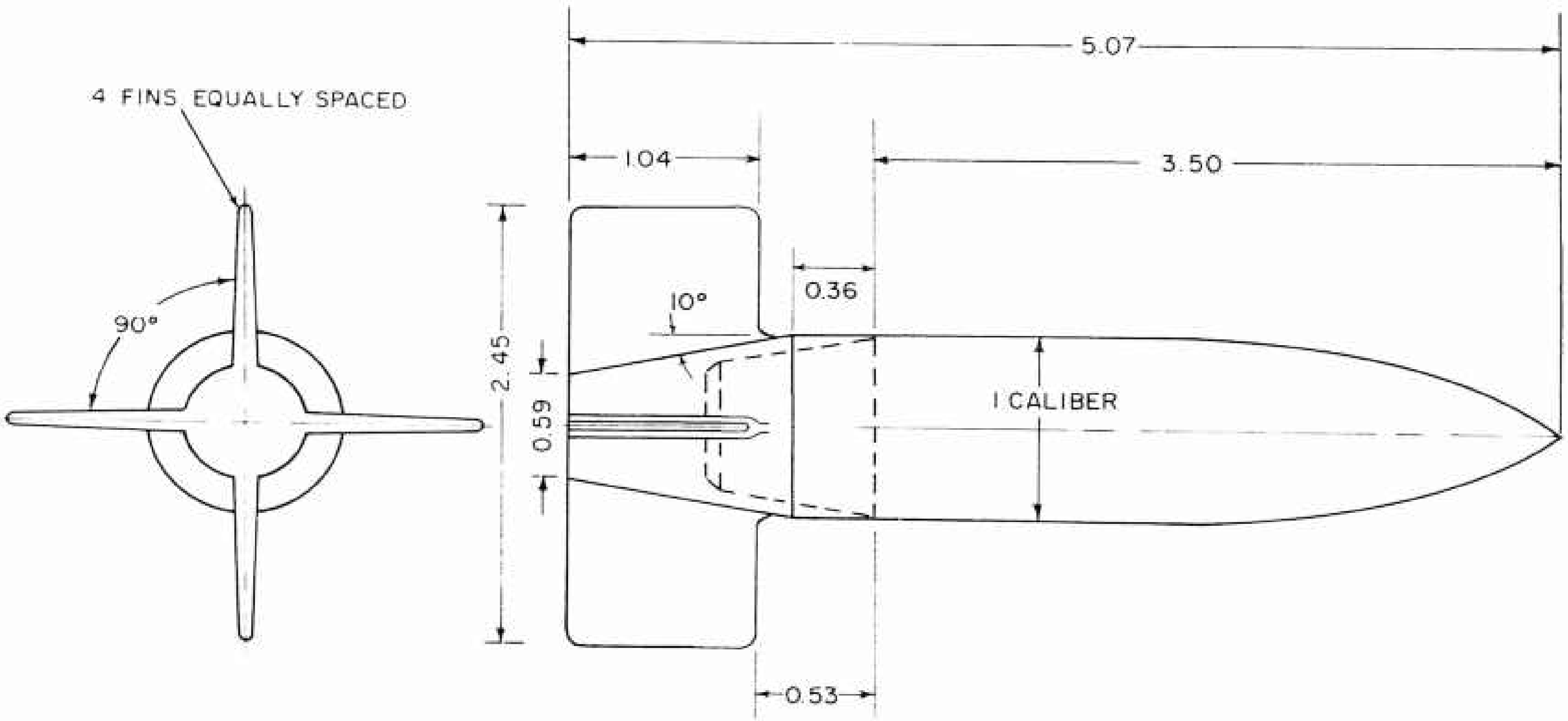

NOTE:
1. DIMENSIONS GIVEN IN CALIBERS
2. 1 CALIBER = 0.428 INCHES
3. C.G. LOCATED 2.27 CALIBERS FROM MODEL BASE

FIG. 10 LAZY DOG CONFIGURATION 8

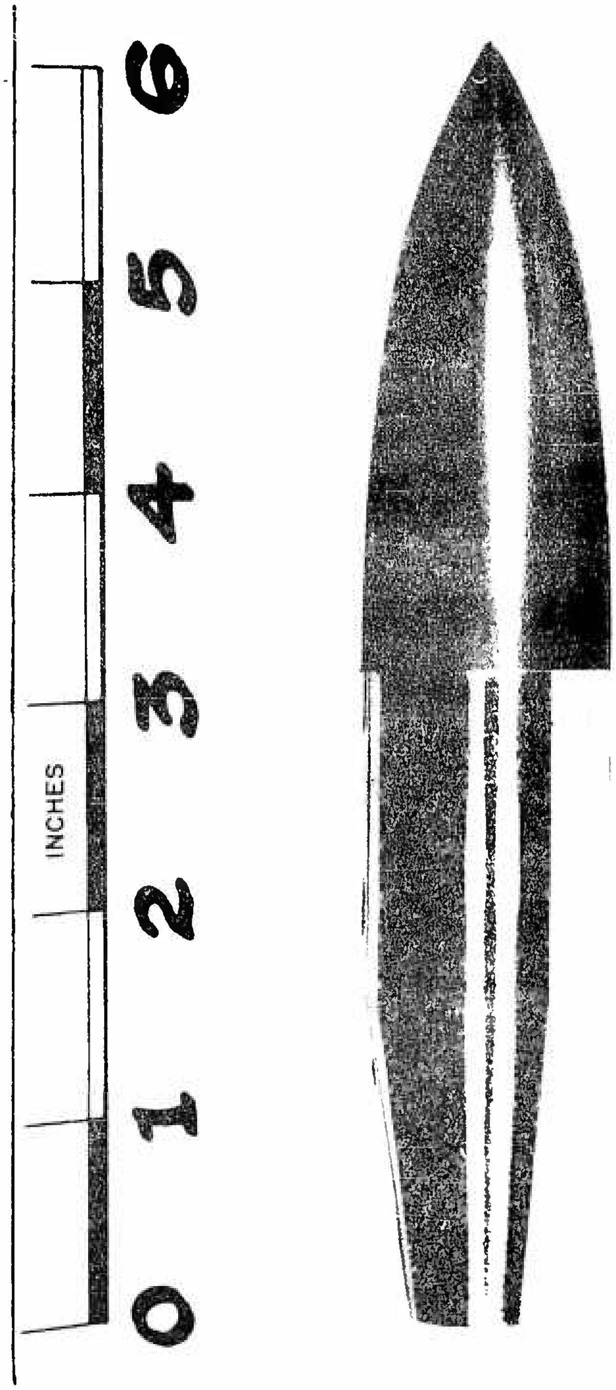

FIG. 11 A 2.92 SCALE, 50 CALIBER CORE MODEL

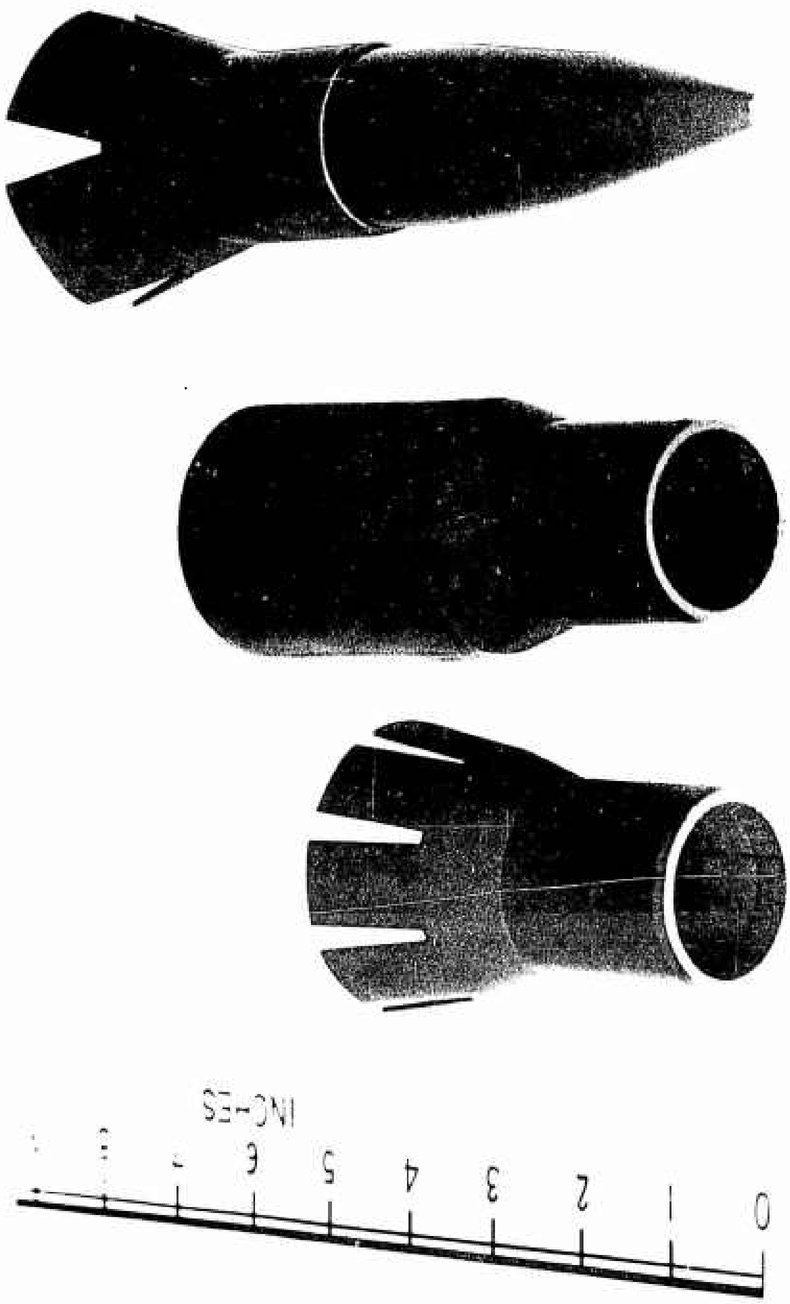

3 1 2
CONFIGURATION

FIG. 12 THE 2.50 SCALE MODELS OF CONFIGURATIONS 1,2 AND 3

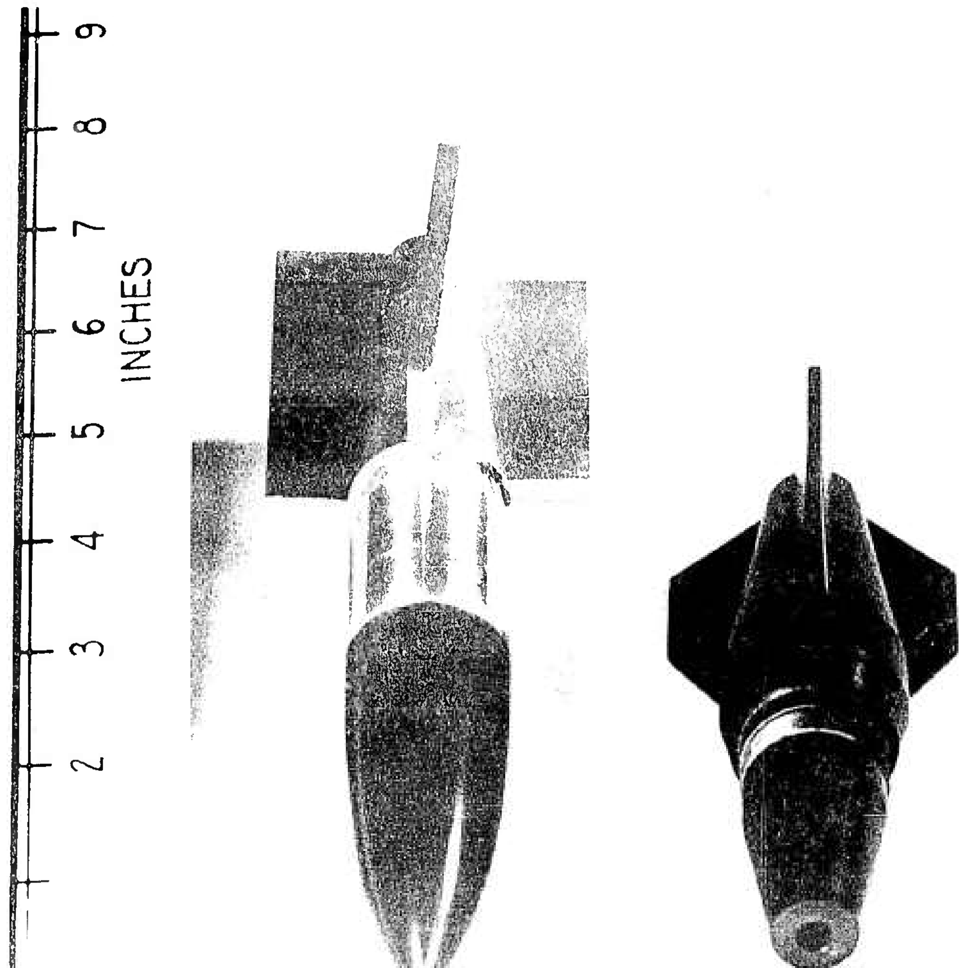

CONFIG. 5 CONFIG. 4

FIG 13 THE .292 SCALE MODELS OF CONFIGURATIONS 4 AND 5

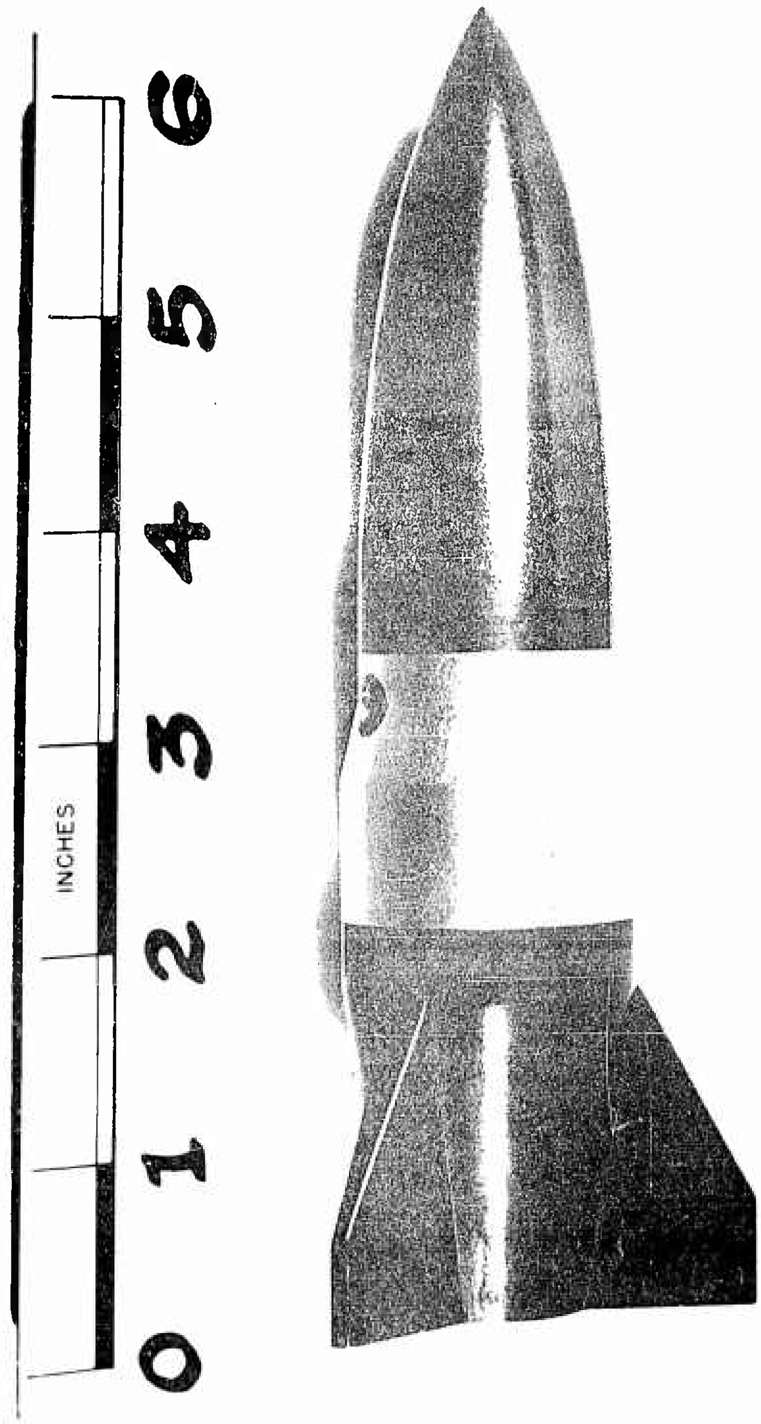

FIG. 14 A 2.92 SCALE MODEL OF CONFIGURATION 6

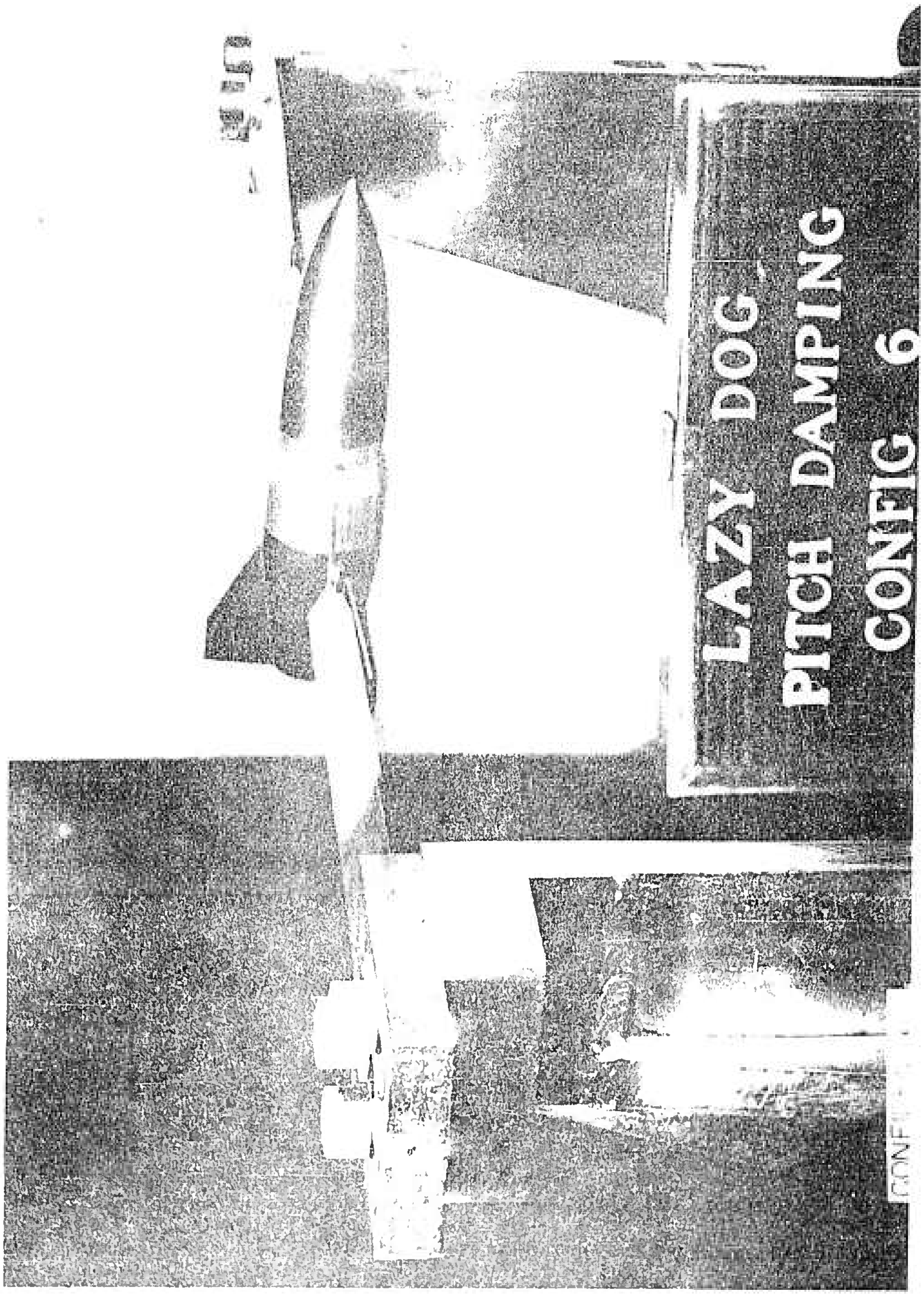

FIG 15 THE 2.92 SCALE, PITCH-DAMPING MODEL OF CONFIGURATION 6

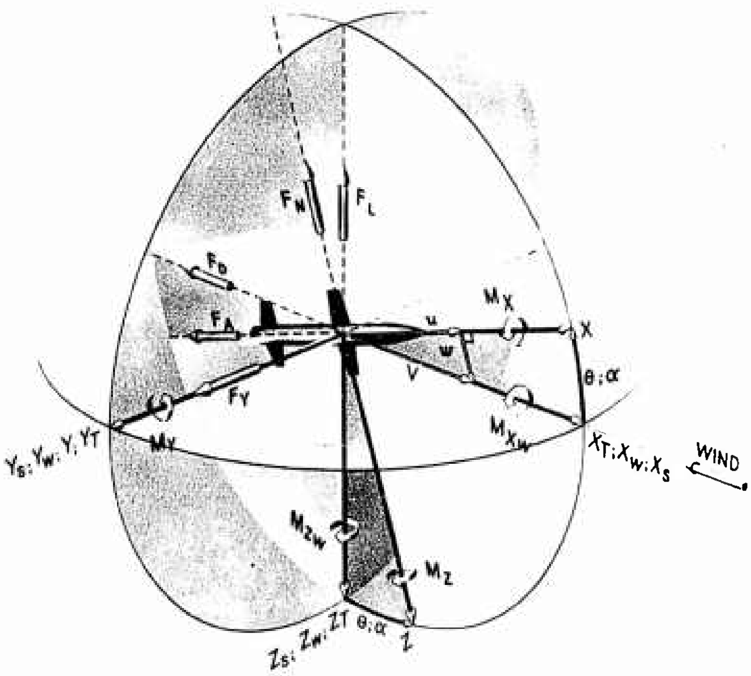

FIG. 16 AXES SYSTEMS, BODY ROTATED THROUGH AN ANGLE OF PITCH.

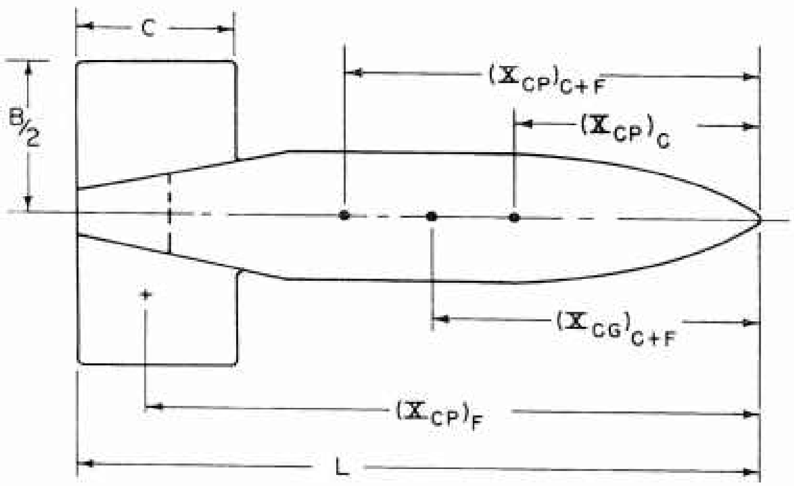

NOMENCLATURE

C = CHORD
B = SPAN
L = LENGTH
$(\ )_C$ ∽ CORE
$(\ )_F$ ∽ FIN

STATIC MARGIN = $(X_{CG})_{C+F} - (X_{CP})_{C+F}$

FIG 17 CENTER OF PRESSURE (X_{CP}) AND CENTER OF GRAVITY (X_{CG}) LOCATIONS FOR THE 50 CALIBER BULLET CORE WITH RECTANGULAR FINS.

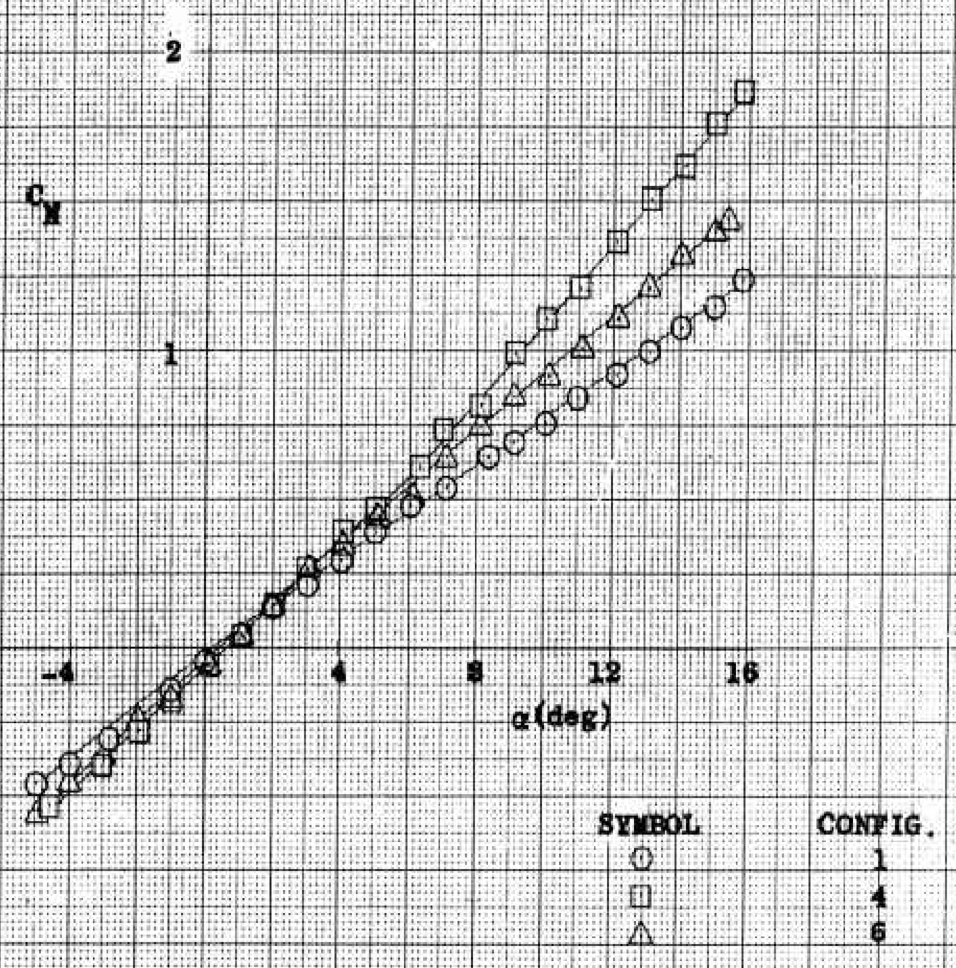

FIG. 18 NORMAL FORCE COEFFICIENT, C_N, AS A FUNCTION OF ANGLE OF ATTACK, α, FOR CONFIGURATIONS 1, 4 AND 6 AT A FREE-STREAM MACH NUMBER OF 0.49

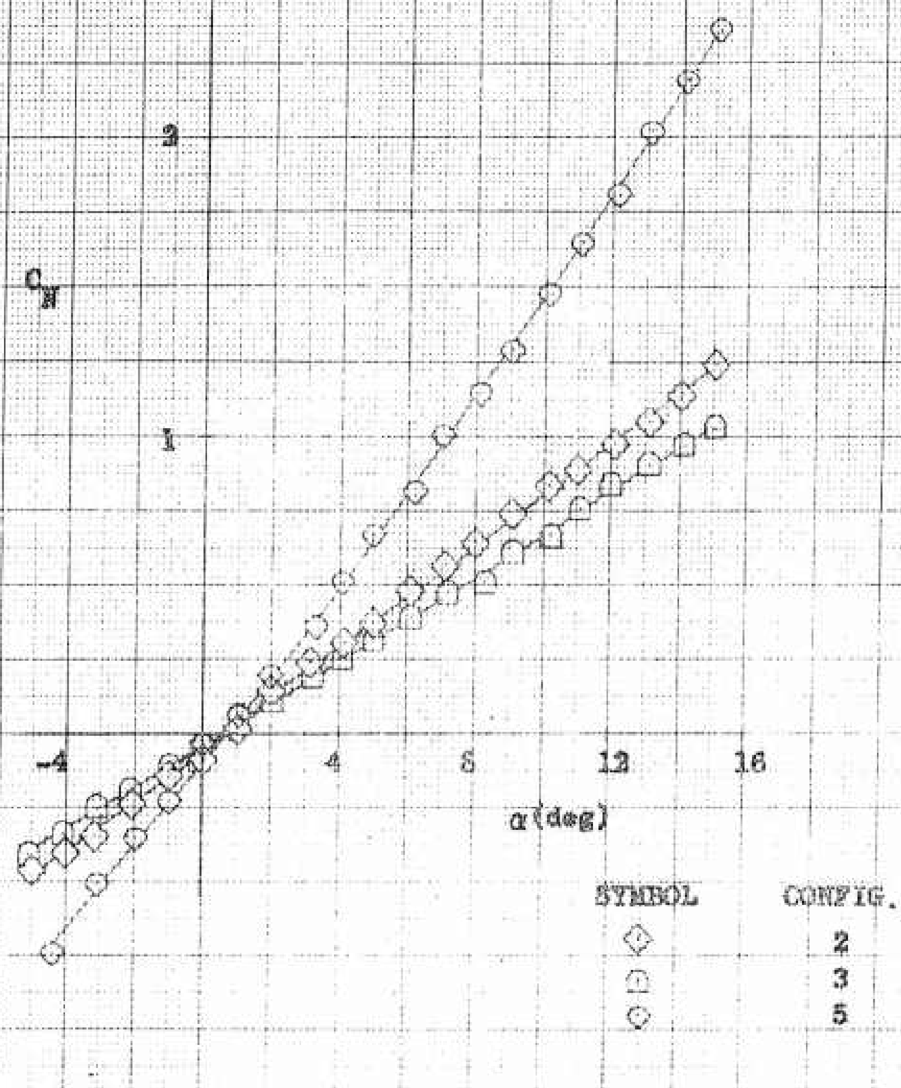

FIG. 19 NORMAL FORCE COEFFICIENT, C_N, AS A FUNCTION OF ANGLE OF ATTACK, α, FOR CONFIGURATIONS 2, 3 AND 5 AT A FREE-STREAM MACH NUMBER OF 0.49

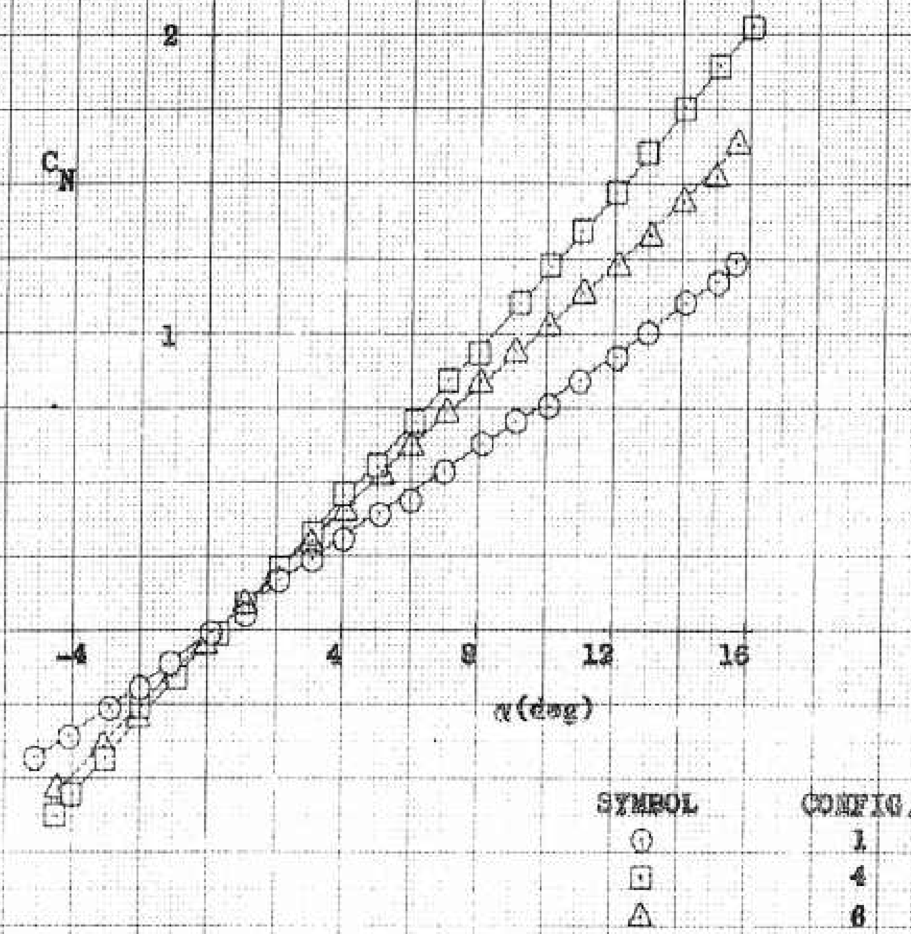

FIG. 20 NORMAL FORCE COEFFICIENT, C_N, AS A FUNCTION OF ANGLE OF ATTACK, α, FOR CONFIGURATIONS 1, 4 AND 6 AT A FREE-STREAM MACH NUMBER OF 0.80

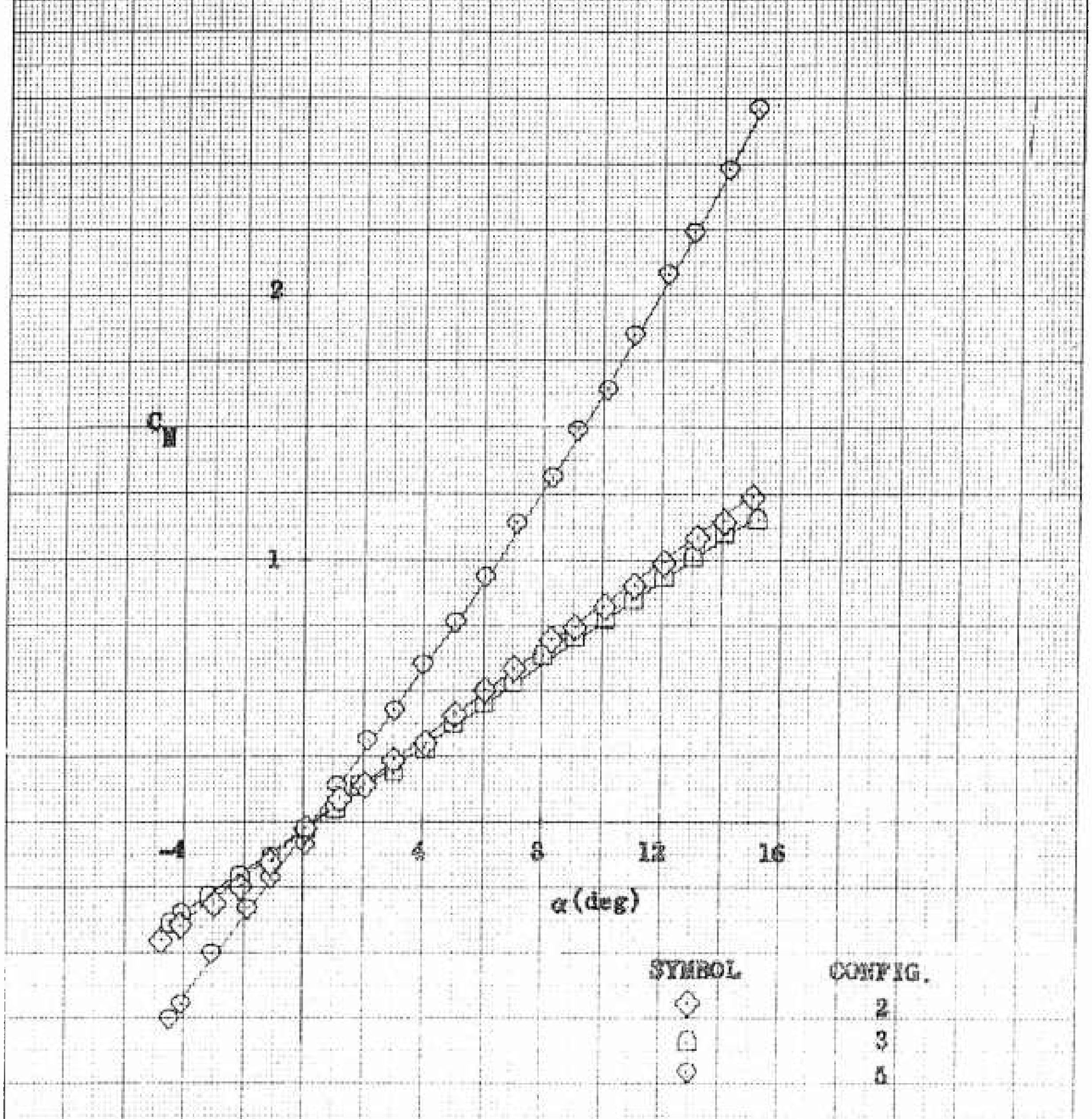

FIG. 21 NORMAL FORCE COEFFICIENT, C_N, AS A FUNCTION OF ANGLE OF ATTACK, α, FOR CONFIGURATIONS 2, 3 AND 5 AT A FREE-STREAM MACH NUMBER OF 0.80

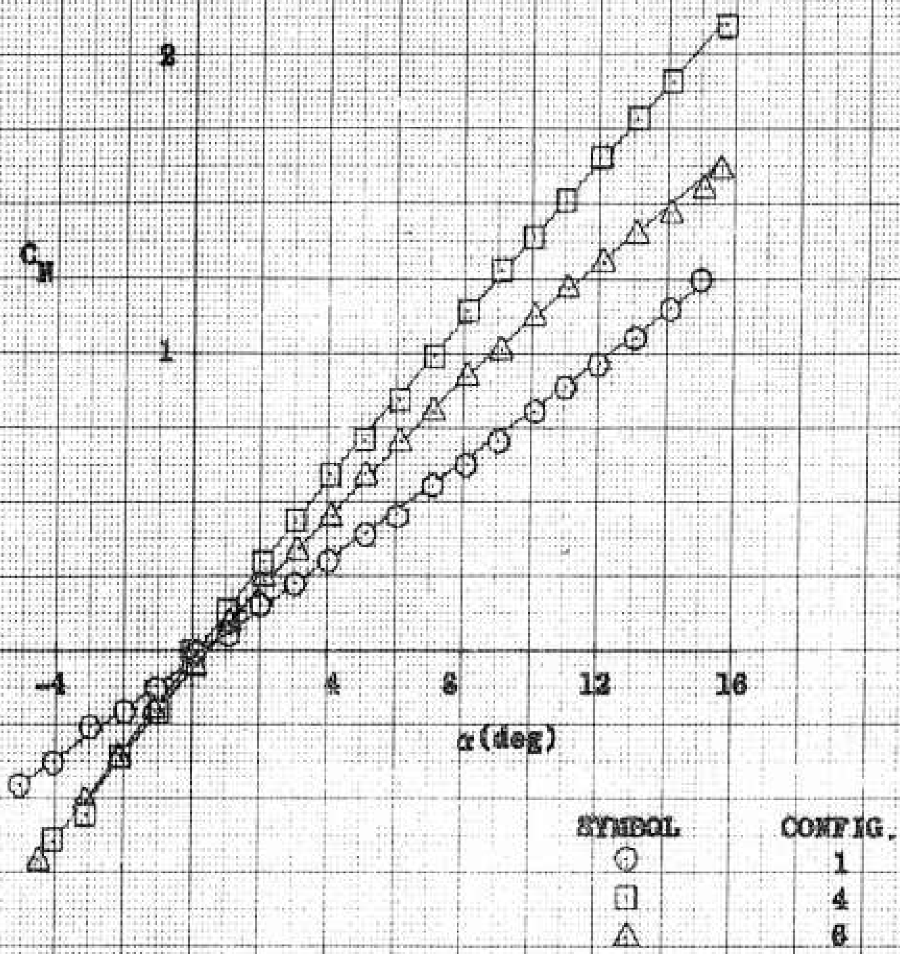

FIG. 22 NORMAL FORCE COEFFICIENT, C_N, AS A FUNCTION OF ANGLE OF ATTACK, α, FOR CONFIGURATIONS 1, 4 AND 6 AT A FREE-STREAM MACH NUMBER OF 0.94

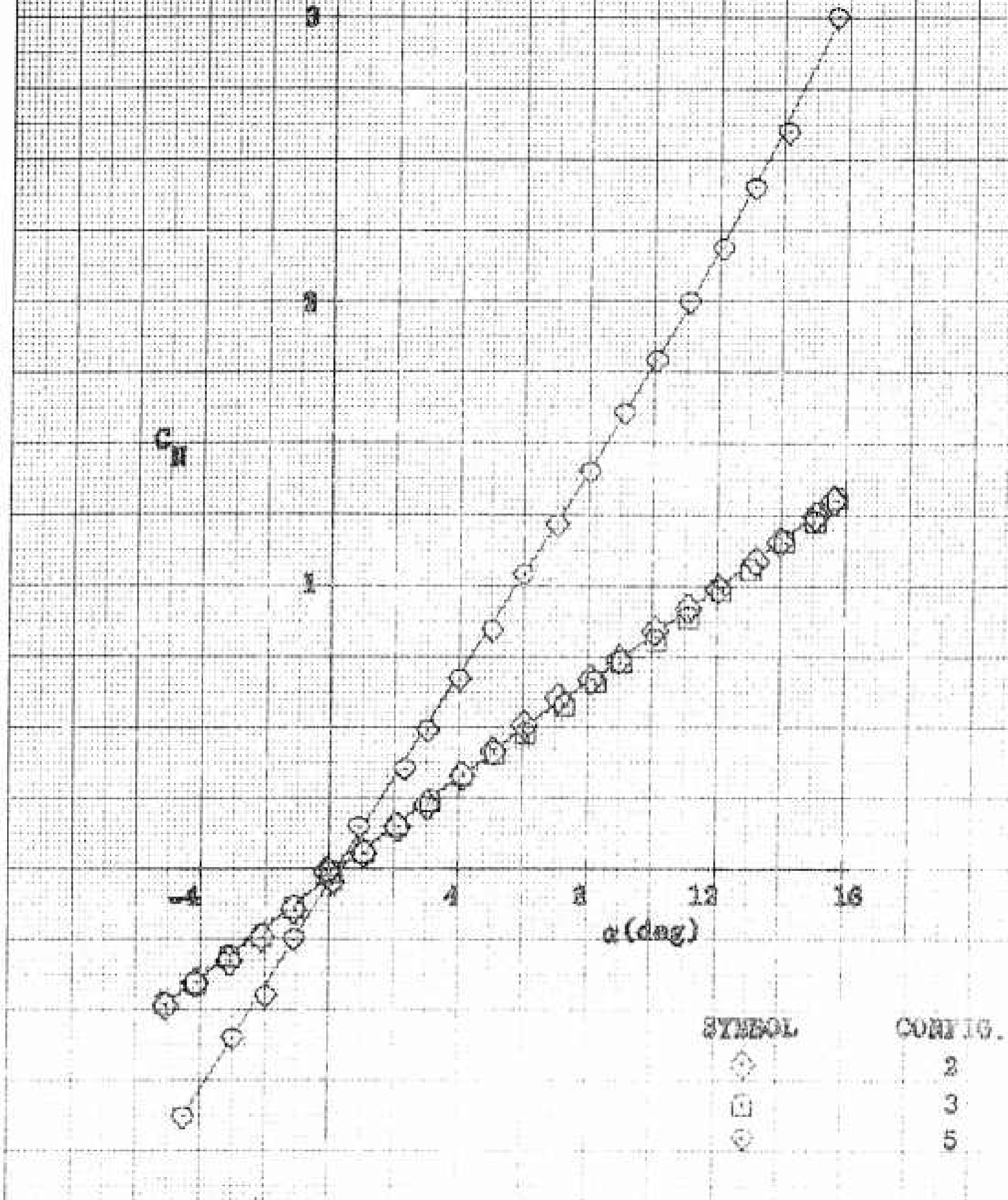

FIG. 23 NORMAL FORCE COEFFICIENT, C_N, AS A FUNCTION OF ANGLE OF ATTACK, α, FOR CONFIGURATIONS 2, 3 AND 5 AT A FREE-STREAM MACH NUMBER OF 0.94

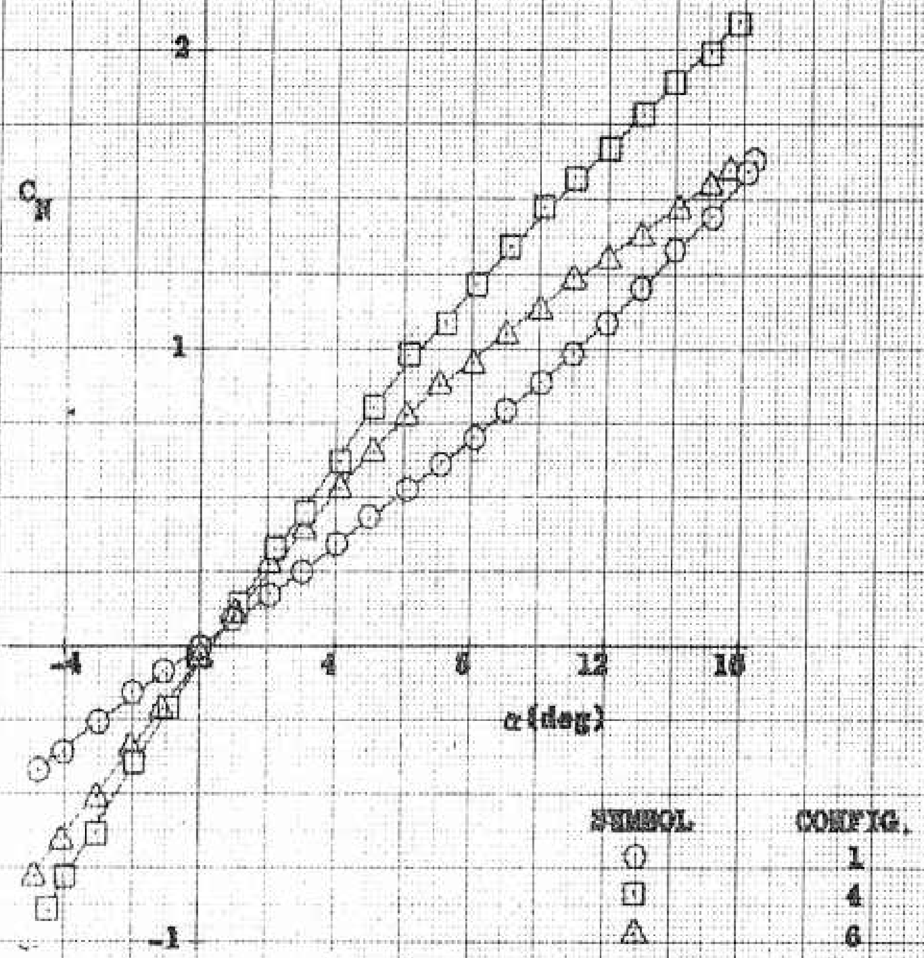

FIG. 24 NORMAL FORCE COEFFICIENT, C_N, AS A FUNCTION OF ANGLE OF ATTACK, α, FOR CONFIGURATIONS 1, 4 AND 6 AT A FREE-STREAM MACH NUMBER OF 1.05

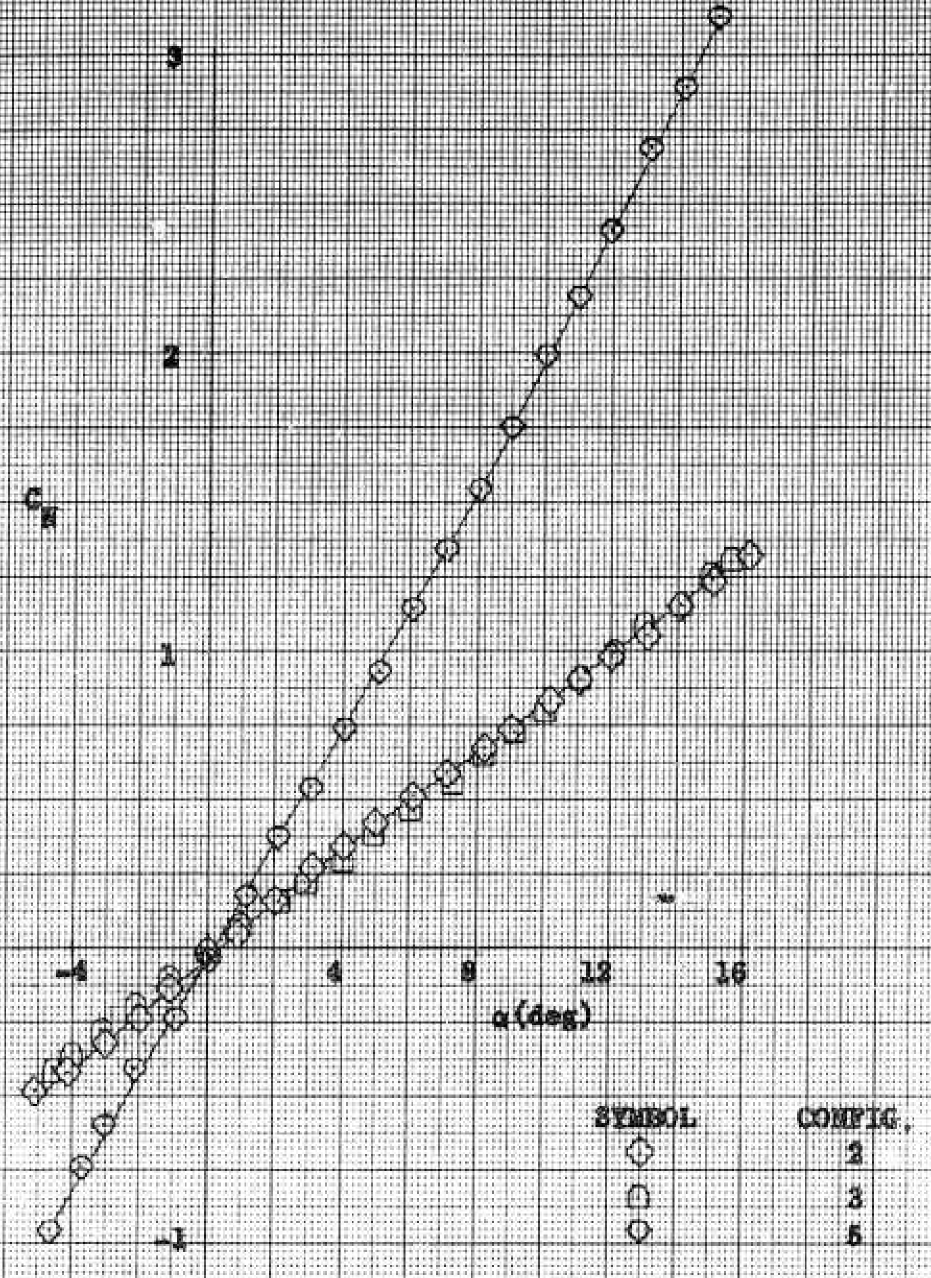

FIG. 25 NORMAL FORCE COEFFICIENT, C_N, AS A FUNCTION OF ANGLE OF ATTACK, α, FOR CONFIGURATIONS 2, 3 AND 5 AT A FREE-STREAM MACH NUMBER OF 1.05

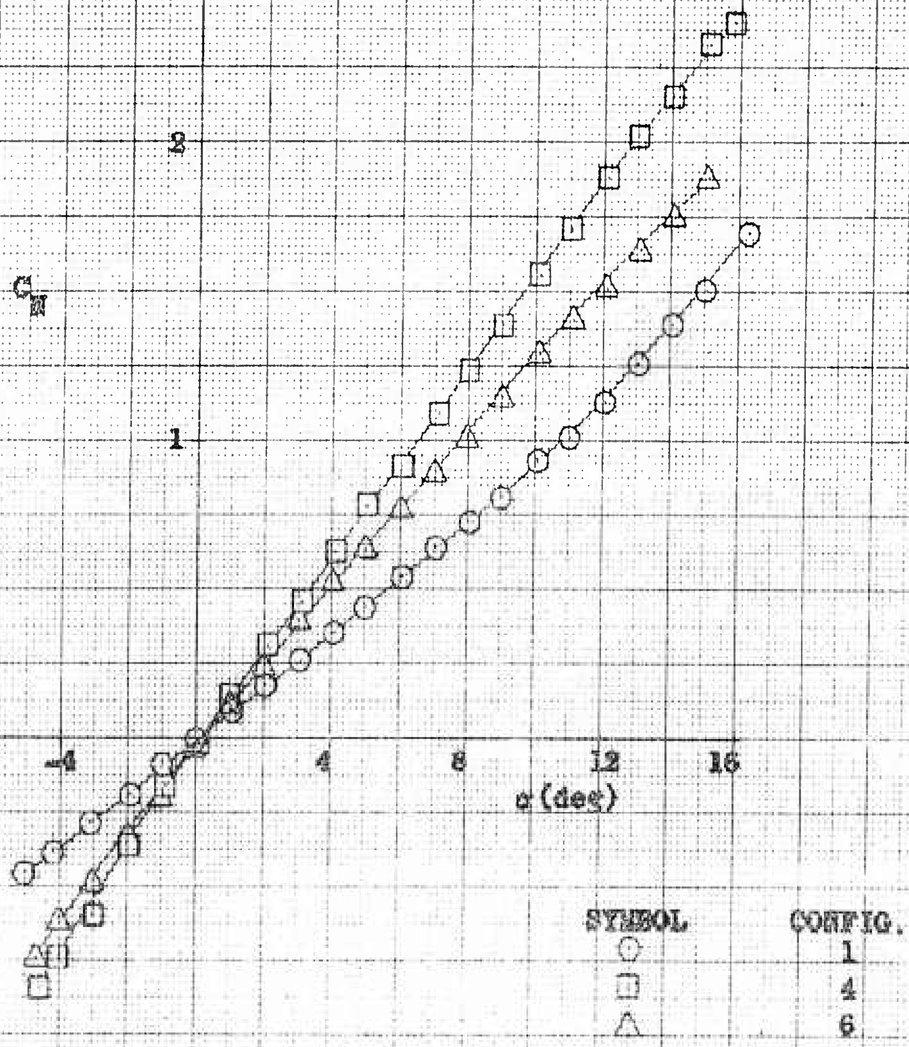

FIG. 25 NORMAL FORCE COEFFICIENT, C_N, AS A FUNCTION OF ANGLE OF ATTACK, α, FOR CONFIGURATIONS 1, 4 AND 6 AT A FREE-STREAM MACH NUMBER OF 1.15

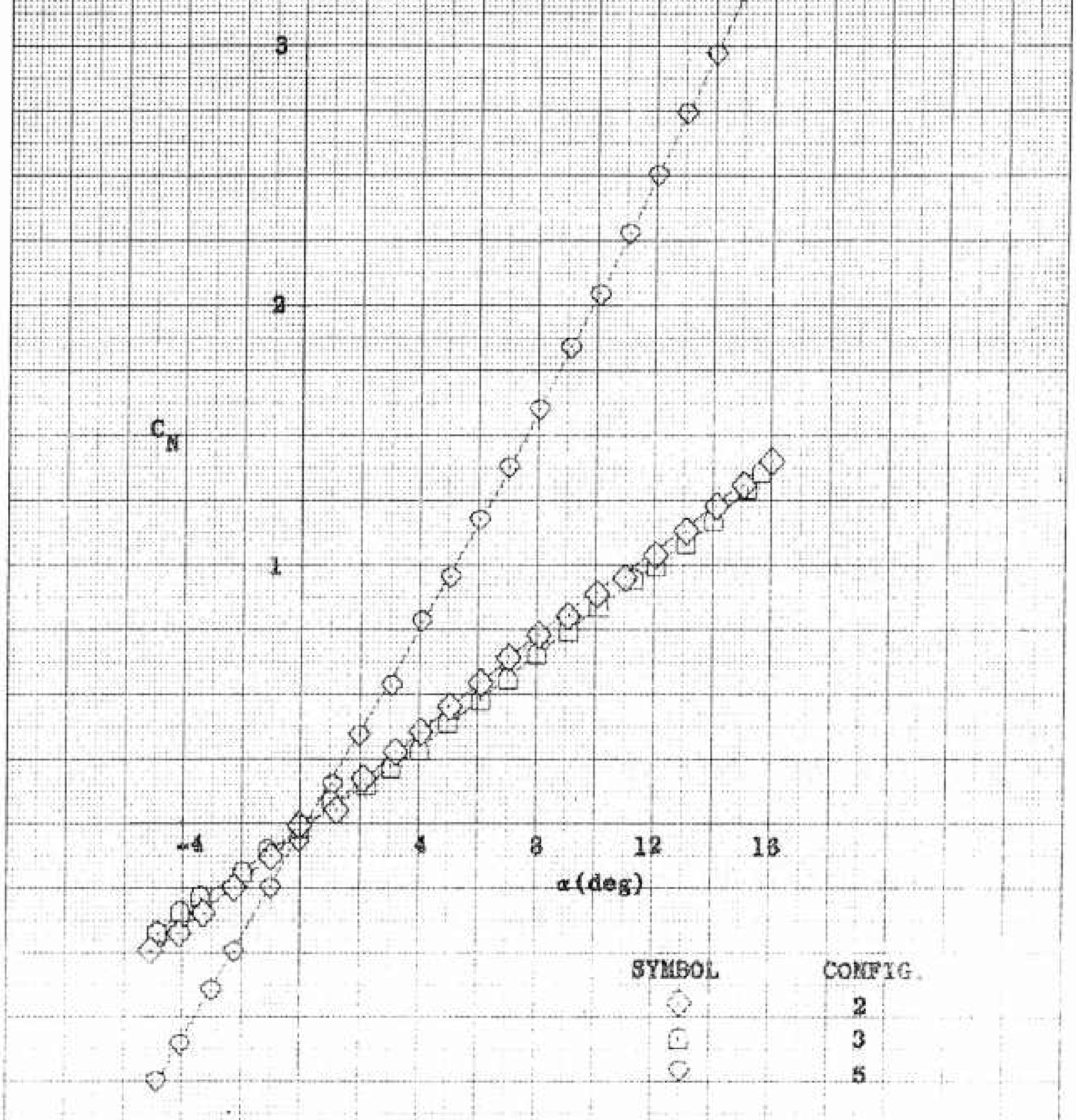

FIG. 27 NORMAL FORCE COEFFICIENT, C_N, AS A FUNCTION OF ANGLE OF ATTACK, α, FOR CONFIGURATIONS 2, 3 AND 5 AT A FREE-STREAM MACH NUMBER OF 1.15

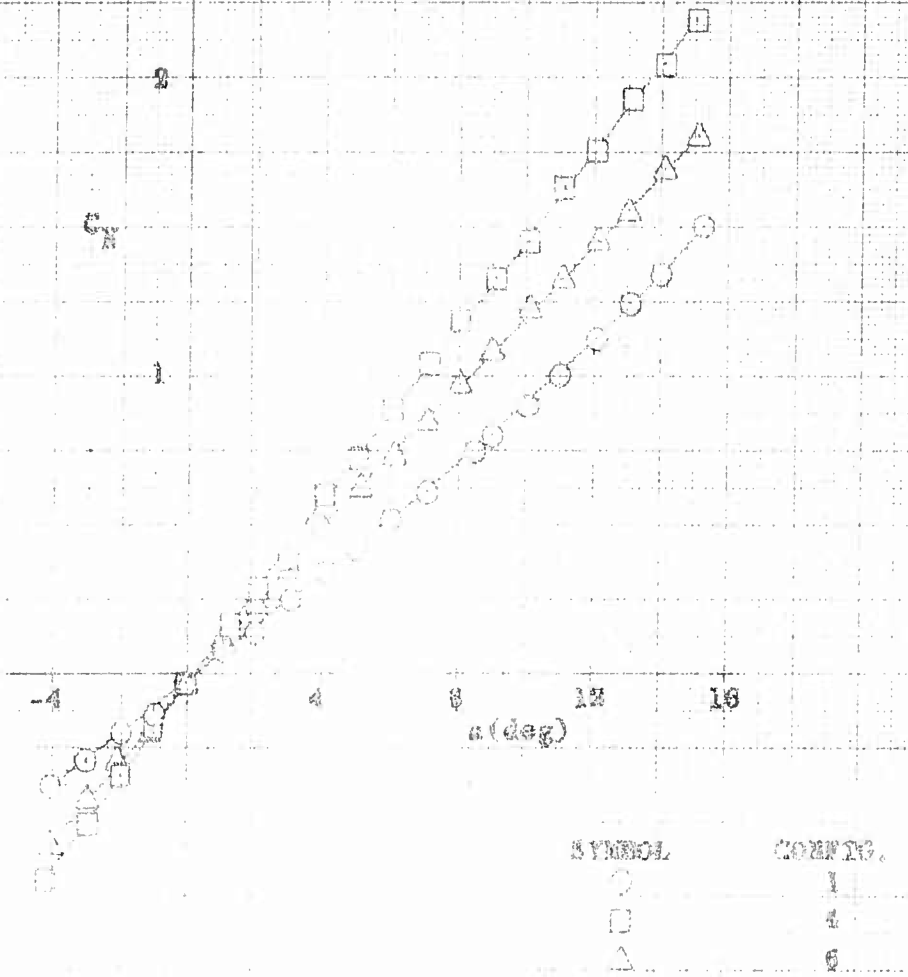

FIG. 28 NORMAL FORCE COEFFICIENT, C_N, AS A FUNCTION OF ANGLE OF ATTACK, α, FOR CONFIGURATIONS 1, 4 AND 6 AT A FREE-STREAM MACH NUMBER OF 1.26

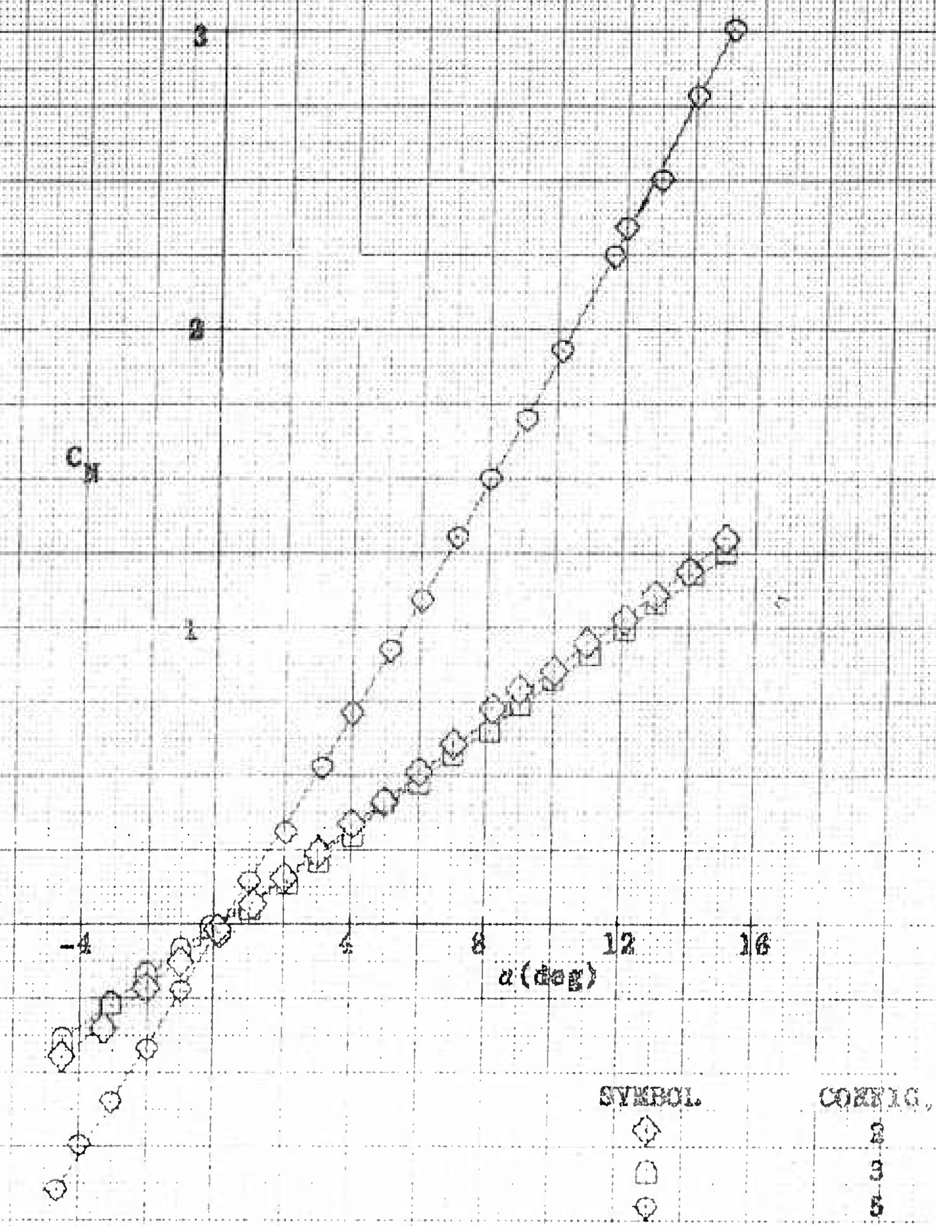

FIG. 29 NORMAL FORCE COEFFICIENT, C_N, AS A FUNCTION OF ANGLE OF ATTACK, α, FOR CONFIGURATIONS 2, 3 AND 5 AT A FREE-STREAM MACH NUMBER OF 1.26

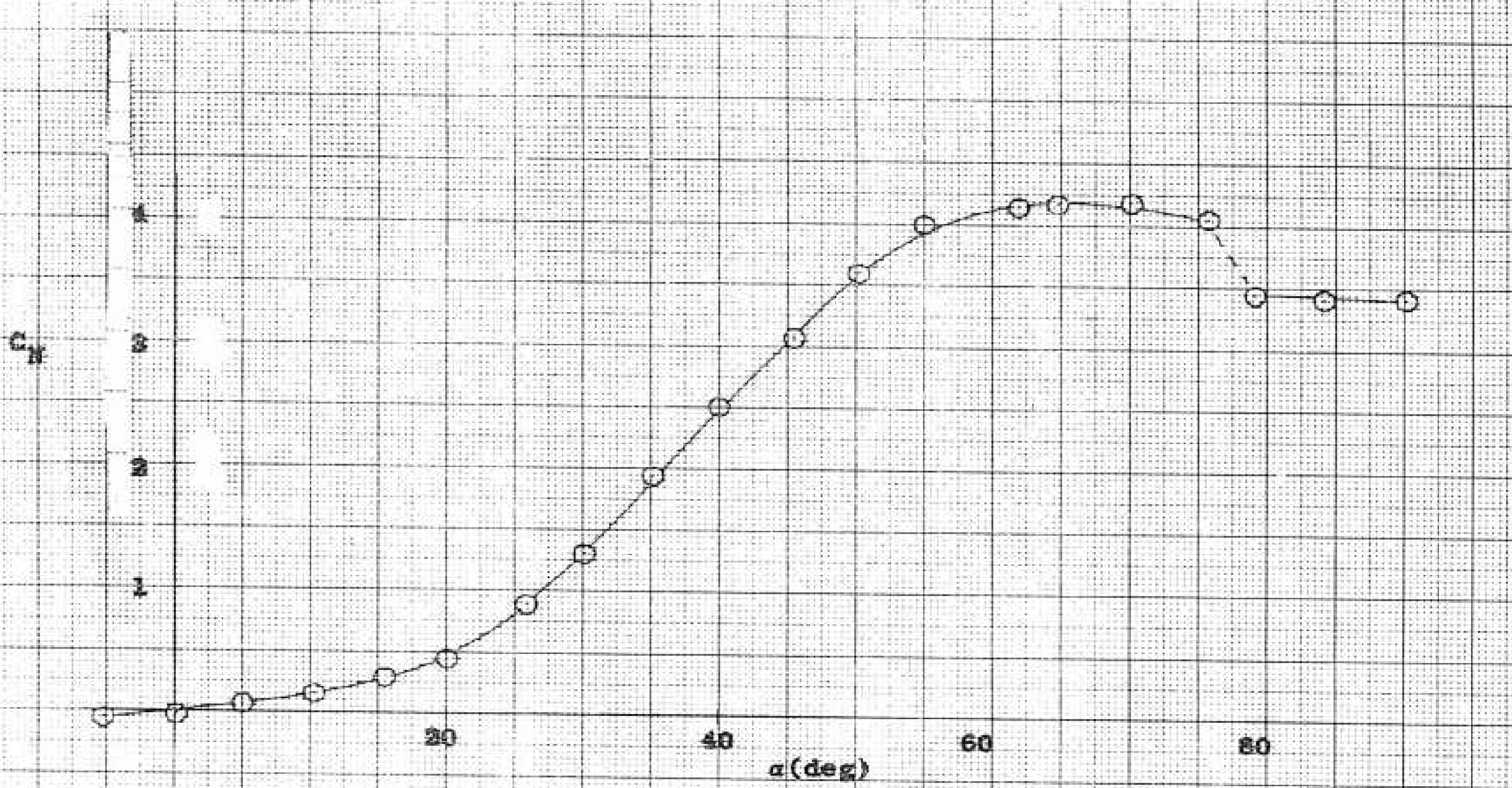

FIG. 30 NORMAL FORCE COEFFICIENT, C_N, AS A FUNCTION OF ANGLE OF ATTACK, α, FOR THE 50 CALIBER BULLET CORE AT A FREE-STREAM MACH NUMBER OF 0.30

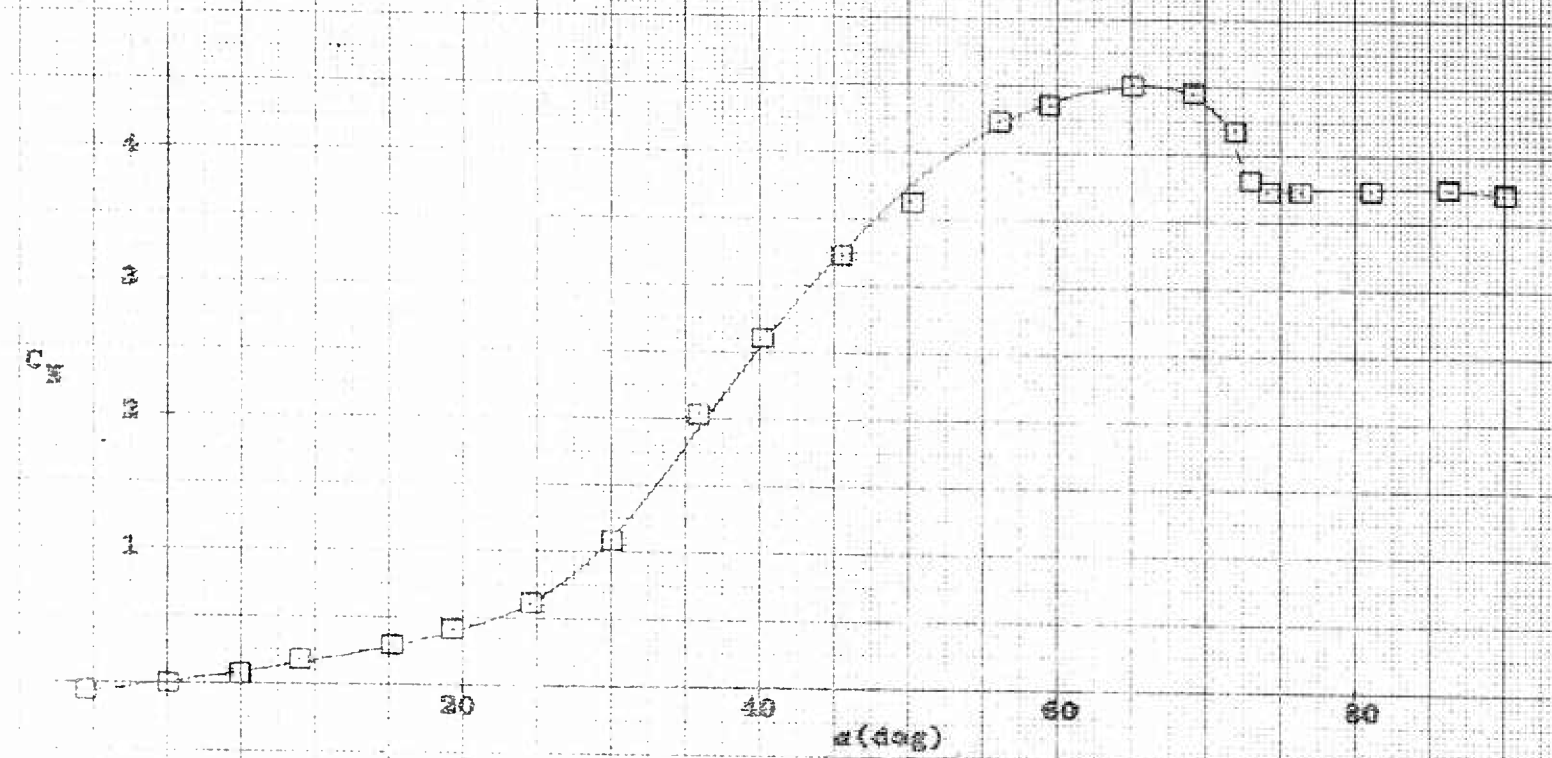

FIG. 31 NORMAL FORCE COEFFICIENT, C_N, AS A FUNCTION OF ANGLE OF ATTACK, α, FOR THE [illegible] CALIBER BULLET CORE AT A FREE-STREAM MACH NUMBER OF [illegible].50

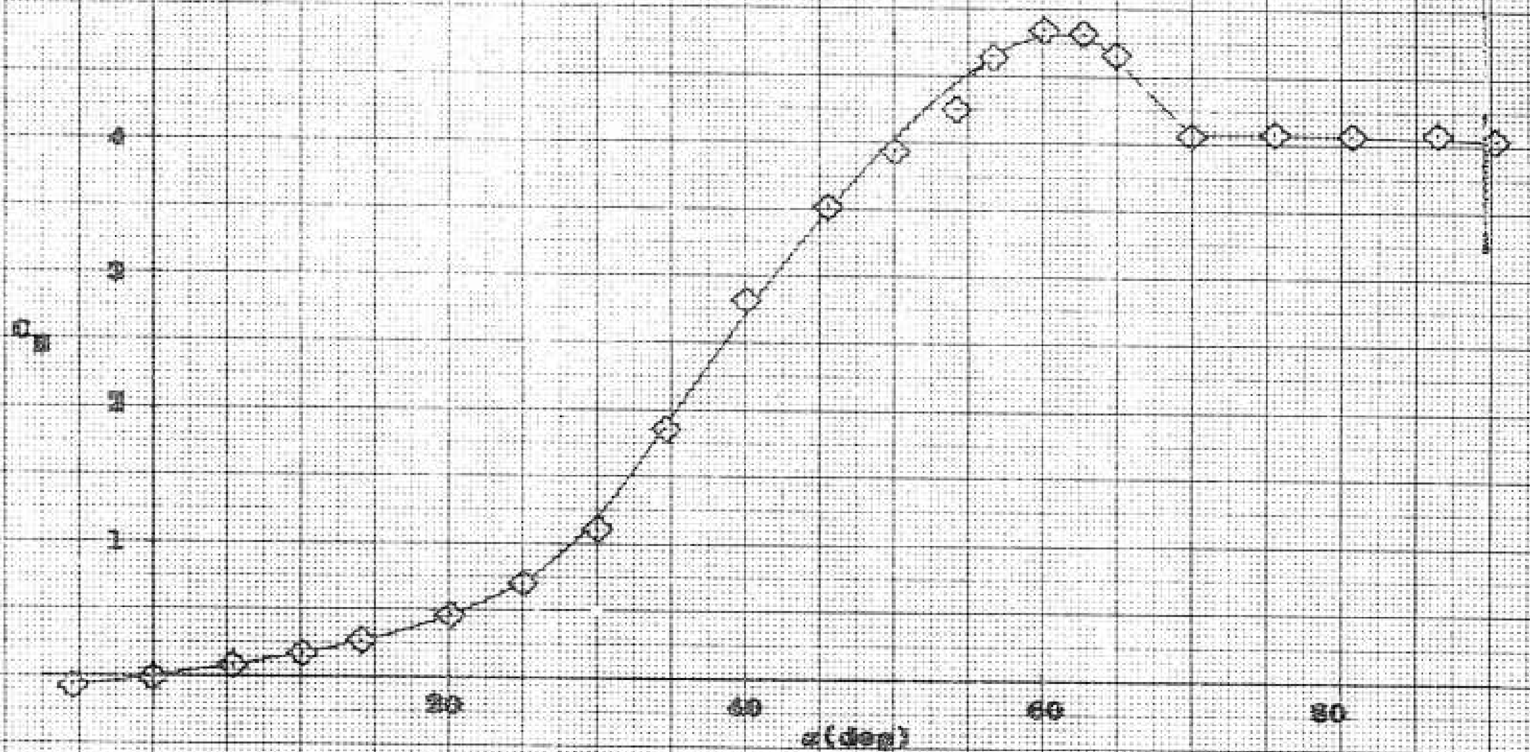

FIG. 32 NORMAL FORCE COEFFICIENT, C_N, AS A FUNCTION OF ANGLE OF ATTACK, α, FOR THE 30 CALIBER BULLET CORE AT A FREE-STREAM MACH NUMBER OF 0.70

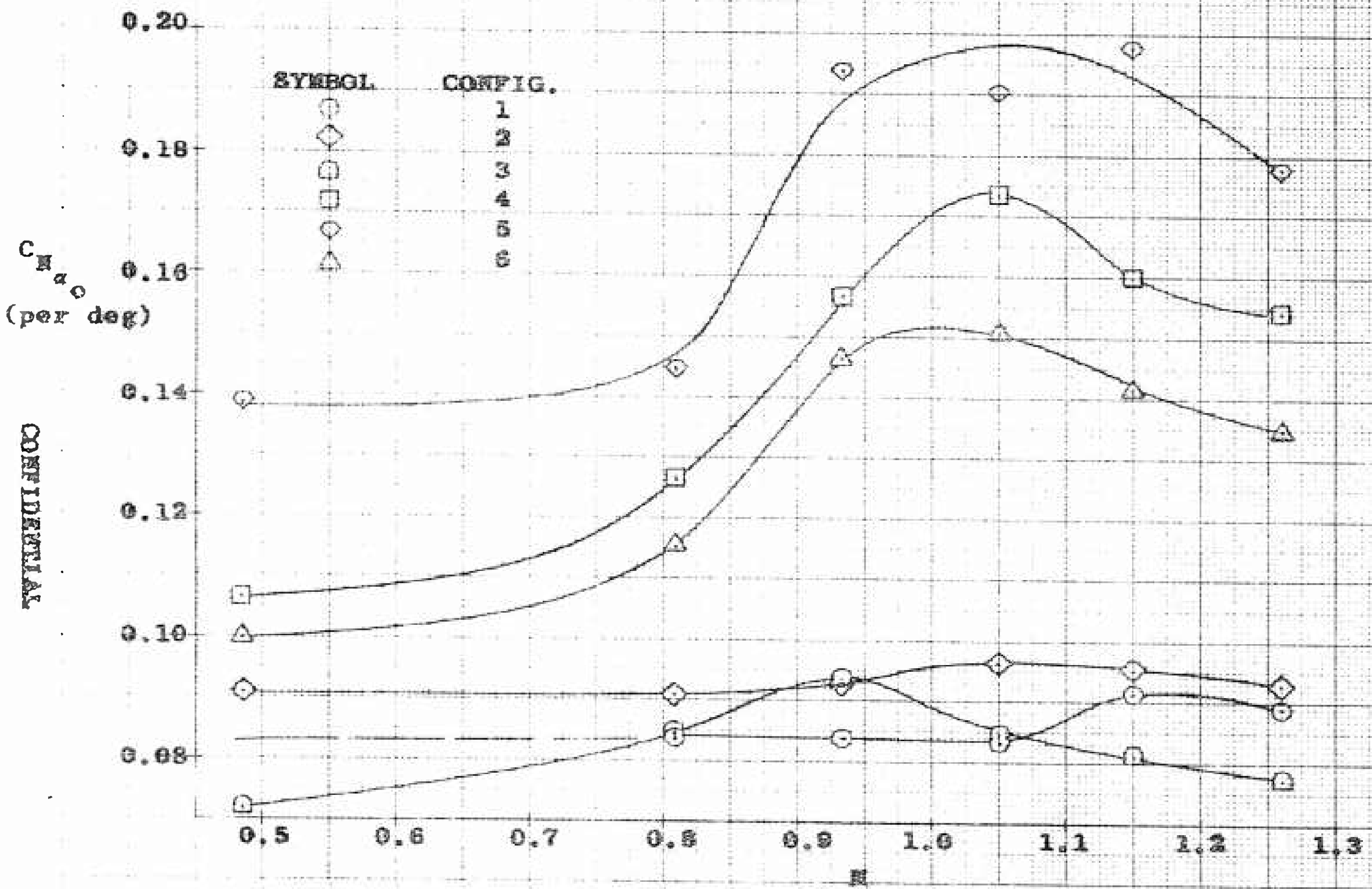

FIG. 33 SLOPE OF THE NORMAL FORCE COEFFICIENT-ANGLE OF ATTACK CURVE, MEASURED AT ZERO ANGLE OF ATTACK, $C_{N_{\alpha_0}}$, AS A FUNCTION OF FREE-STREAM MACH NUMBER FOR CONFIGURATIONS 1 THROUGH 6.

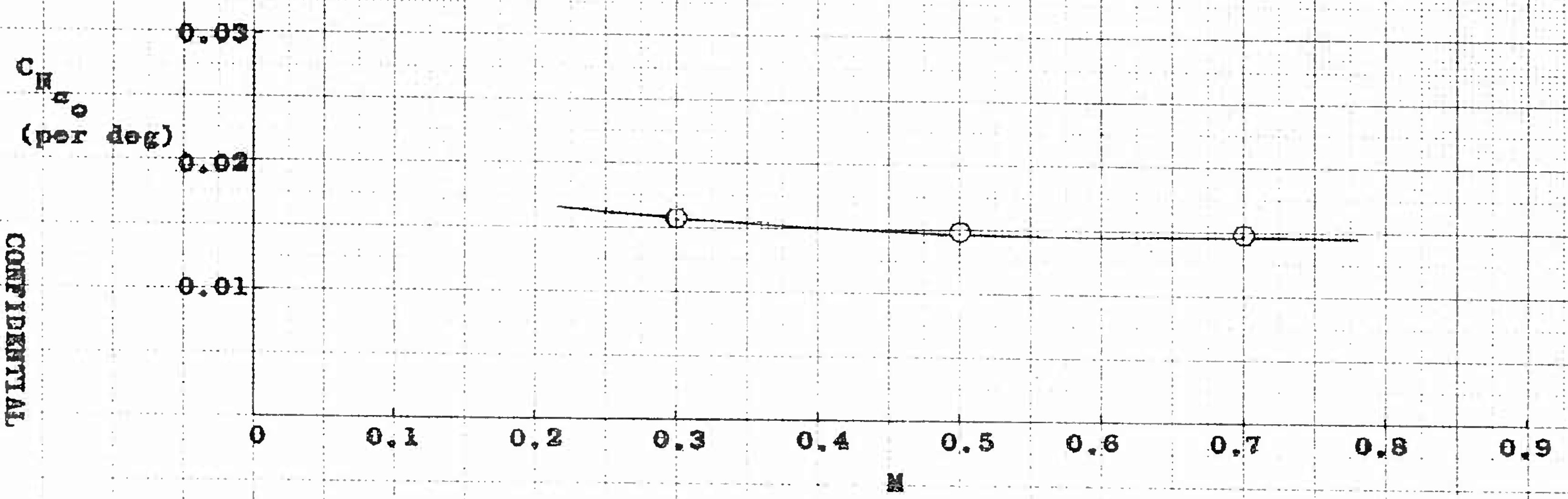

FIG. 34 SLOPE OF THE NORMAL FORCE COEFFICIENT-ANGLE OF ATTACK CURVE, MEASURED AT ZERO ANGLE OF ATTACK, $C_{N_{\alpha_o}}$, AS A FUNCTION OF FREE-STREAM MACH NUMBER FOR THE 50 CALIBER BULLET CORE.

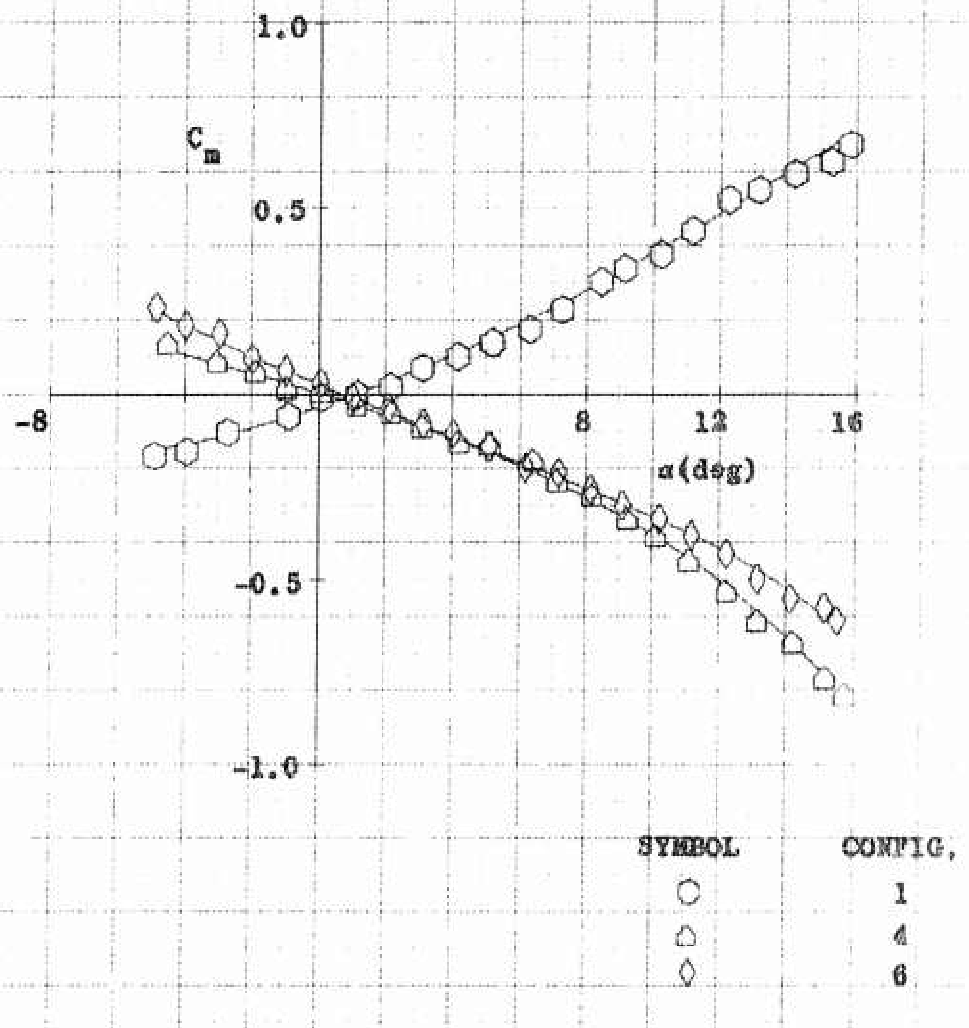

FIG. 35 PITCHING MOMENT COEFFICIENT, C_m, AS A FUNCTION OF ANGLE OF ATTACK, α, FOR CONFIGURATIONS 1, 4 AND 6 AT A FREE-STREAM MACH NUMBER OF 0.49

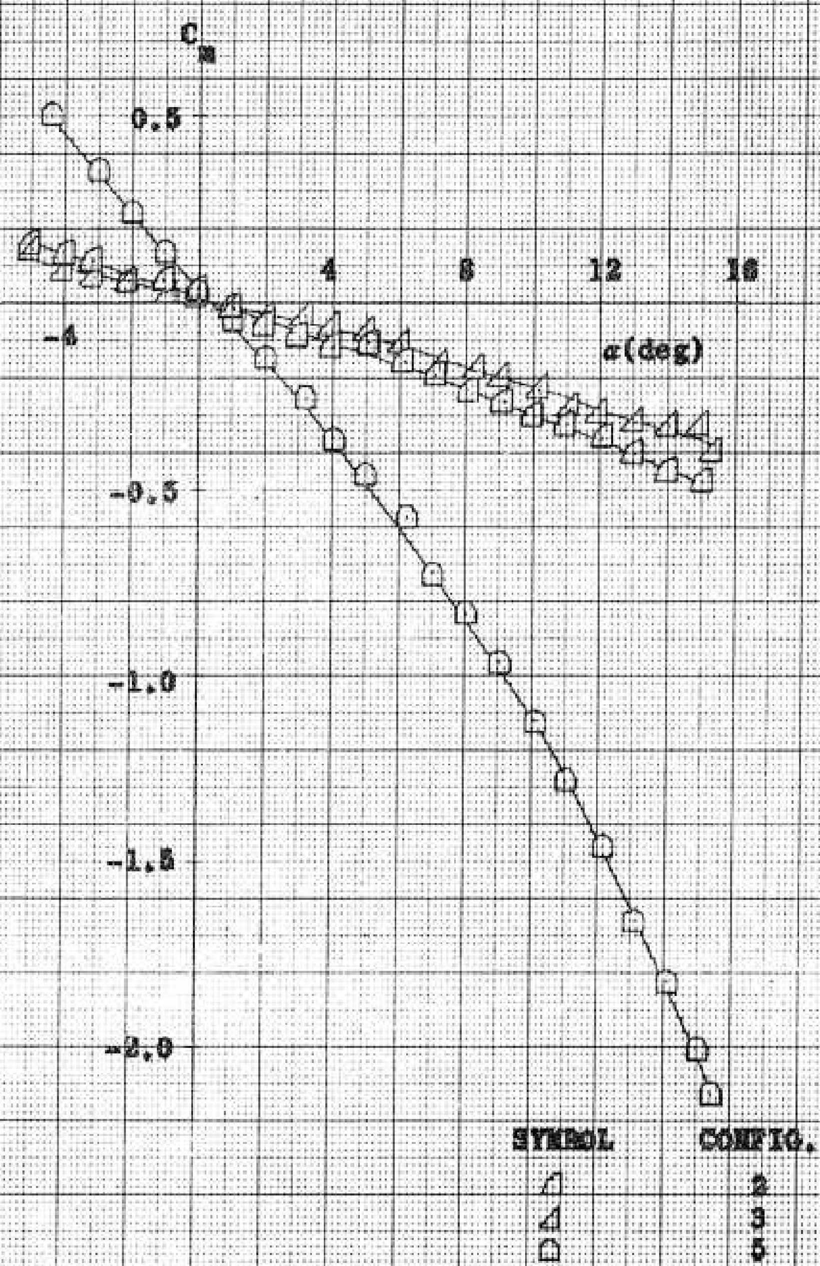

FIG. 36 PITCHING MOMENT COEFFICIENT, C_m, AS A FUNCTION OF ANGLE OF ATTACK, α, FOR CONFIGURATIONS 2, 3 AND 5 AT A FREE-STREAM MACH NUMBER OF 0.49

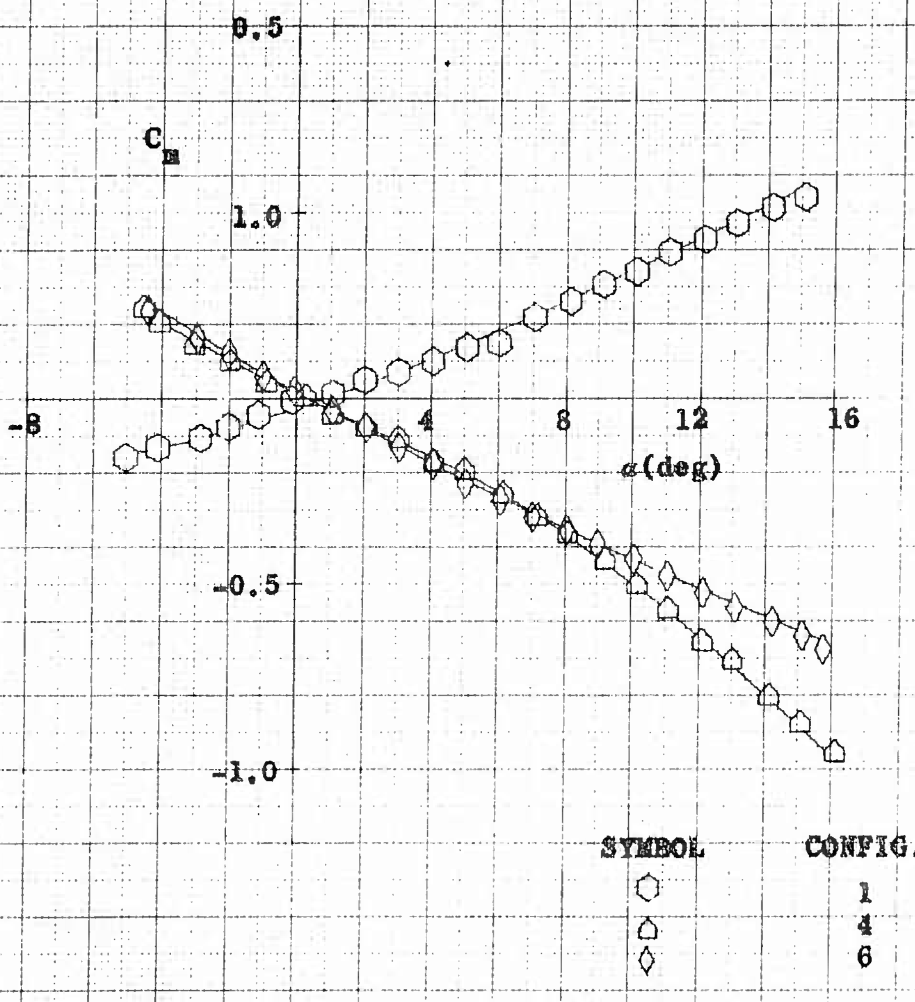

FIG. 37 PITCHING MOMENT COEFFICIENT, C_m, AS A FUNCTION OF ANGLE OF ATTACK, α, FOR CONFIGURATIONS 1, 4 AND 6 AT A FREE-STREAM MACH NUMBER OF 0.80

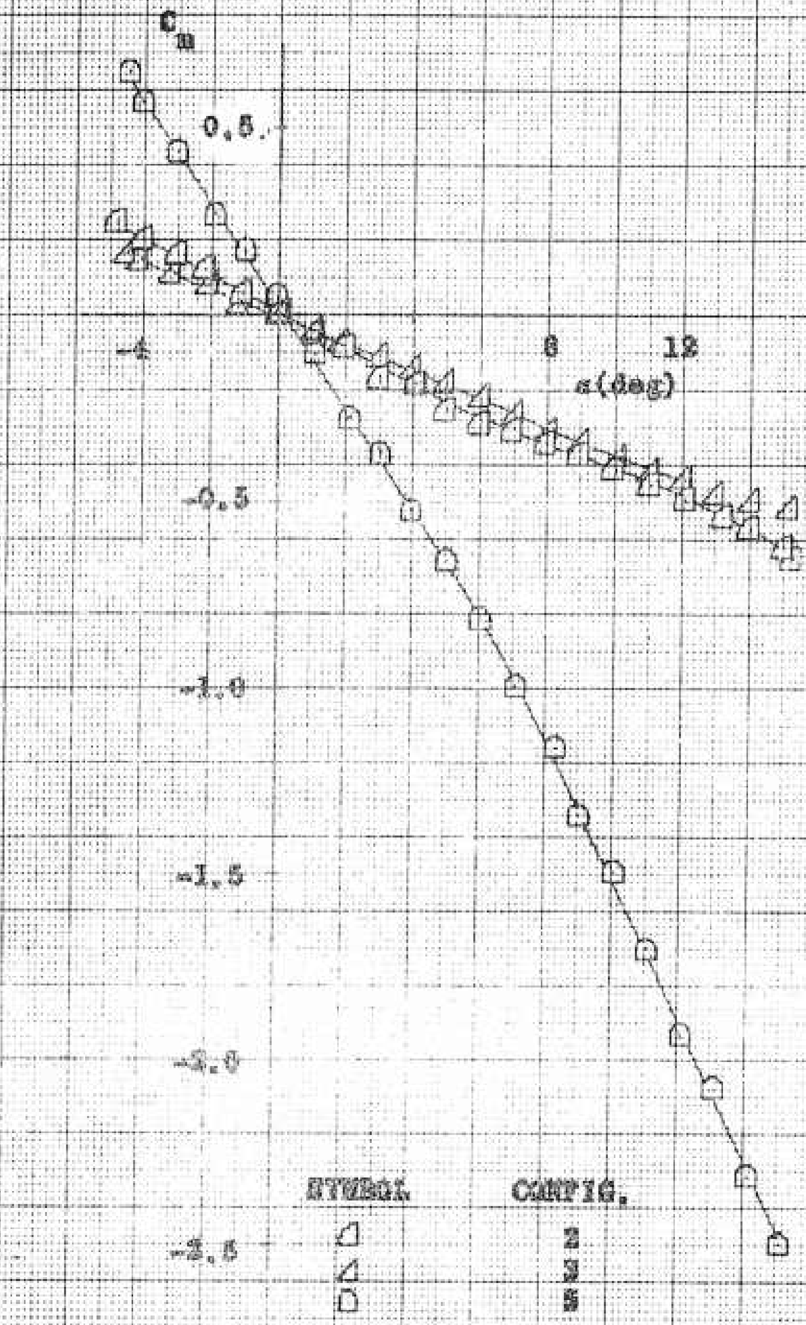

FIG. 38 PITCHING MOMENT COEFFICIENT, C_m, AS A FUNCTION OF ANGLE OF ATTACK, α, FOR CONFIGURATIONS 2, 3 AND 5 AT A FREE-STREAM MACH NUMBER OF 0.80

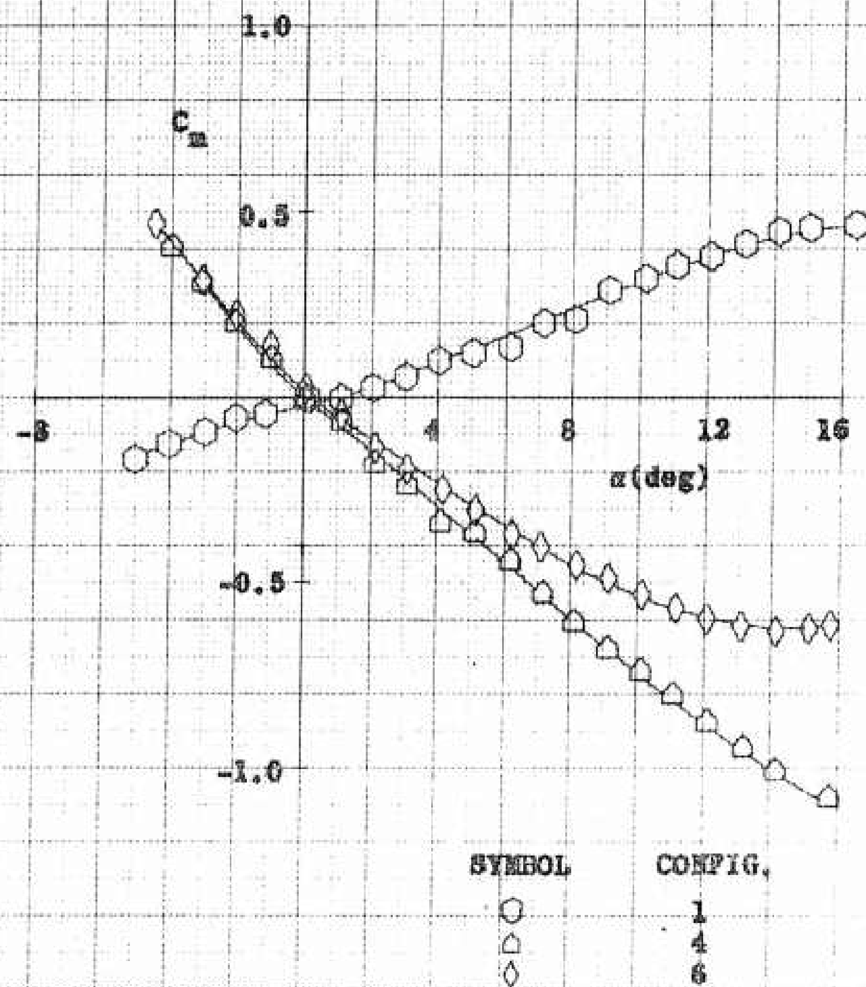

FIG. 39 PITCHING MOMENT COEFFICIENT, C_m, AS A FUNCTION OF ANGLE OF ATTACK, α, FOR CONFIGURATIONS 1, 4 AND 6 AT A FREE-STREAM MACH NUMBER OF 0.94

CONFIDENTIAL
NOLTR 63-47

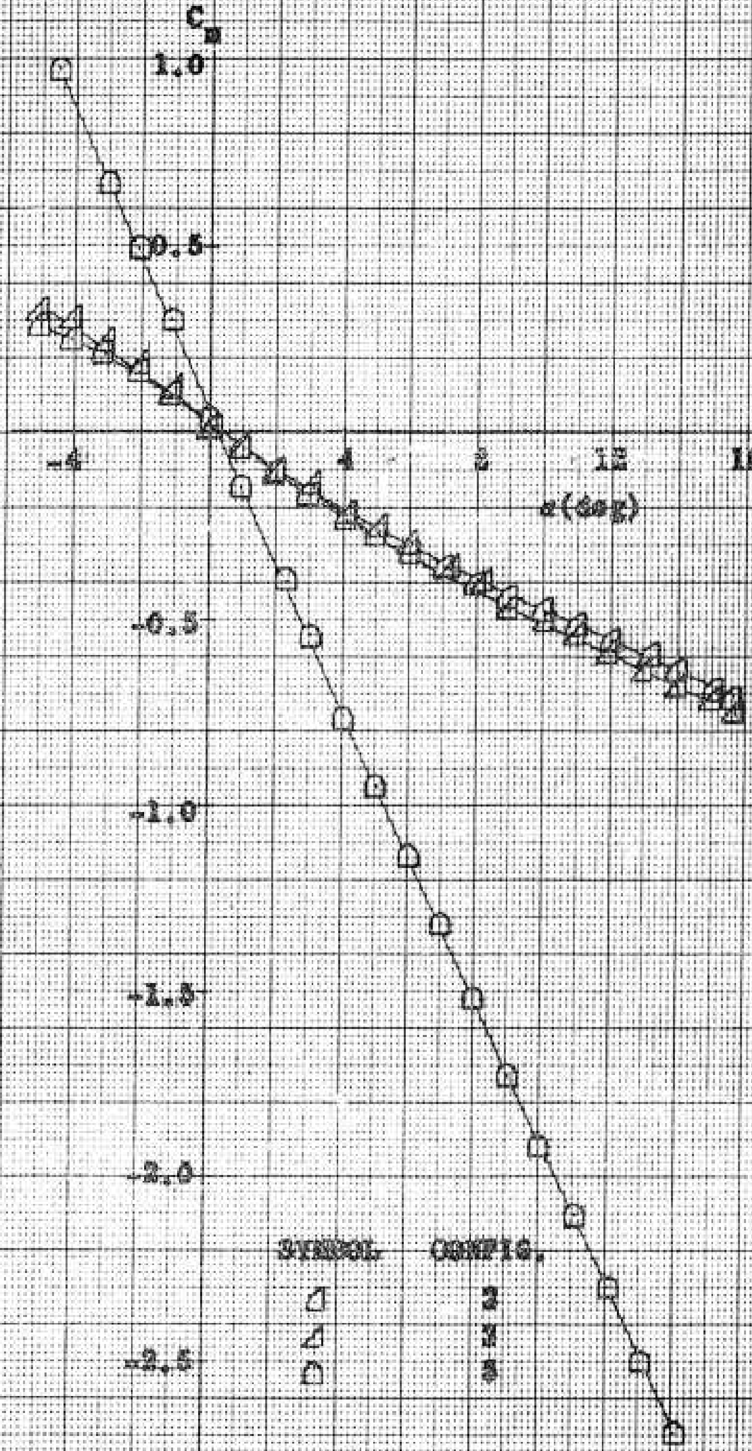

FIG. 40 PITCHING MOMENT COEFFICIENT, C_m, AS A FUNCTION OF ANGLE OF ATTACK, α, FOR CONFIGURATIONS 2, 3 AND 5 AT A FREE-STREAM MACH NUMBER OF 0.94

CONFIDENTIAL

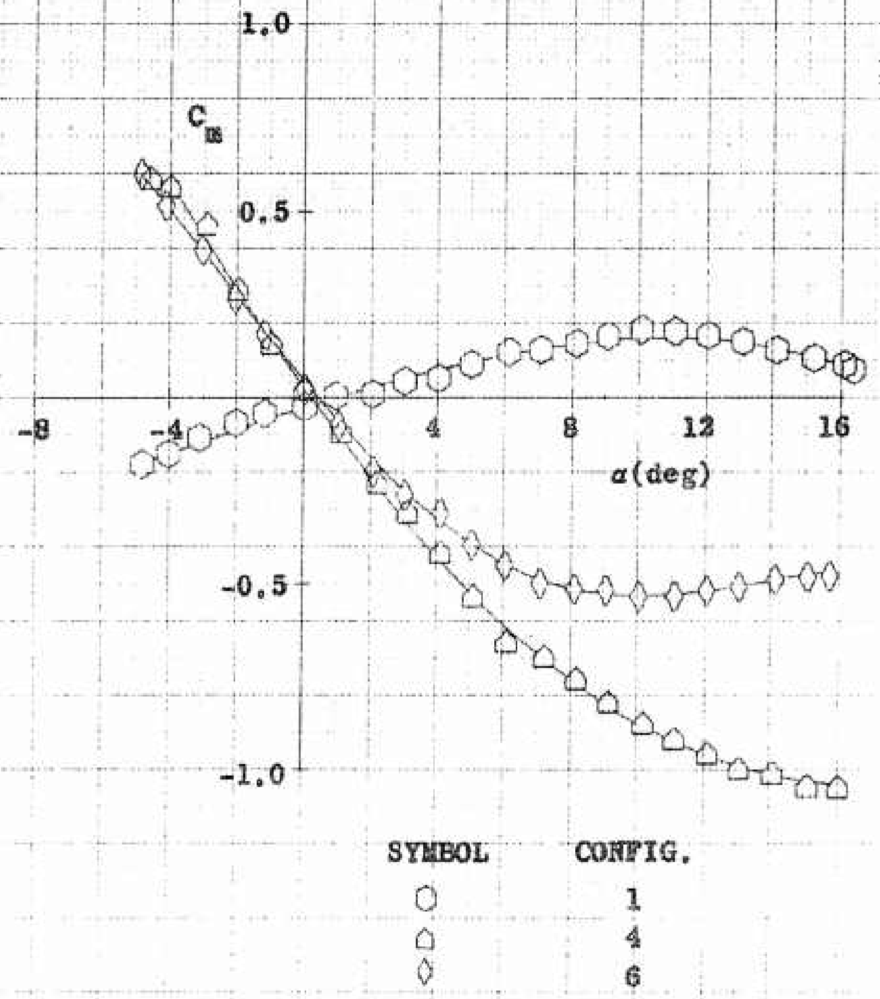

FIG. 41 PITCHING MOMENT COEFFICIENT, C_m, AS A FUNCTION OF ANGLE OF ATTACK, α, FOR CONFIGURATIONS 1, 4 AND 6 AT A FREE-STREAM MACH NUMBER OF 1.05.

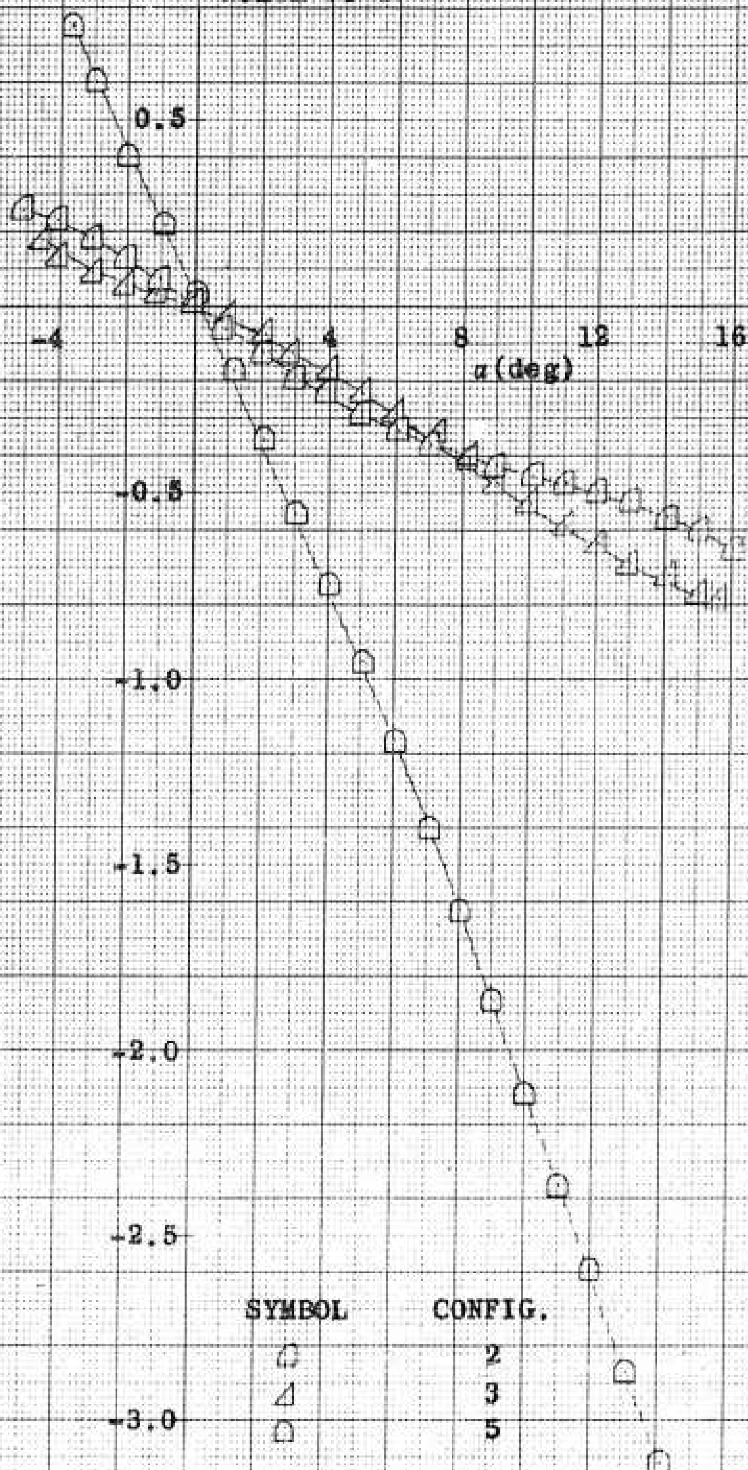

FIG. 42 PITCHING MOMENT COEFFICIENT, C_m, AS A FUNCTION OF ANGLE OF ATTACK, α, FOR CONFIGURATIONS 2, 3 AND 5 AT A FREE-STREAM MACH NUMBER OF 1.05

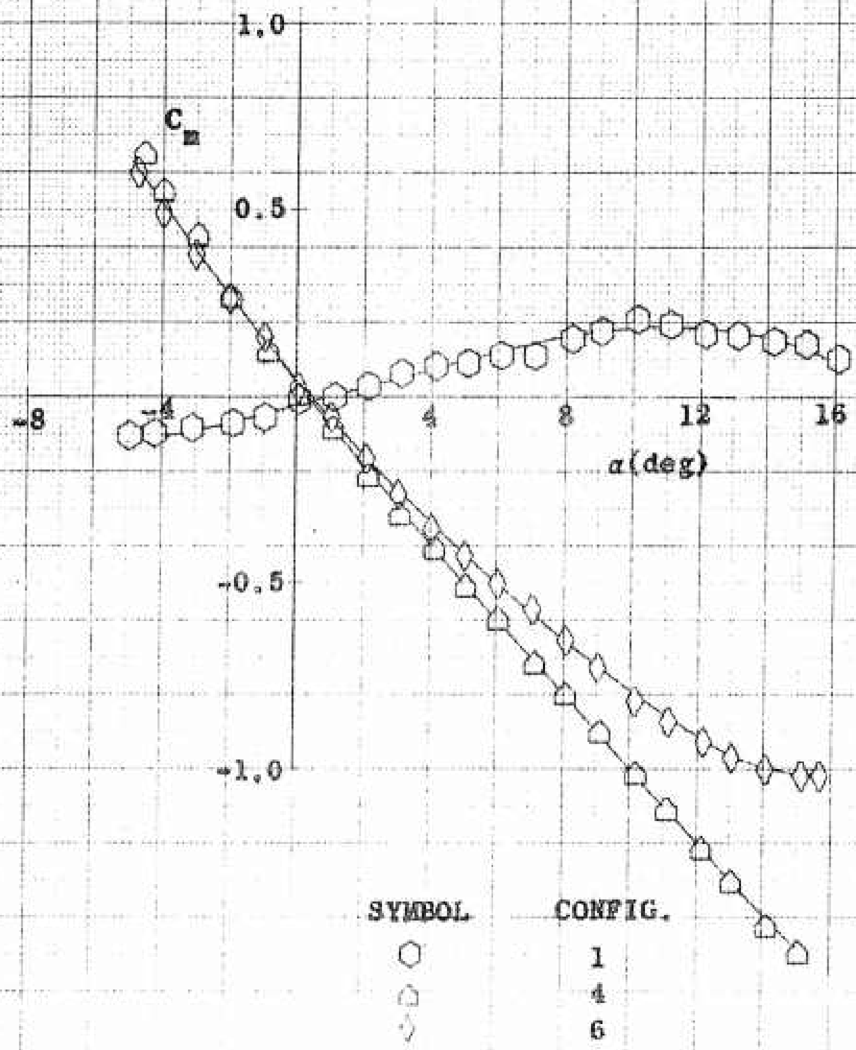

FIG. 43 PITCHING MOMENT COEFFICIENT, C_m, AS A FUNCTION OF ANGLE OF ATTACK, α, FOR CONFIGURATIONS 1, 4 AND 6 AT A FREE-STREAM MACH NUMBER OF 1.15

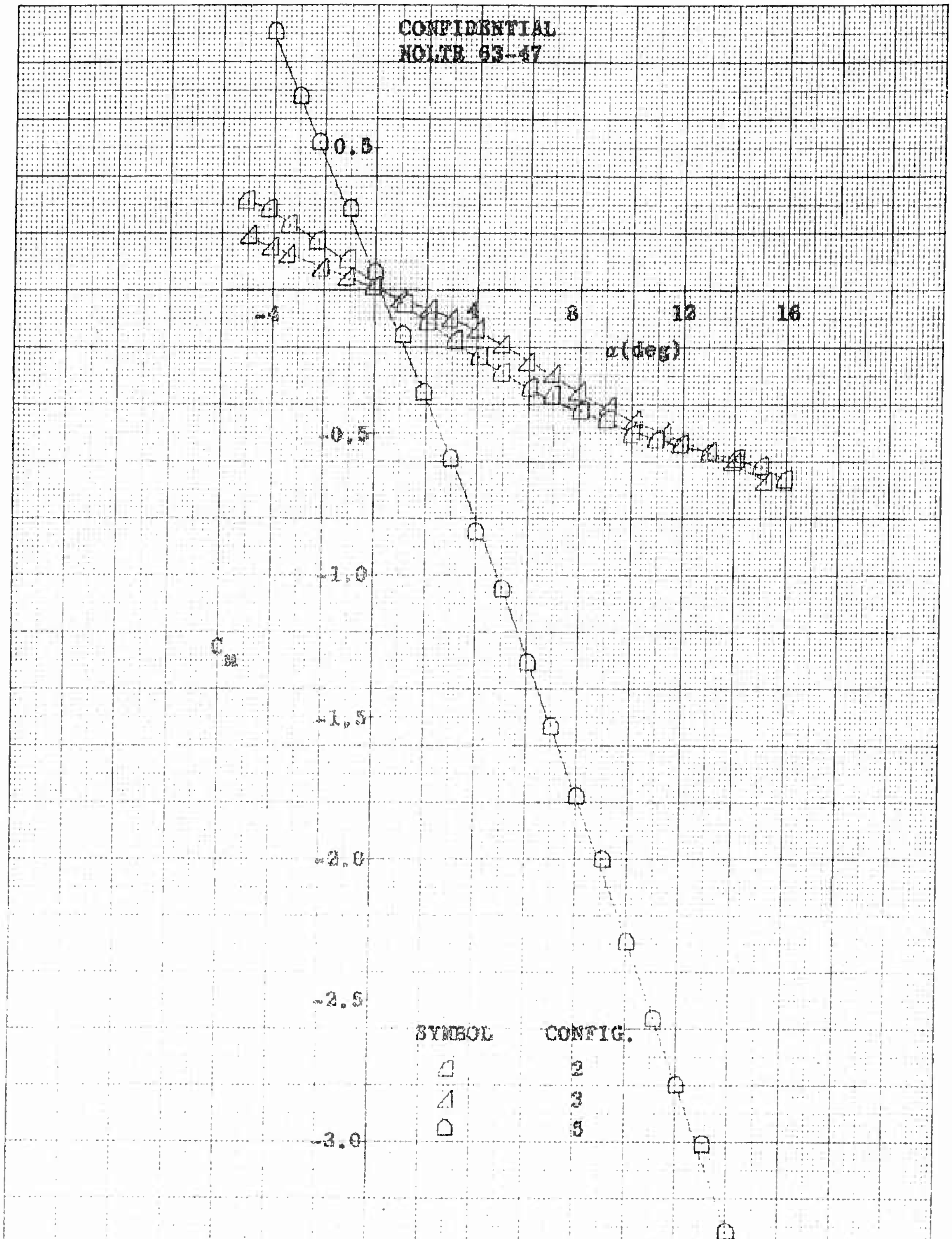

FIG. 44 PITCHING MOMENT COEFFICIENT, C_m, AS A FUNCTION OF ANGLE OF ATTACK, α, FOR CONFIGURATIONS 2, 3 AND 5 AT A FREE-STREAM MACH NUMBER OF 1.15

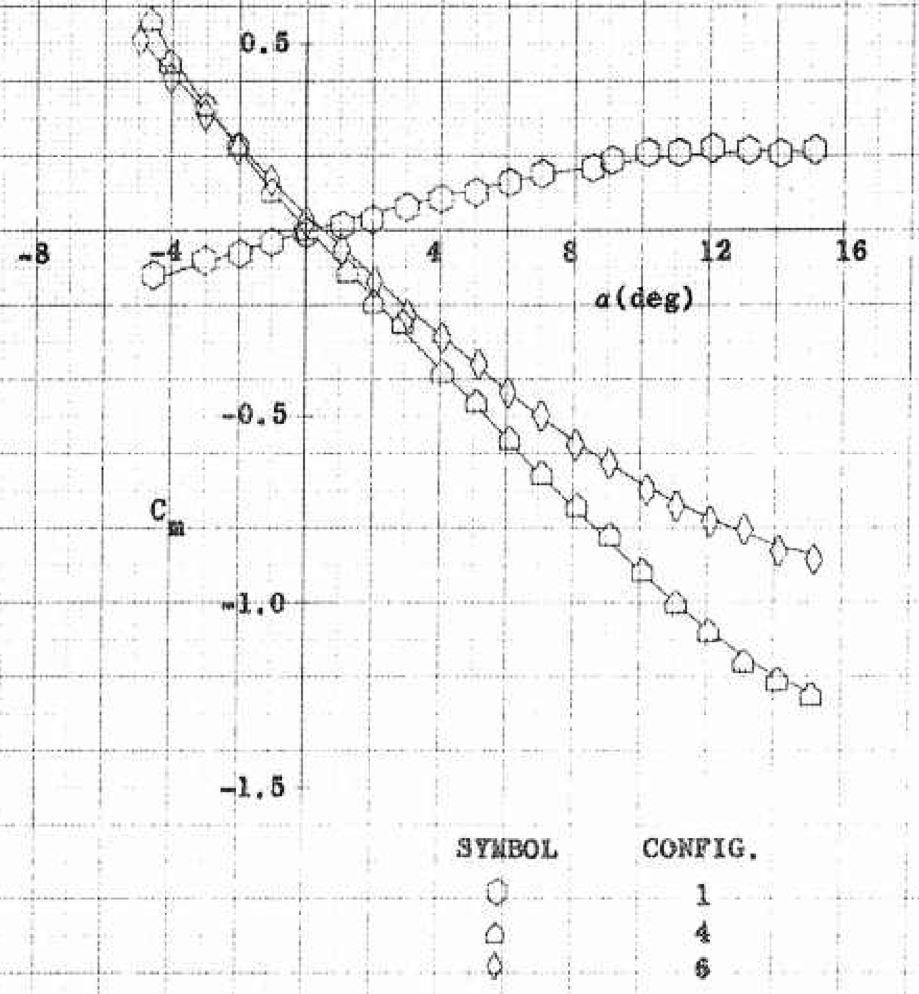

FIG. 45 PITCHING MOMENT COEFFICIENT, C_m, AS A FUNCTION OF ANGLE OF ATTACK, α, FOR CONFIGURATIONS 1, 4 AND 6 AT A FREE-STREAM MACH NUMBER OF 1.26

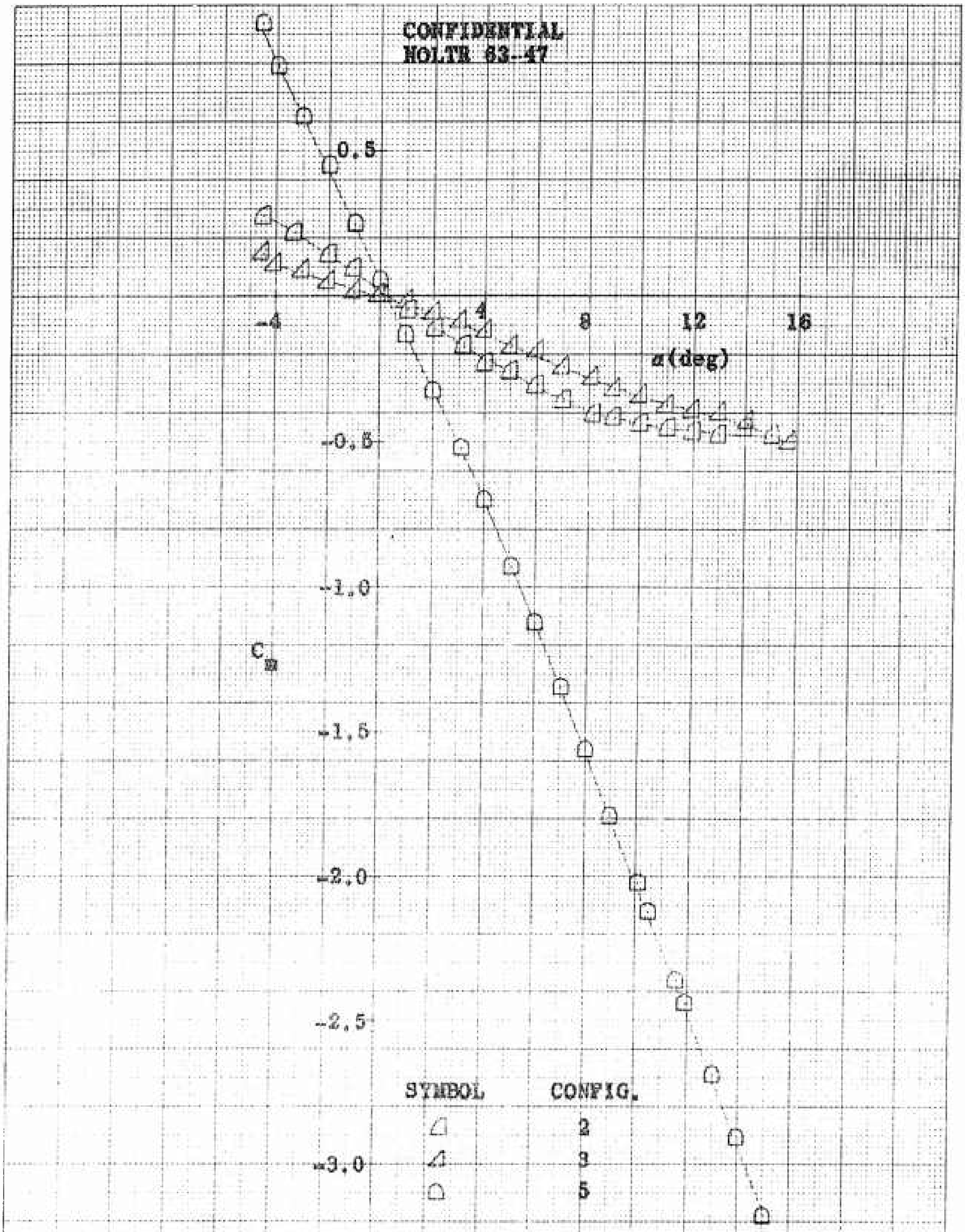

FIG. 46 PITCHING MOMENT COEFFICIENT, C_m, AS A FUNCTION OF ANGLE OF ATTACK, α, FOR CONFIGURATIONS 2, 3 AND 5 AT A FREE-STREAM MACH NUMBER OF 1.26

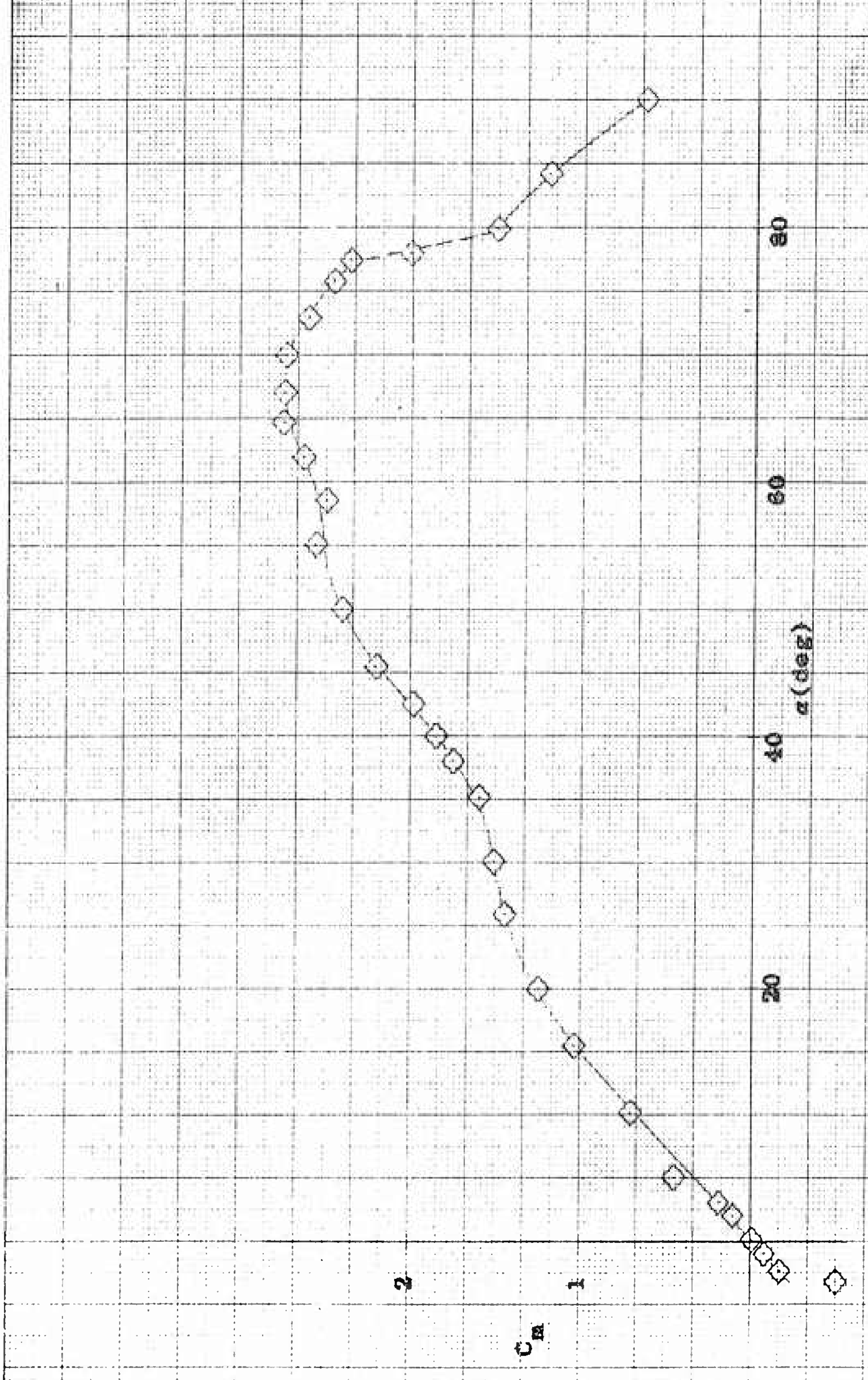

FIG. 47 PITCHING MOMENT COEFFICIENT, C_m, AS A FUNCTION OF ANGLE OF ATTACK, α, FOR THE .30 CALIBER BULLET CORE AT A FREE-STREAM MACH NUMBER OF 0.30

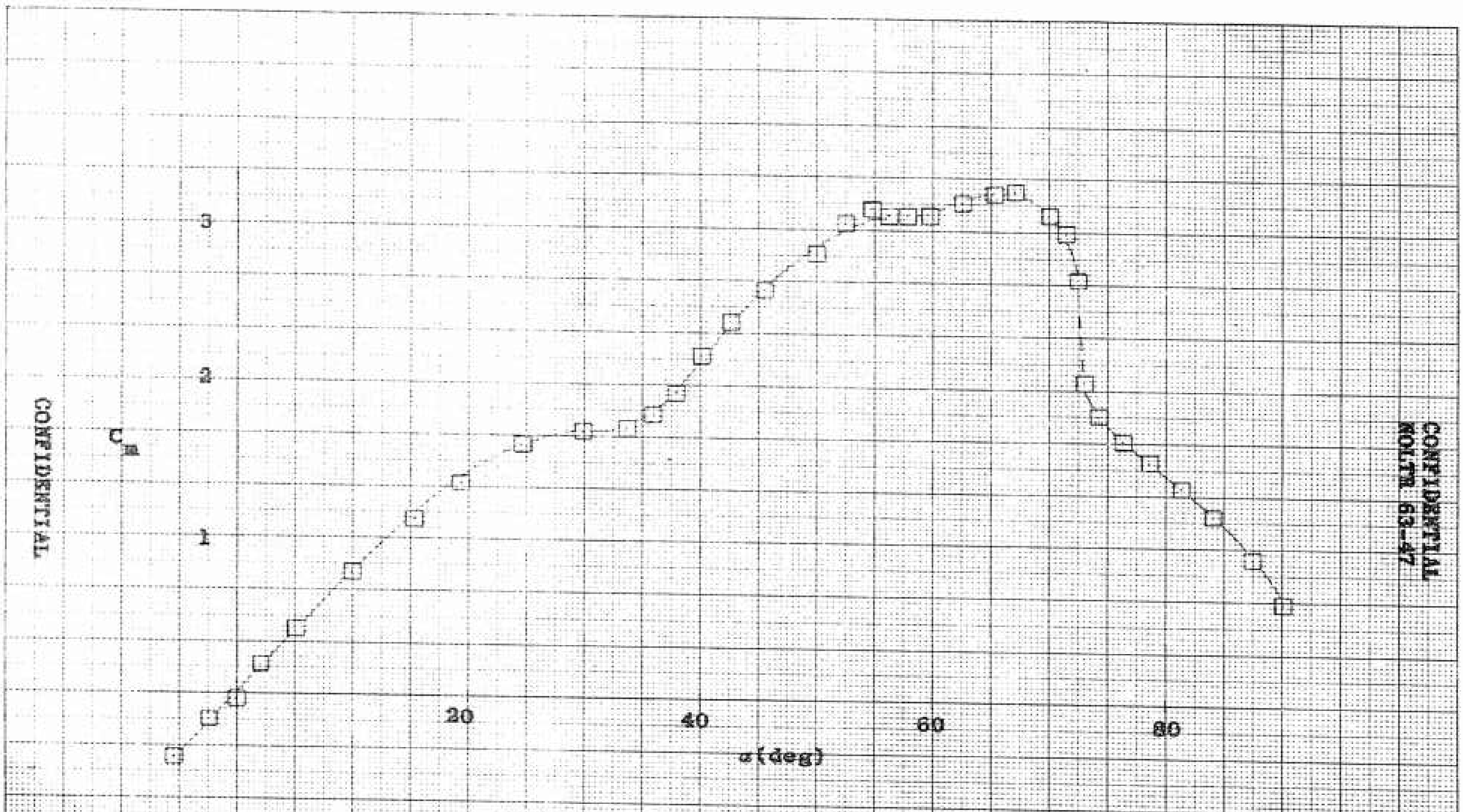

FIG. 48 PITCHING MOMENT COEFFICIENT, C_m, AS A FUNCTION OF ANGLE OF ATTACK, α, FOR THE 50 CALIBER BULLET CORE AT A FREE-STREAM MACH NUMBER OF 0.50

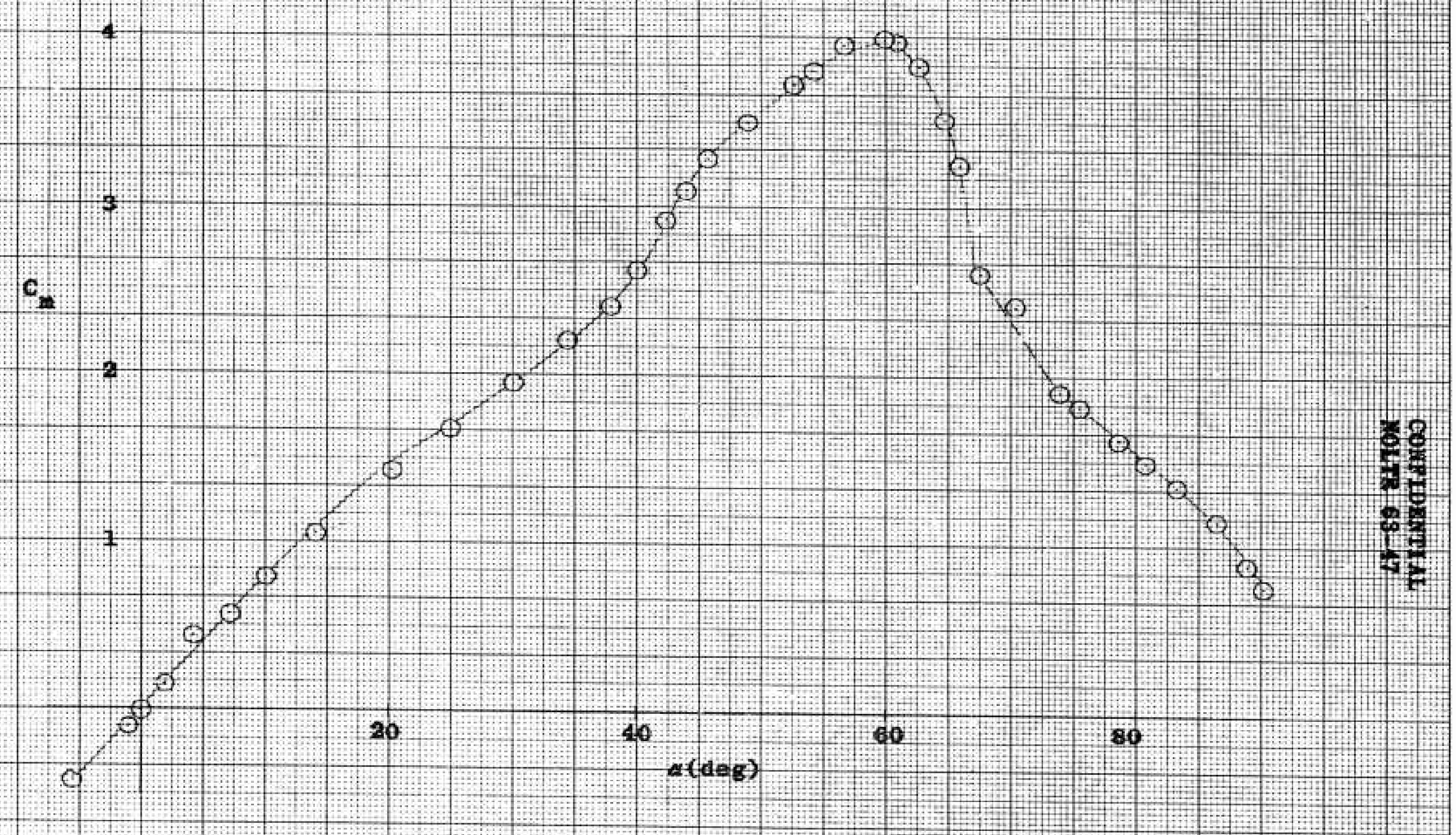

FIG. 49 PITCHING MOMENT COEFFICIENT, C_m, AS A FUNCTION OF ANGLE OF ATTACK, α, FOR THE 50 CALIBER BULLET CORE AT A FREE-STREAM MACH NUMBER OF 0.70

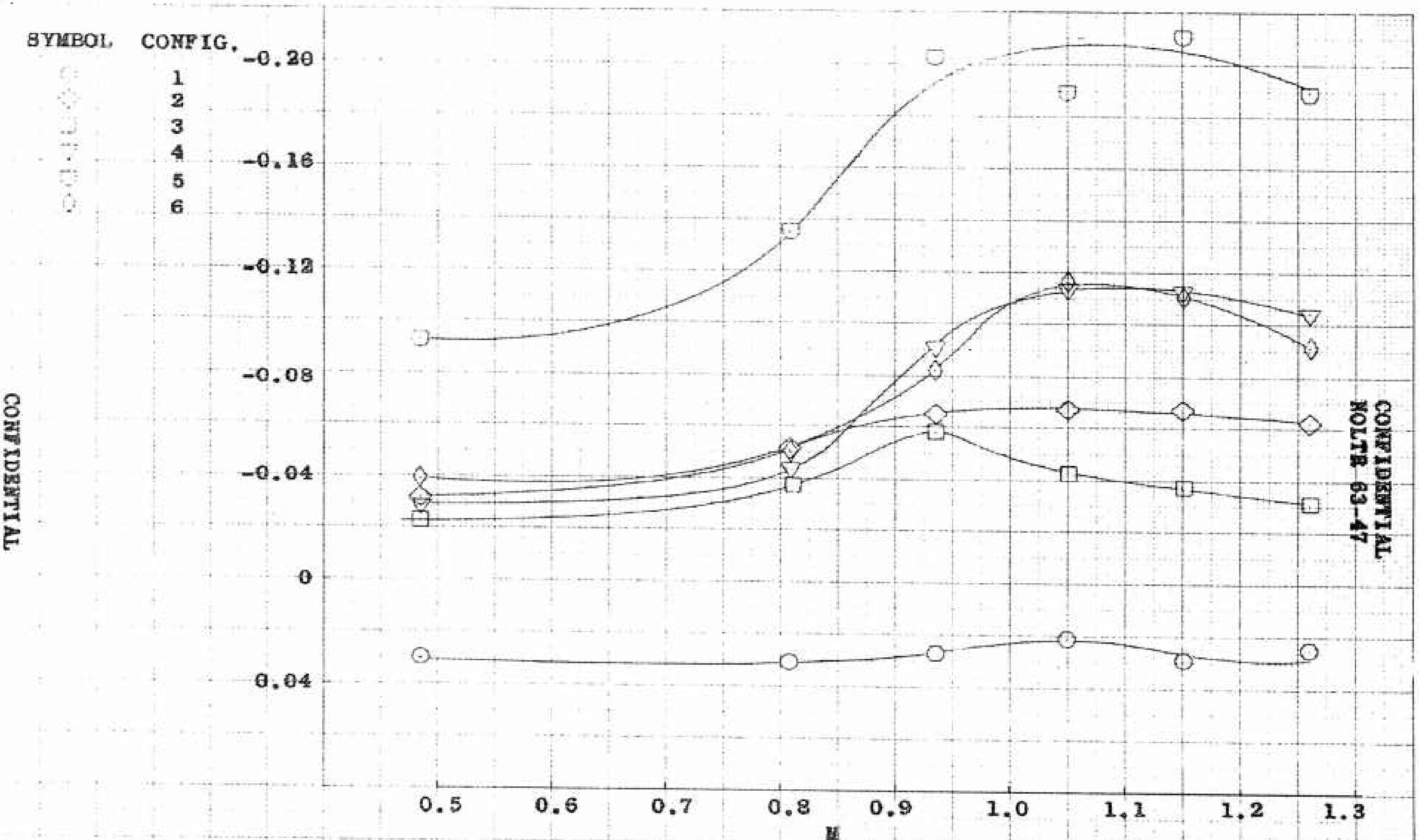

FIG. 50 SLOPE OF THE PITCHING MOMENT COEFFICIENT-ANGLE OF ATTACK CURVE, MEASURED AT ZERO ANGLE OF ATTACK, $C_{m_{\alpha_o}}$, AS A FUNCTION OF FREE-STREAM MACH NUMBER FOR CONFIGURATIONS 1 THROUGH 6.

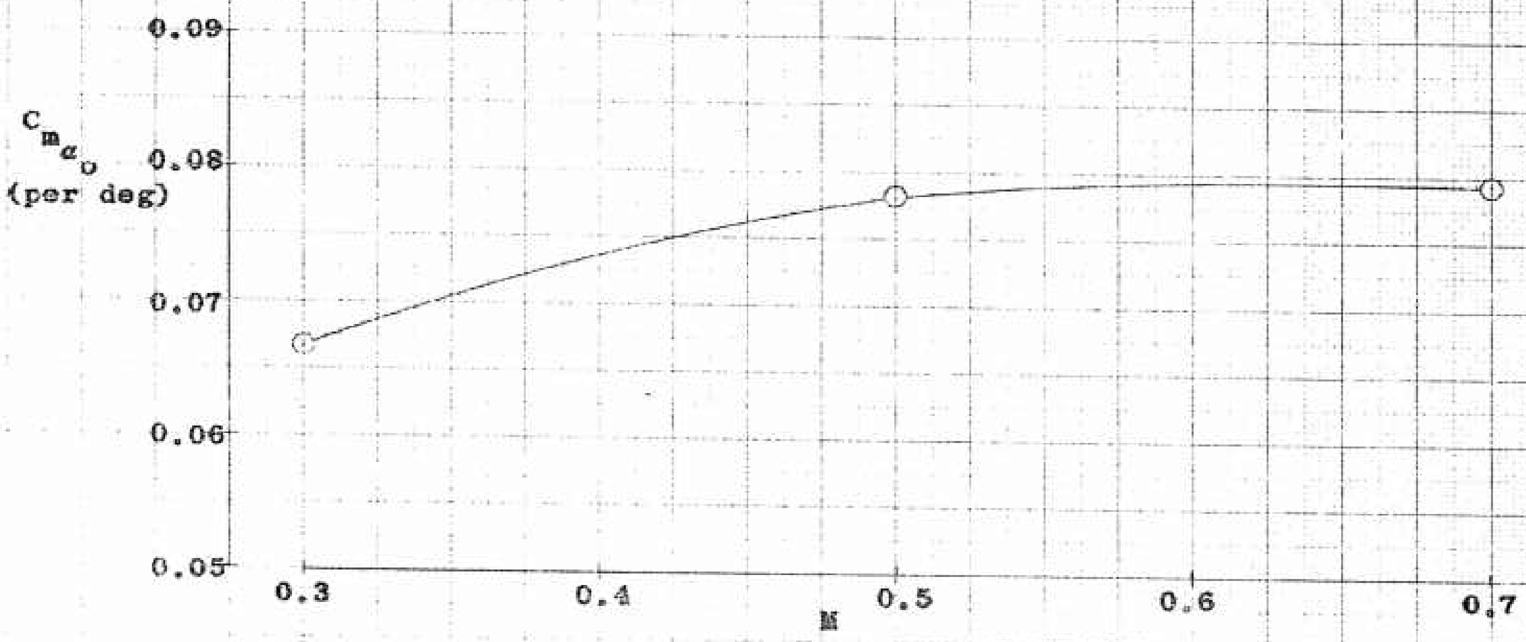

FIG. 51 SLOPE OF THE PITCHING MOMENT COEFFICIENT-ANGLE OF ATTACK CURVE, MEASURED AT ZERO ANGLE OF ATTACK, $C_{m_{\alpha_o}}$, AS A FUNCTION OF FREE-STREAM MACH NUMBER FOR THE 50 CALIBER BULLET CORE.

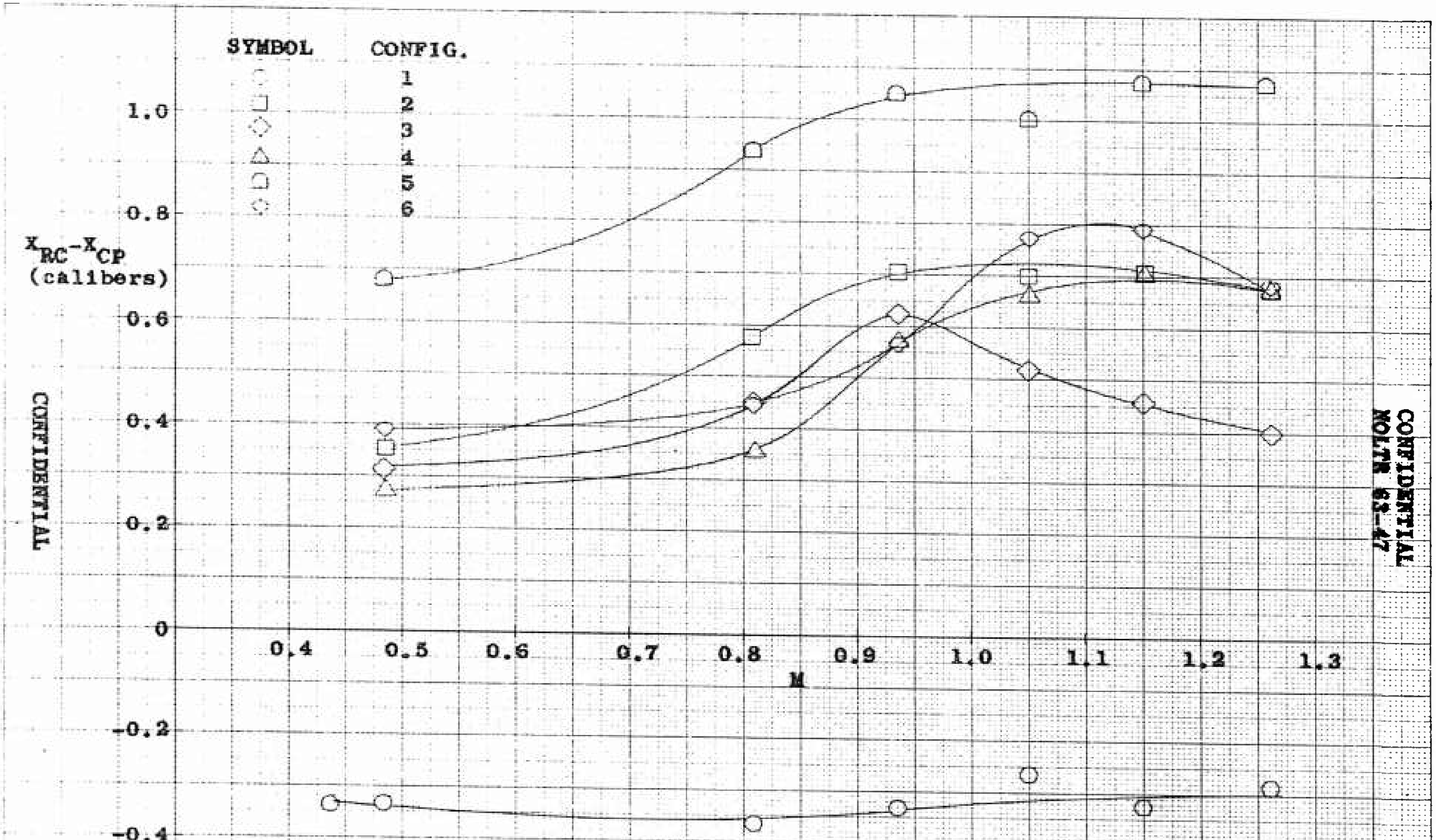

FIG. 52 DISTANCE FROM THE MOMENT REFERENCE CENTER (X_{RC}) TO THE CENTER OF PRESSURE (X_{CP}) AS A FUNCTION OF FREE-STREAM MACH NUMBER FOR CONFIGURATIONS 1 THROUGH 6

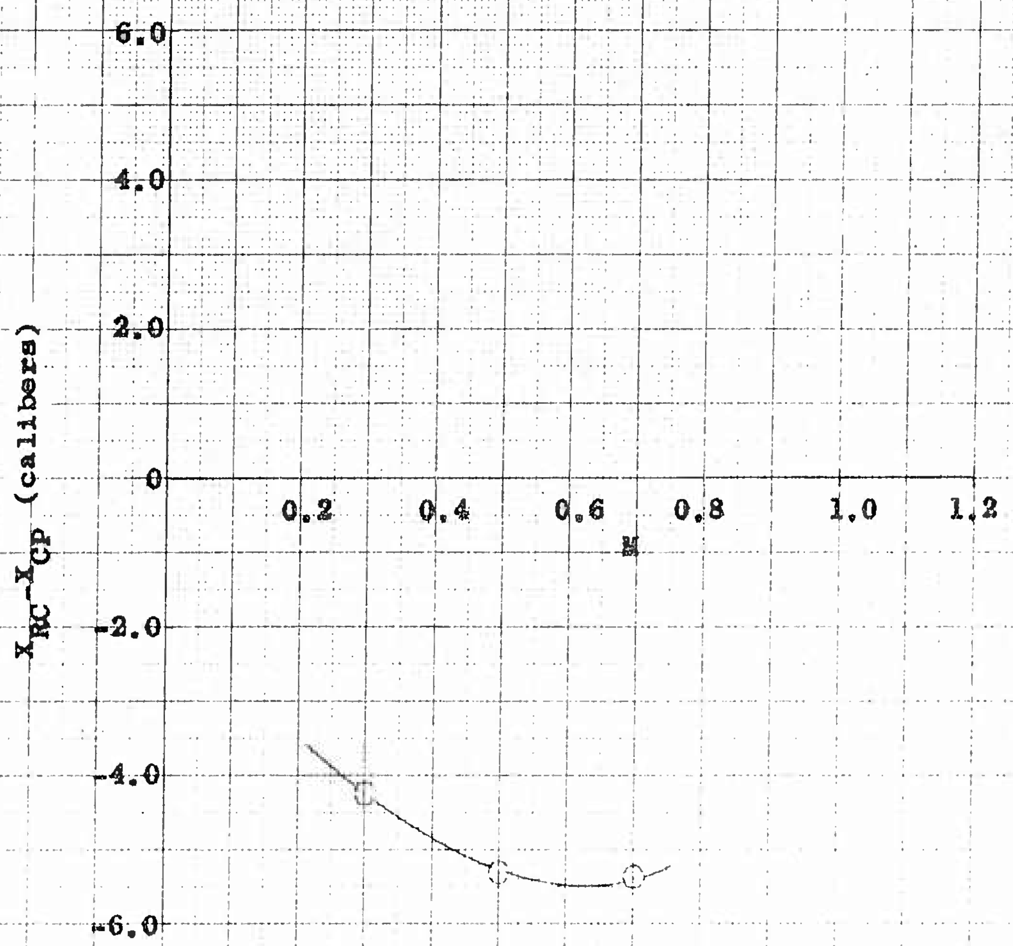

FIG. 53 DISTANCE FROM THE MOMENT REFERENCE CENTER (X_{RC}) TO THE CENTER OF PRESSURE (X_{CP}) AS A FUNCTION OF FREE-STREAM MACH NUMBER FOR THE 50 CALIBER BULLET CORE

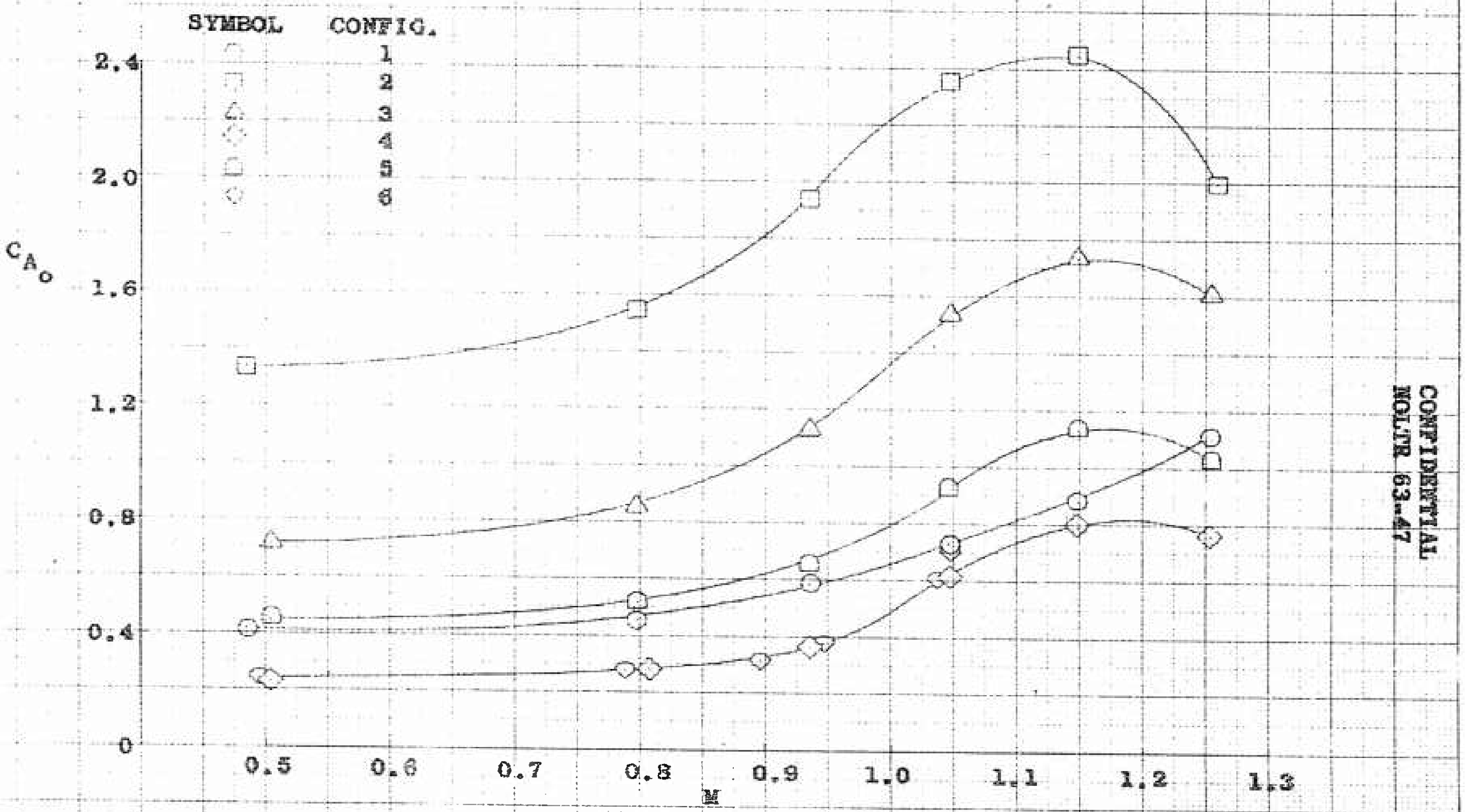

FIG. 54 AXIAL FORCE COEFFICIENT AT ZERO ANGLE OF ATTACK, C_{A_o}, AS A FUNCTION OF FREE-STREAM MACH NUMBER FOR CONFIGURATIONS 1 THROUGH 6

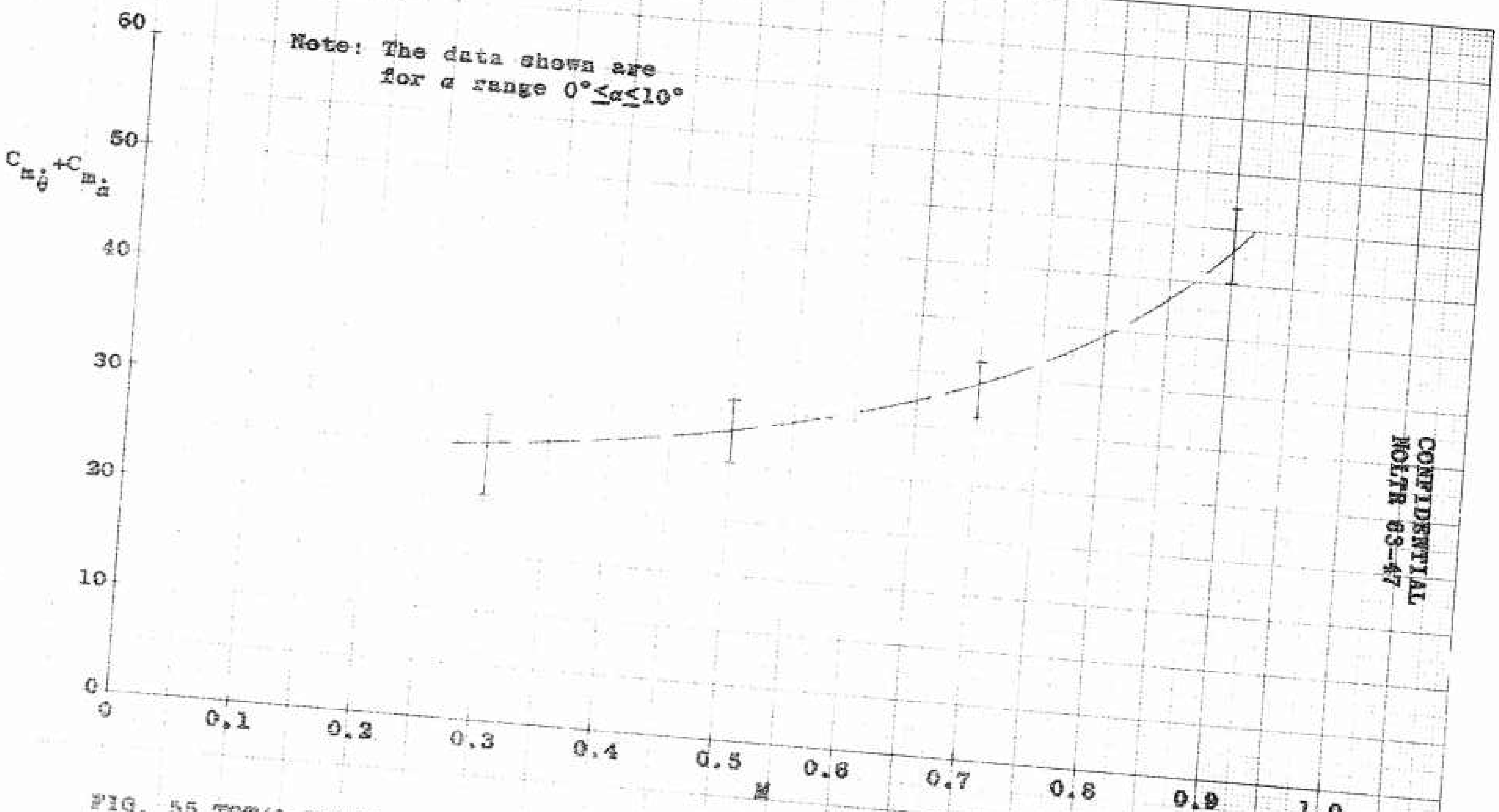

FIG. 55 TOTAL PITCH DAMPING COEFFICIENT, $C_{m_{\dot{\theta}}}+C_{m_{\dot{\alpha}}}$, AS A FUNCTION OF FREE-STREAM MACH NUMBER FOR CONFIGURATION 6

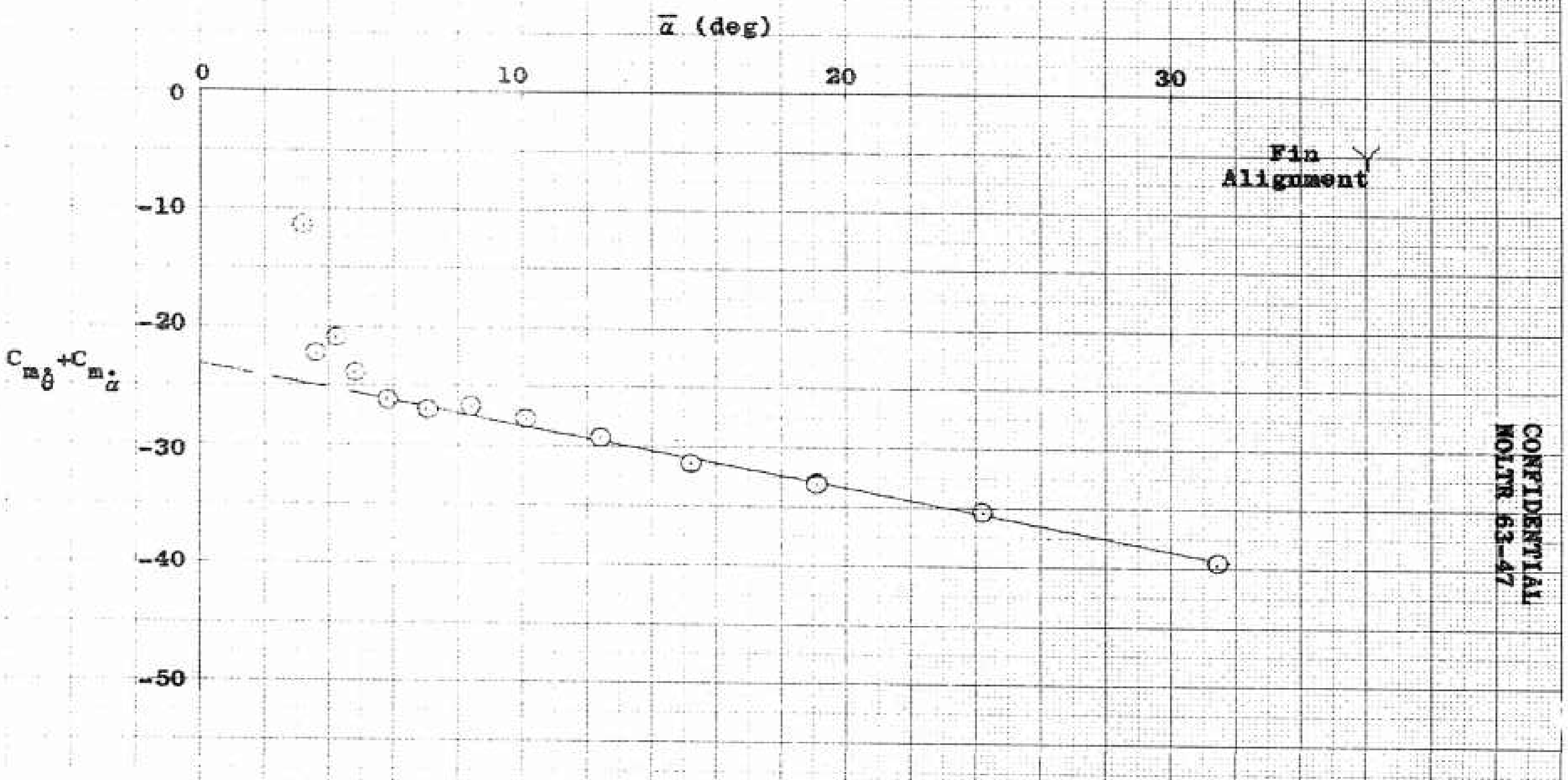

FIG. 56 PITCH DAMPING COEFFICIENT, $C_{m_{\dot\theta}}+C_{m_{\dot\alpha}}$, AS A FUNCTION OF MEAN ANGLE OF ATTACK, $\bar{\alpha}$, FOR CONFIGURATION 6 AT A FREE-STREAM MACH NUMBER OF 0.30

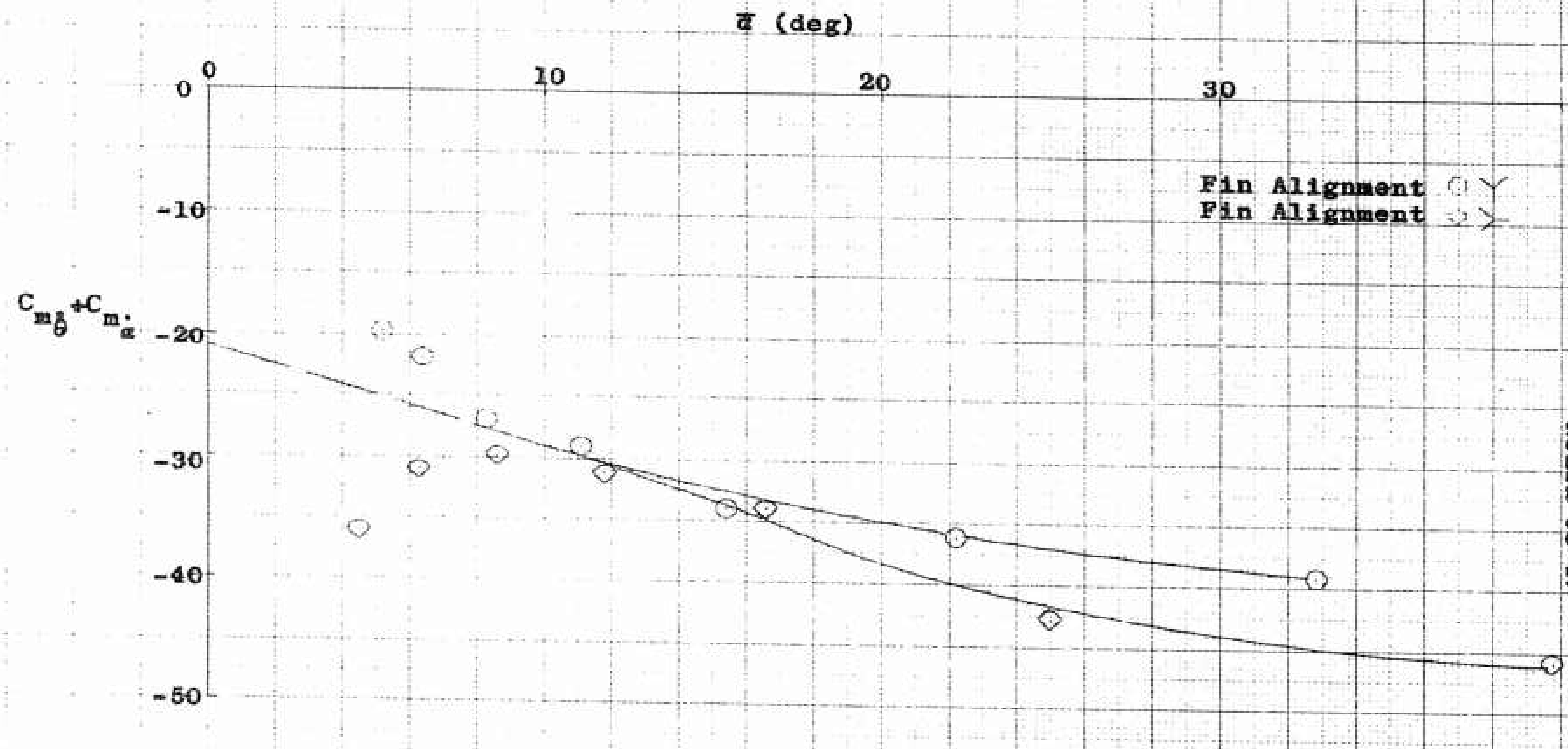

FIG. 57 PITCH DAMPING COEFFICIENT, $C_{m_{\dot\theta}}+C_{m_{\dot\alpha}}$, AS A FUNCTION OF MEAN ANGLE OF ATTACK, $\bar{\alpha}$, FOR CONFIGURATION 6 AT A FREE-STREAM MACH NUMBER OF 0.50

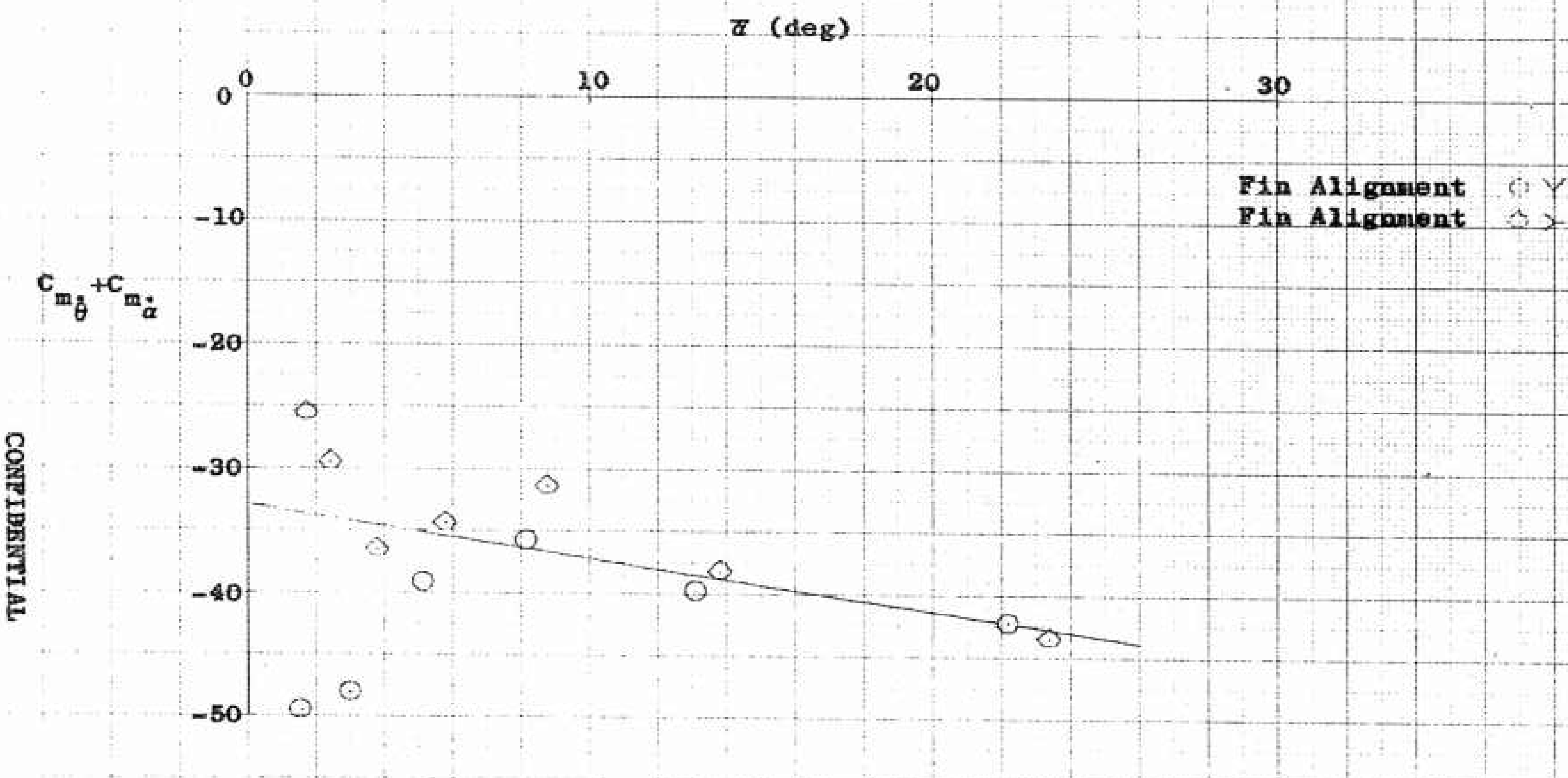

FIG. 58 PITCH DAMPING COEFFICIENT, $C_{m_{\dot{\theta}}}+C_{m_{\dot{\alpha}}}$, AS A FUNCTION OF MEAN ANGLE OF ATTACK, $\bar{\alpha}$, FOR CONFIGURATION 6 AT A FREE-STREAM MACH NUMBER OF 0.70

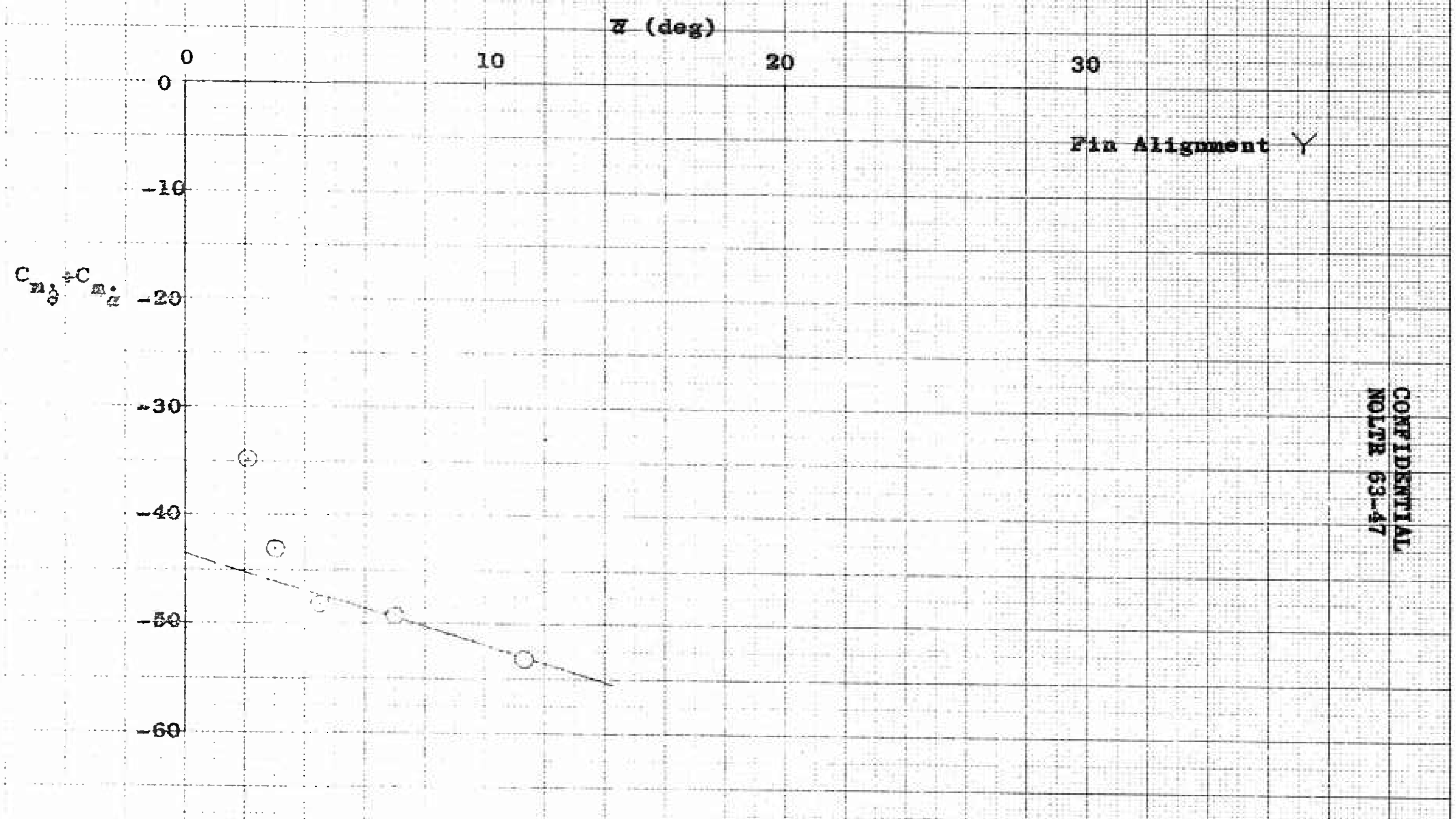

FIG. 59 PITCH DAMPING COEFFICIENT, $C_{m_{\dot{\theta}}}+C_{m_{\dot{\alpha}}}$, AS A FUNCTION OF MEAN ANGLE OF ATTACK, $\bar{\alpha}$, FOR CONFIGURATION 6 AT A FREE-STREAM MACH NUMBER OF 0.90

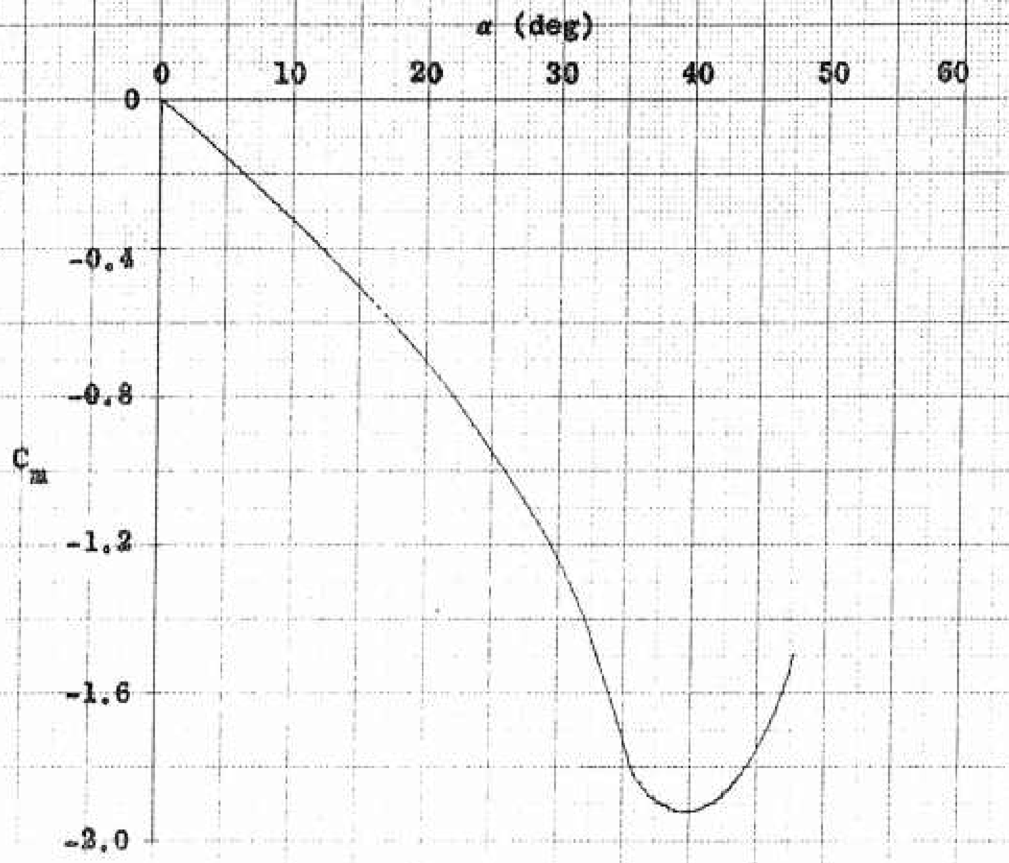

FIG. 60 PITCHING MOMENT COEFFICIENT, C_m, AS A FUNCTION OF ANGLE OF ATTACK, α, FOR CONFIGURATION 6 AT A FREE-STREAM MACH NUMBER OF 0.30 AS OBTAINED FROM PITCH DAMPING DATA

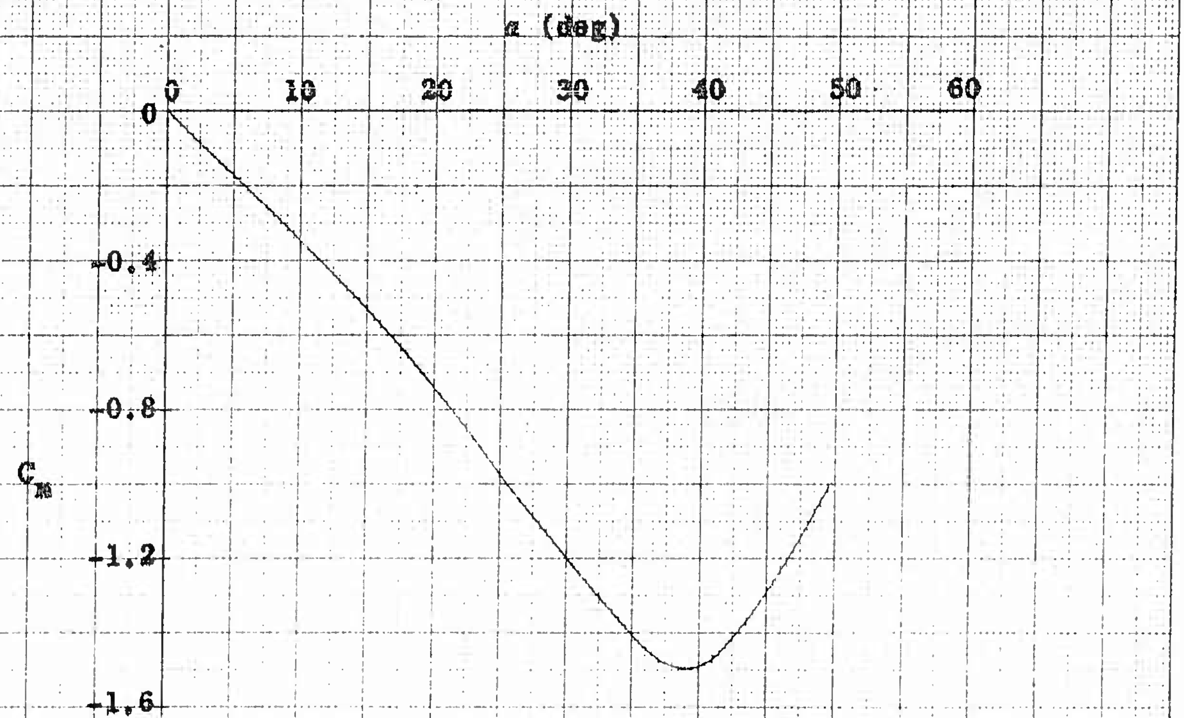

FIG. 61 PITCHING MOMENT COEFFICIENT, C_m, AS A FUNCTION OF ANGLE OF ATTACK, α, FOR CONFIGURATION 6 AT A FREE-STREAM MACH NUMBER OF 0.50 AS OBTAINED FROM PITCH DAMPING DATA

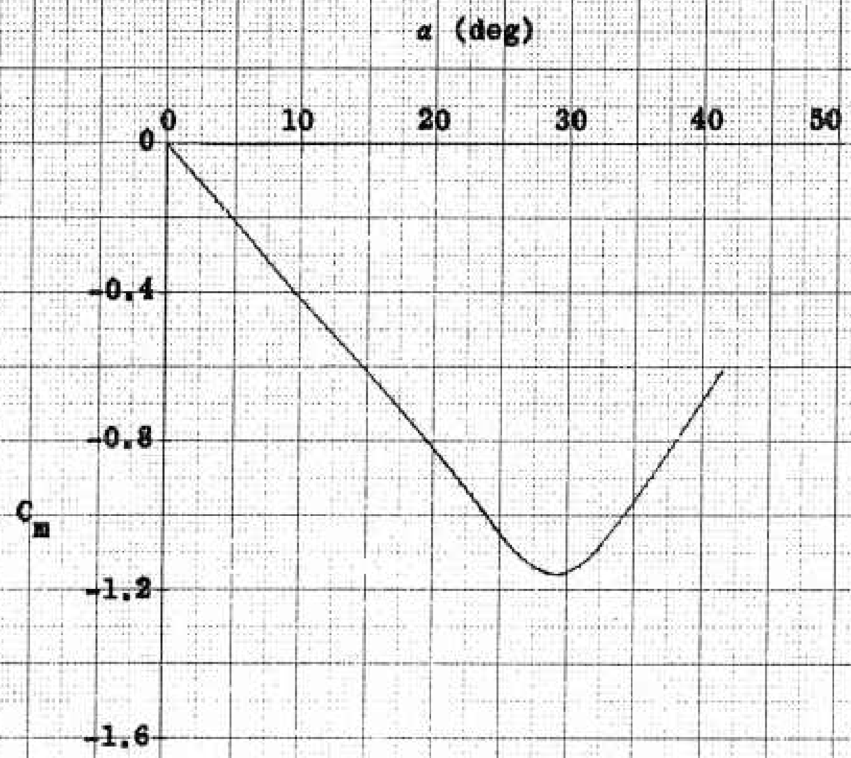

FIG. 62 PITCHING MOMENT COEFFICIENT, C_m, AS A FUNCTION OF ANGLE OF ATTACK, α, FOR CONFIGURATION 6 AT A FREE-STREAM MACH NUMBER OF 0.70 AS OBTAINED FROM PITCH DAMPING DATA

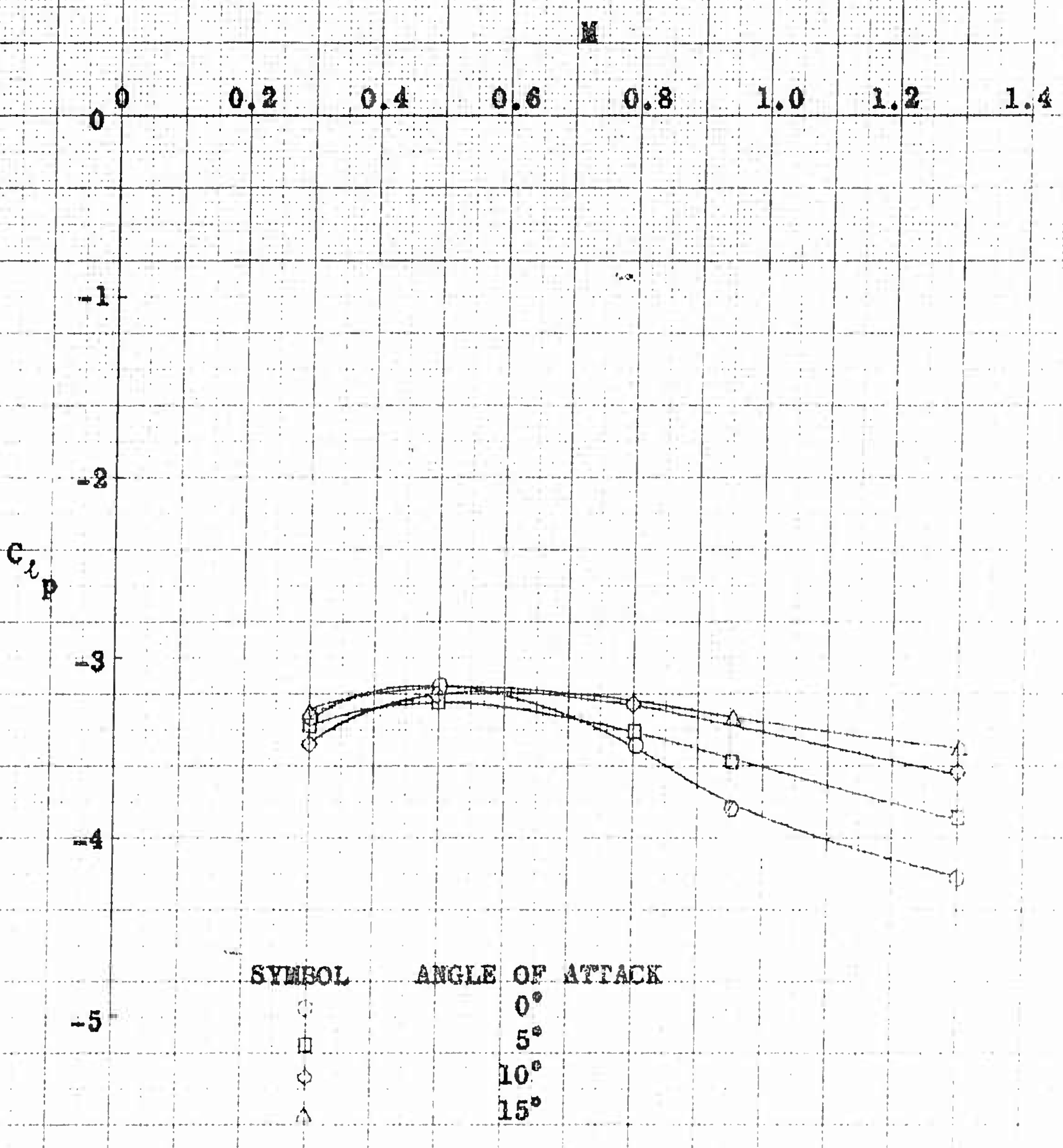

FIG. 63 ROLL DAMPING COEFFICIENT, C_{l_p}, AS A FUNCTION OF FREE-STREAM MACH NUMBER FOR CONFIGURATION 6 AT CONSTANT ANGLES OF ATTACK OF 0, 5, 10 AND 15 DEGREES

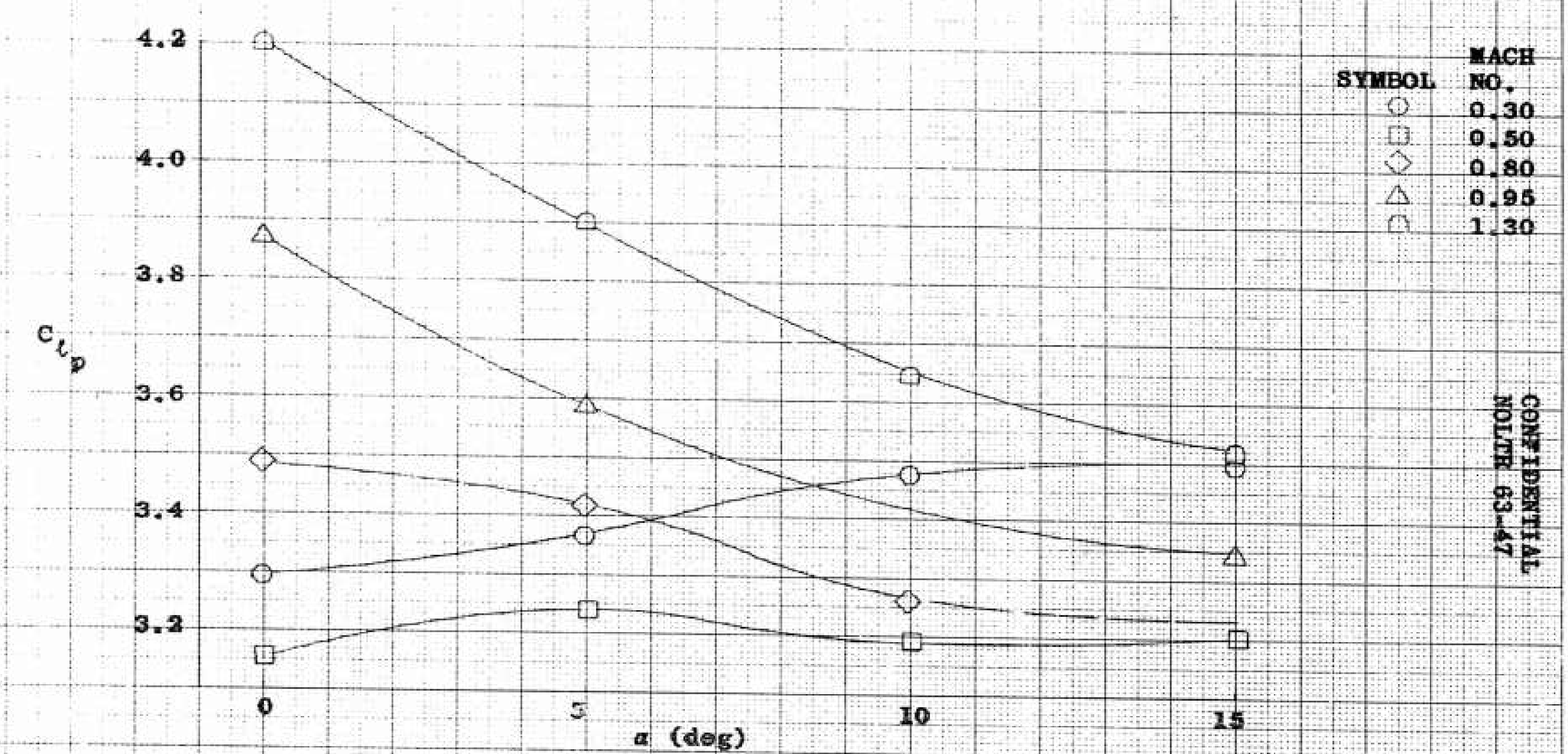

FIG. 64 ROLL DAMPING COEFFICIENT, C_{l_p}, AS A FUNCTION OF ANGLE OF ATTACK FOR CONFIGURATION 8 AT FREE-STREAM MACH NUMBERS OF 0.30, 0.50, 0.80, 0.95 AND 1.30

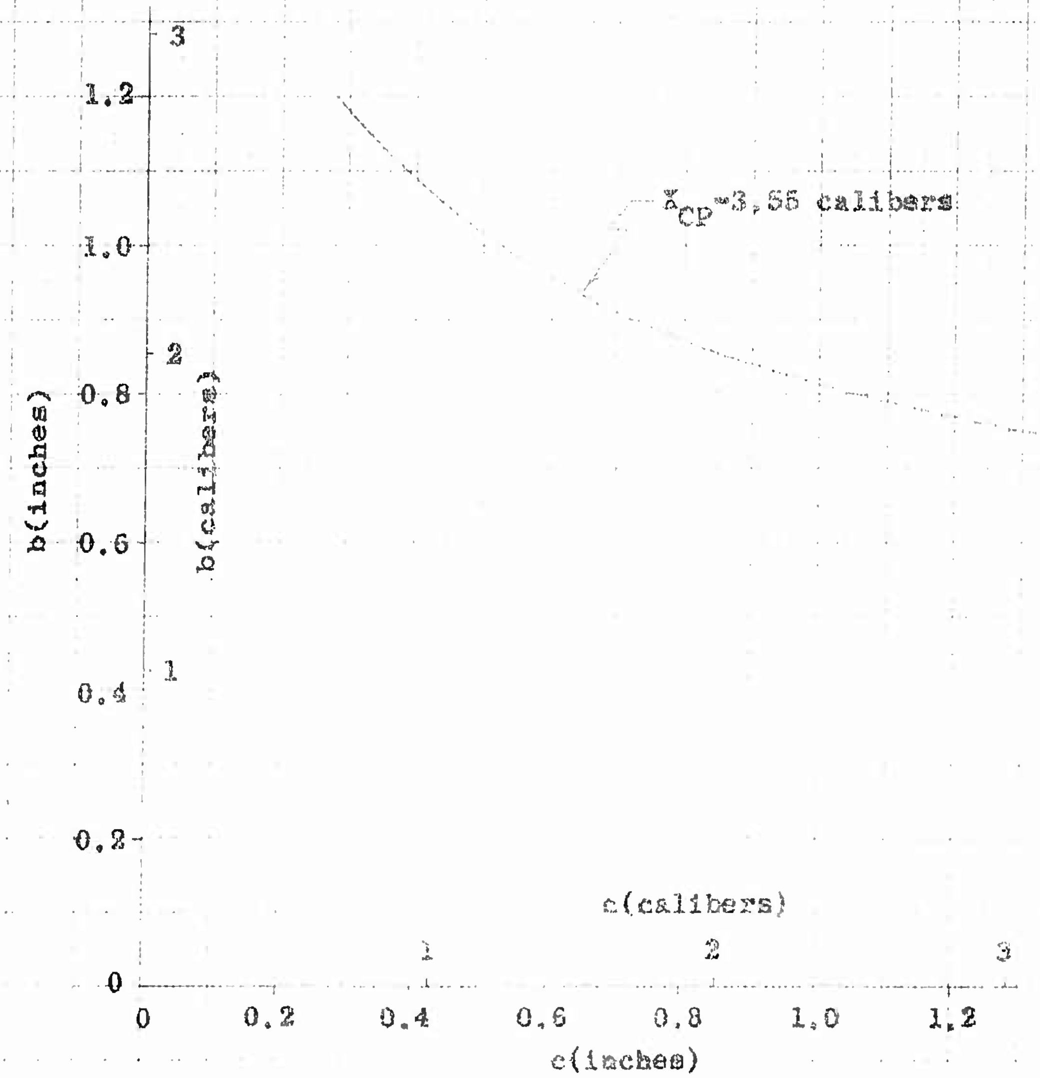

FIG. 65 FIN SPAN, b, VERSUS CHORD LENGTH, c, FOR THE 50 CALIBER BULLET CORE WITH RECTANGULAR FINS FOR A MODEL WITH THE CENTER OF PRESSURE 1.54 INCHES AFT OF THE NOSE

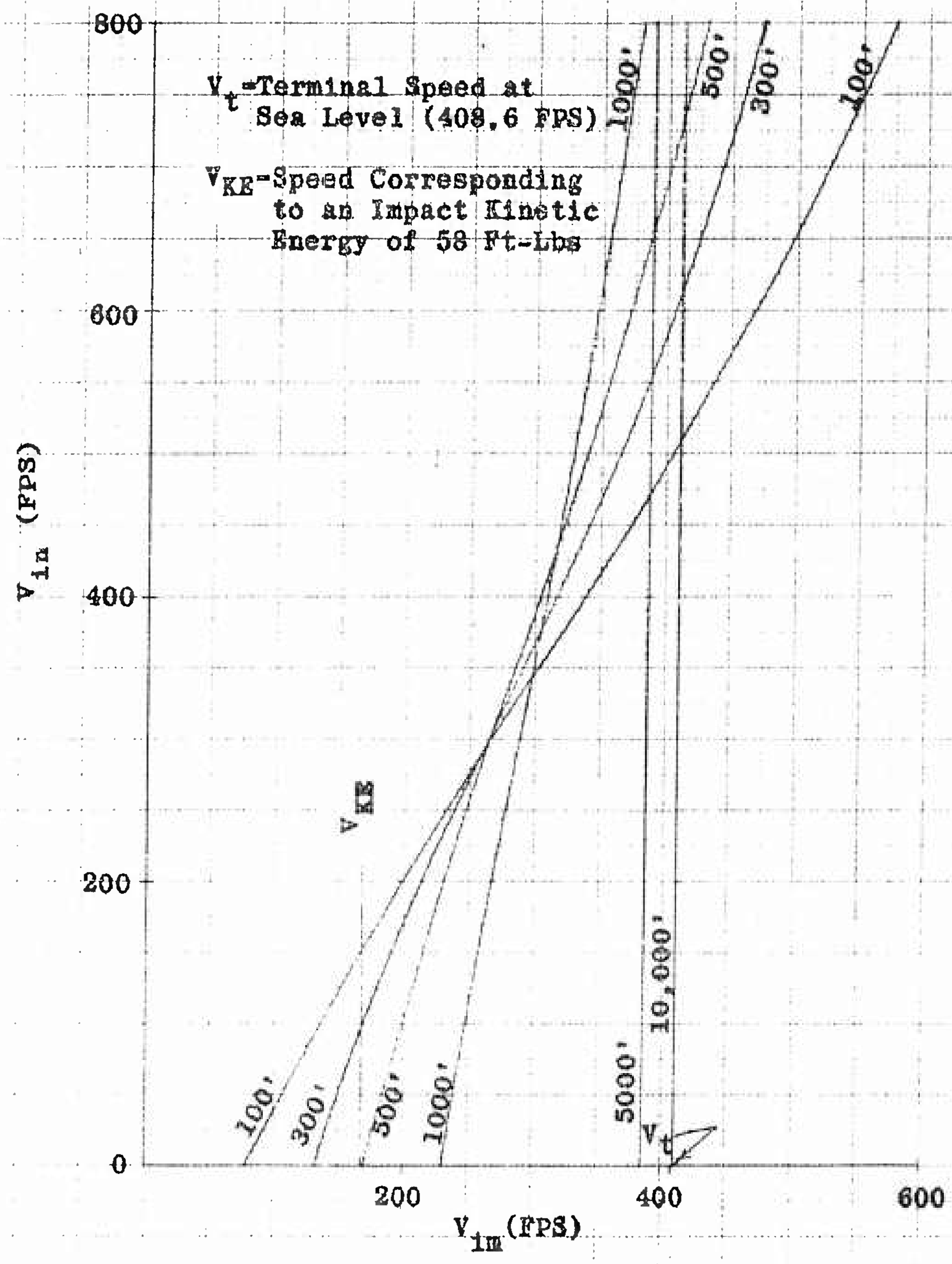

FIG. 66 VELOCITY AT IMPACT (V_{im}) FOR SEVERAL LAUNCH ALTITUDES AND INITIAL HORIZONTAL LAUNCH VELOCITIES (V_{in}) FOR A PARTICLE HAVING A FIXED W/C_D OF 0.25

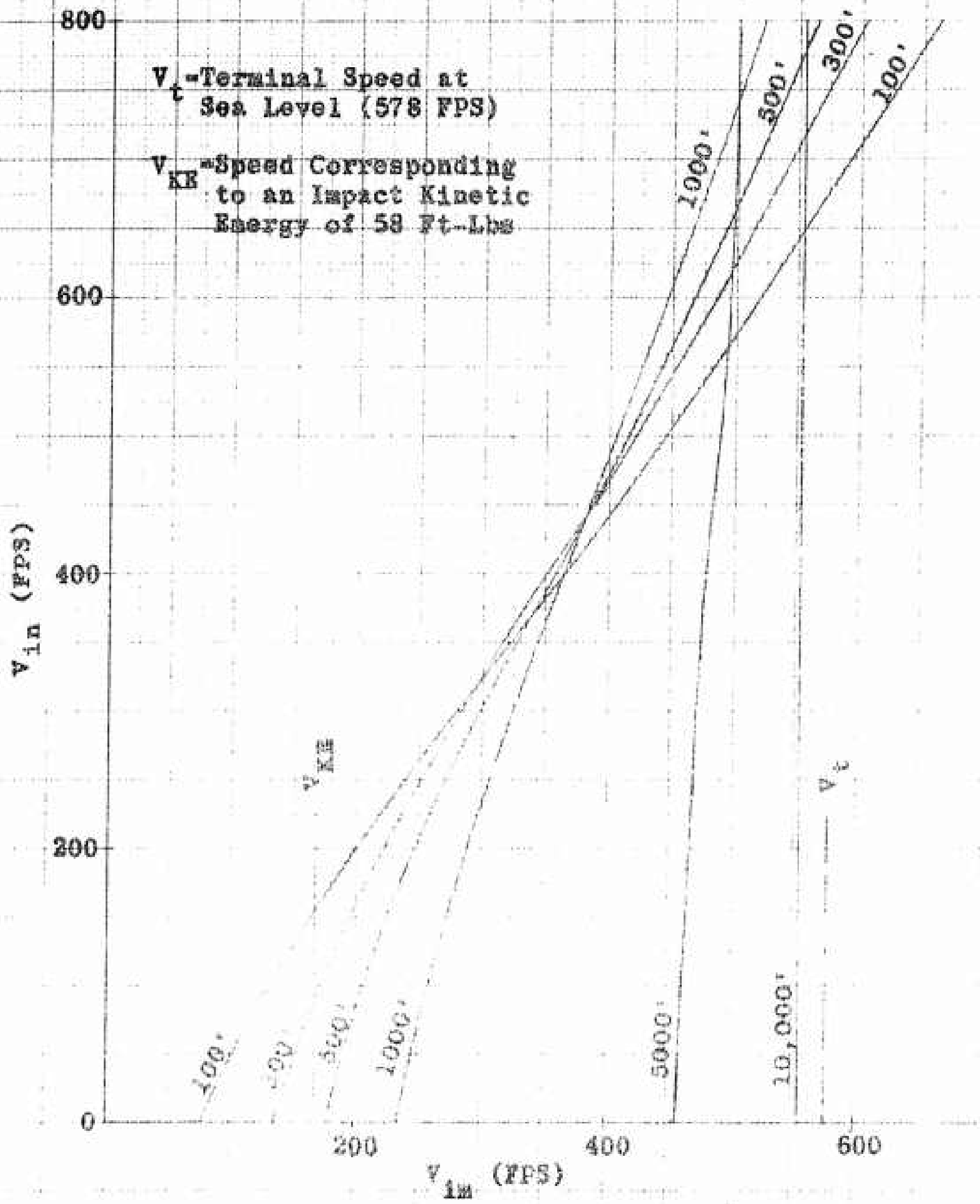

FIG. 67 VELOCITY AT IMPACT (V_{im}) FOR SEVERAL LAUNCH ALTITUDES AND INITIAL HORIZONTAL LAUNCH VELOCITIES (V_{in}) FOR A PARTICLE HAVING A FIXED W/C_D OF 0.50

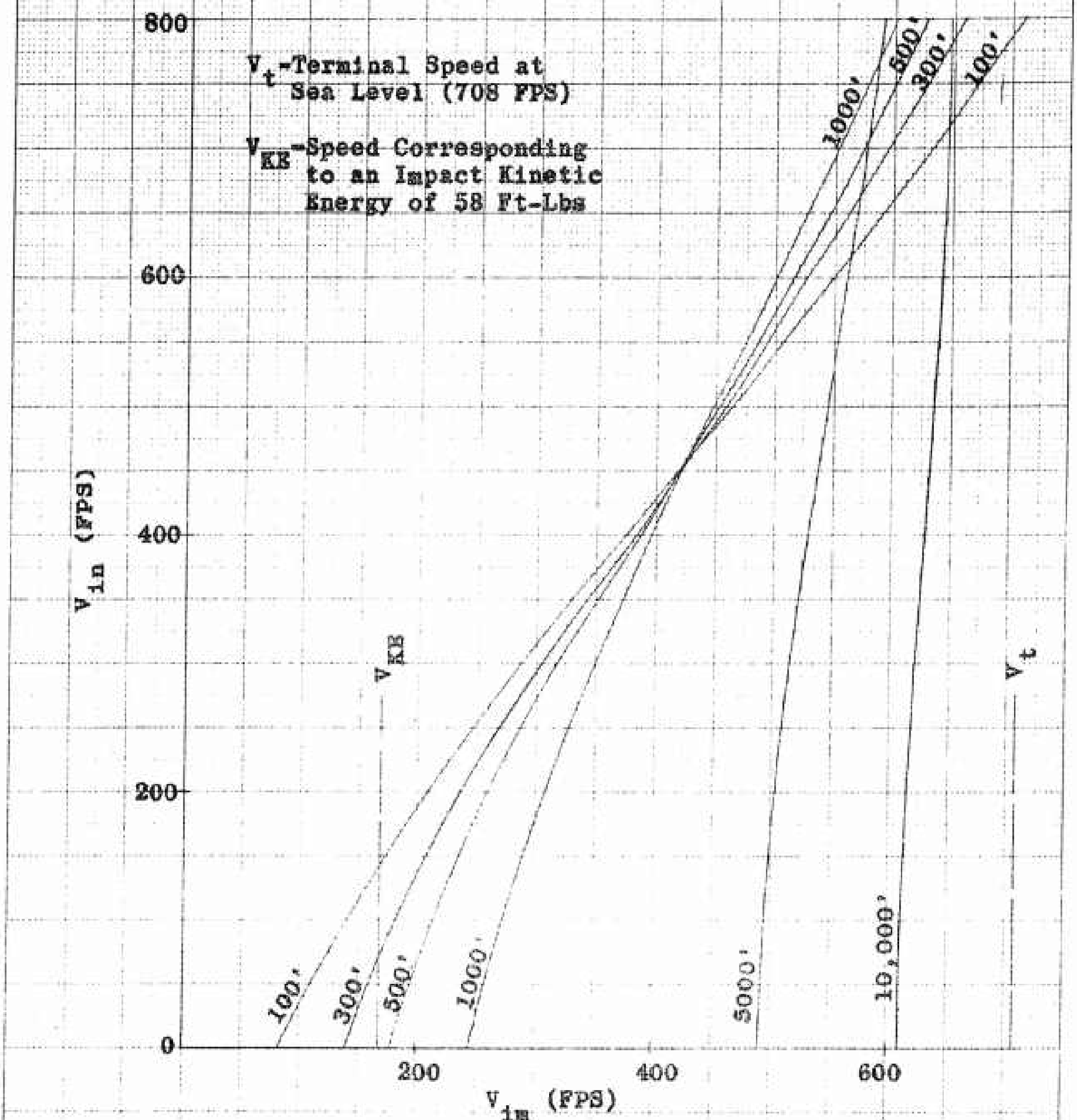

FIG. 68 VELOCITY AT IMPACT (V_{im}) FOR SEVERAL LAUNCH ALTITUDES AND INITIAL HORIZONTAL LAUNCH VELOCITIES (V_{in}) FOR A PARTICLE HAVING A FIXED W/C_D OF 0.75

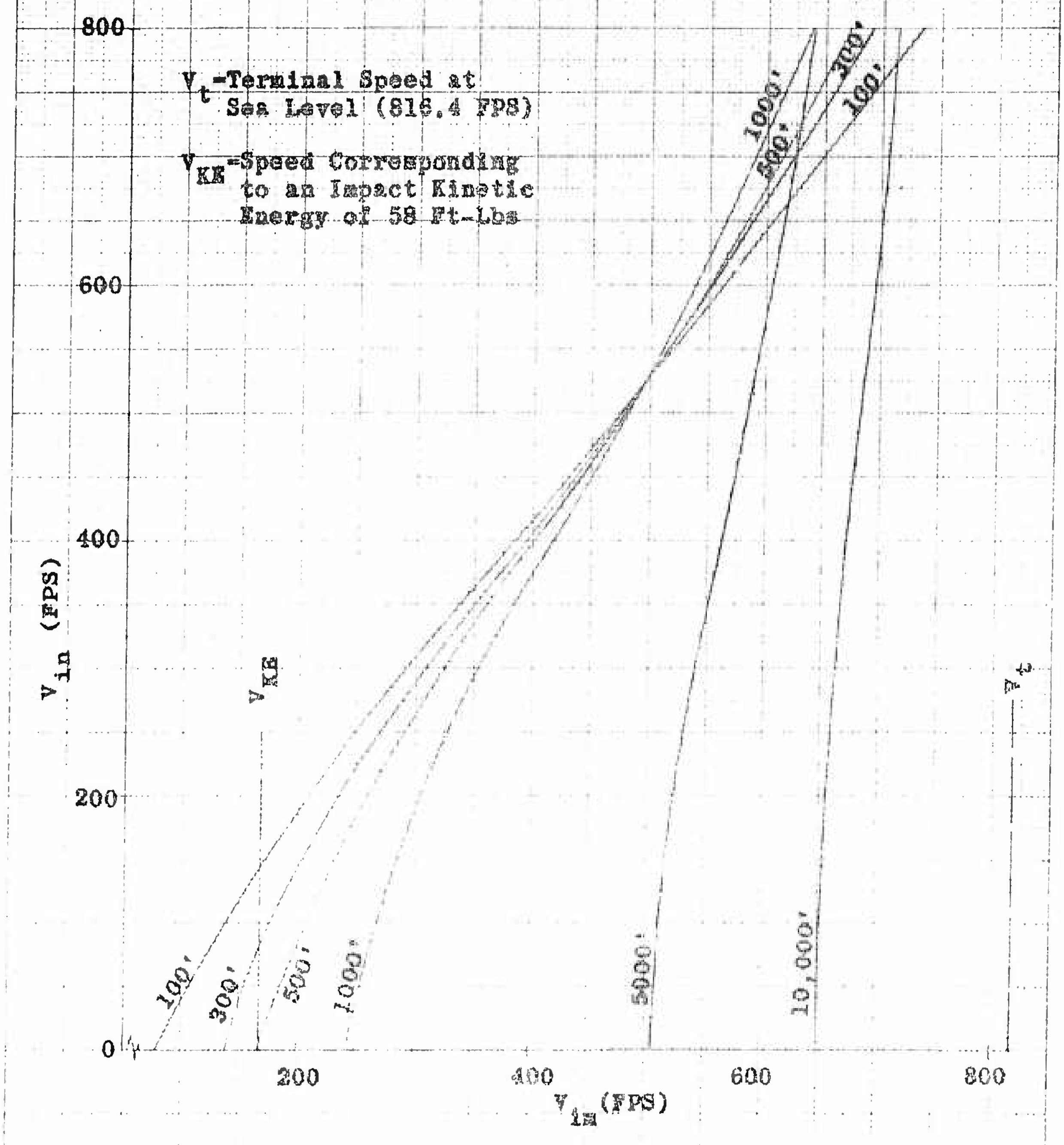

FIG. 69 VELOCITY AT IMPACT (V_{im}) FOR SEVERAL LAUNCH ALTITUDES AND INITIAL HORIZONTAL LAUNCH VELOCITIES (V_{in}) FOR A PARTICLE HAVING A FIXED W/C_D OF 1.00

AERODYNAMICS DEPARTMENT
EXTERNAL DISTRIBUTION LIST (A1)

No. of Copies

Chief, Bureau of Naval Weapons
Department of the Navy
Washington 25, D. C.
Attn: DLI-30
Attn: R-14
Attn: RRRE-4
Attn: RMGA-811
Attn: RMMO-42

Office of Naval Research
Room 2709, T-3
Washington 25, D. C.
Attn: Head, Mechanics Branch
Attn: Head, Fluid Dynamics Branch

Director, David Taylor Model Basin
Aerodynamics Laboratory
Washington 7, D. C.
Attn: Library

Commander, U. S. Naval Ordnance Test Station
China Lake, California
Attn: Technical Library
Attn: Code 406

Director, Naval Research Laboratory
Washington 25, D. C.
Attn: Code 2027

Commanding Officer
Officer of Naval Research
Branch Office
Box 39, Navy 100
Fleet Post Office
New York, New York

NASA
High Speed Flight Station
Box 273
Edwards Air Force Base, California
Attn: W. C. Williams

NASA
Ames Research Center
Moffett Field, California
Attn: Librarian

AERODYNAMICS DEPARTMENT
EXTERNAL DISTRIBUTION LIST (A1)

	No. of Copies
NASA Langley Research Center Langley Field, Virginia Attn: Librarian Attn: C. H. McLellan Attn: Adolf Busemann Attn: Comp. Res. Div. Attn: Theoretical Aerodynamics Division	3
NASA Lewis Research Center 21000 Brookpark Road Cleveland 11, Ohio Attn: Librarian Attn: Chief, Propulsion Aerodynamics Div.	
NASA 600 Independence Avenue, S. W. Washington 25, D. C. Attn: Chief, Division of Research Information Attn: Dr. H. H. Kurzweg, Asst. Director of Research	
Office of the Assistant Secretary of Defense (R&D) Room 3E1065, The Pentagon Washington 25, D. C. Attn: Technical Library	
Research and Development Board Room 3D1041, The Pentagon Washington 25, D. C. Attn: Library	
Defense Documentation Center Cameron Station Alexandria Va 22314	20
Commander, Pacific Missile Range Point Mugu, California Attn: Technical Library	
Commanding General Aberdeen Proving Ground, Maryland Attn: Technical Information Branch Attn: Ballistic Research Laboratory	

AERODYNAMICS DEPARTMENT
EXTERNAL DISTRIBUTION LIST (A1)

	No. of Copies
Commander, Naval Weapons Laboratory Dahlgren, Virginia Attn: Library	
Director, Special Projects Department of the Navy Washington 25, D. C. Attn: SP-2722	
Director of Intelligence Headquarters, USAF Washington 25, D. C. Attn: AFOIN-3B	
Headquarters - Aero. Systems Division Wright-Patterson Air Force Base Dayton, Ohio Attn: WWAD	2
Attn: RRLA-Library	
Commander Air Force Ballistic Systems Division Norton Air Force Base San Bernardino, California Attn: BSRVA	2
Chief, Defense Atomic Support Agency Washington 25, D. C. Attn: Document Library	
Headquarters, Arnold Engineering Development Center Air Research and Development Center Arnold Air Force Station, Tennessee Attn: Technical Library Attn: AEOR Attn: AEOIM	
Commanding Officer, Harry Diamond Laboratories Washington 25, D. C. Attn: Library, Room 211, Bldg. 92	
Commanding General U. S. Army Missile Command Redstone Arsenal Redstone Arsenal, Alabama Attn. Mr. N. Shapiro (AMSMI-RR) Attn. Redstone Scientific Information Center (AMSMI-RB)	

AERODYNAMICS DEPARTMENT
EXTERNAL DISTRIBUTION LIST (A1)

	No. of Copies
NASA George C. Marshall Space Flight Center Huntsville, Alabama Attn: Dr. E. Geissler Attn: Mr. T. Reed Attn: Mr. H. Paul Attn: Mr. W. Dahm Attn: Mr. H. A. Connell Attn: Mr. J. Kingsbury Attn: ORDAB-DA	
APL/JHU (C/NOw 7386) 8621 Georgia Avenue Silver Spring, Maryland Attn: Technical Reports Group	2
Attn: Mr. D. Fox Attn: Dr. F. Hill Via: INSORD	
Air Force Systems Command Scientific & Technical Liaison Office Room 3710, Main Navy Department of the Navy Washington 25, D. C. Attn: Alonzo P. Mercier	
NASA 600 Independence Avenue, S.W. Washington 25, D.C. Attn: I. Shantz P. A. Cerreta	

CATALOGING INFORMATION FOR LIBRARY USE

BIBLIOGRAPHIC INFORMATION

	DESCRIPTORS	CODES		DESCRIPTORS	CODES
SOURCE	NOL technical report	NOLTR	SECURITY CLASSIFICATION AND CODE COUNT	Confidential - 33	CØ33
REPORT NUMBER	63-47	63ØØ47	CIRCULATION LIMITATION		
REPORT DATE	18 May 1964	Ø564	CIRCULATION LIMITATION OR BIBLIOGRAPHIC		
			BIBLIOGRAPHIC (SUPPL., VOL., ETC.)		

SUBJECT ANALYSIS OF REPORT

DESCRIPTORS	CODES	DESCRIPTORS	CODES	DESCRIPTORS	CODES
Lazy Dog	LAZY	0.3	ØX3Ø	50	ØØ5Ø
Static	STAC	1.0	1XØØ	Caliber	CALB
Dynamic	DYNA	1.25	1X25	Bullets	BULT
Stability	STBI	1.5	1X5Ø	High speed	HIGS
Subsonic	SUBS	Free fall	FREF	Aircraft	AIRC
Transonic	TRNS	Missile	MISL	Air launched	AIRR
Speed	VELC	Aerodynamic	AERD	Fin stabilized	FINT
Wind tunnel	WINU	Body	BODY	Low drag	LOWD
Testing	TEST	Ballistic ranges	BALR	Afterbody	AFTE
Configuration	COFI	Test facility	TESF		
Mach number	MACH	Antipersonnel	ANTO		
Range	RANG	Weapons	WEAP		

PRNC-NOL-5070 78 (5-62)

Naval Ordnance Laboratory, White Oak, Md.
(NOL technical report 63-47)
STATIC AND DYNAMIC STABILITY STUDIES ON SEVERAL LAZY DOG CONFIGURATIONS AT SUBSONIC AND TRANSONIC SPEEDS (U), by J. B. Eades, jr. and C. Powers. 18 May 1964. 78p. illus., tables. (Aerodynamics research report 191) BuWeps task RMMO-42-005/212-1/F008-09-01.

CONFIDENTIAL

A summary is presented of the investigations conducted in the Naval Ordnance Laboratory's supersonic tunnel no. 1 on several of the Navy's Lazy Dog weapon configurations. Lazy Dog is a free-fall missile employing a 50 caliber bullet or its core as the basic aerodynamic body.

1. Missile - Aerodynamics
2. Missiles - Lazy Dog
I. Title
II. Eades, James B., jr.
III. Powers, Charlotte W., jt. author
IV. Series
V. Project

Abstract card is unclassified.

Naval Ordnance Laboratory, White Oak, Md.
(NOL technical report 63-47)
STATIC AND DYNAMIC STABILITY STUDIES ON SEVERAL LAZY DOG CONFIGURATIONS AT SUBSONIC AND TRANSONIC SPEEDS (U), by J. B. Eades, jr. and C. Powers. 18 May 1964. 78p. illus., tables. (Aerodynamics research report 191) BuWeps task RMMO-42-005/212-1/F008-09-01.

CONFIDENTIAL

A summary is presented of the investigations conducted in the Naval Ordnance Laboratory's supersonic tunnel no. 1 on several of the Navy's Lazy Dog weapon configurations. Lazy Dog is a free-fall missile employing a 50 caliber bullet or its core as the basic aerodynamic body.

1. Missile - Aerodynamics
2. Missiles - Lazy Dog
I. Title
II. Eades, James B., jr.
III. Powers, Charlotte W., jt. author
IV. Series
V. Project

Abstract card is unclassified.

Naval Ordnance Laboratory, White Oak, Md.
(NOL technical report 63-47)
STATIC AND DYNAMIC STABILITY STUDIES ON SEVERAL LAZY DOG CONFIGURATIONS AT SUBSONIC AND TRANSONIC SPEEDS (U), by J. B. Eades, jr. and C. Powers. 18 May 1964. 78p. illus., tables. (Aerodynamics research report 191) BuWeps task RMMO-42-005/212-1/F008-09-01.

CONFIDENTIAL

A summary is presented of the investigations conducted in the Naval Ordnance Laboratory's supersonic tunnel no. 1 on several of the Navy's Lazy Dog weapon configurations. Lazy Dog is a free-fall missile employing a 50 caliber bullet or its core as the basic aerodynamic body.

1. Missile - Aerodynamics
2. Missiles - Lazy Dog
I. Title
II. Eades, James B., jr.
III. Powers, Charlotte W., jt. author
IV. Series
V. Project

Abstract card is unclassified.

Naval Ordnance Laboratory, White Oak, Md.
(NOL technical report 63-47)
STATIC AND DYNAMIC STABILITY STUDIES ON SEVERAL LAZY DOG CONFIGURATIONS AT SUBSONIC AND TRANSONIC SPEEDS (U), by J. B. Eades, jr. and C. Powers. 18 May 1964. 78p. illus., tables. (Aerodynamics research report 191) BuWeps task RMMO-42-005/212-1/F008-09-01.

CONFIDENTIAL

A summary is presented of the investigations conducted in the Naval Ordnance Laboratory's supersonic tunnel no. 1 on several of the Navy's Lazy Dog weapon configurations. Lazy Dog is a free-fall missile employing a 50 caliber bullet or its core as the basic aerodynamic body.

1. Missile - Aerodynamics
2. Missiles - Lazy Dog
I. Title
II. Eades, James B., jr.
III. Powers, Charlotte W., jt. author
IV. Series
V. Project

Abstract card is unclassified.

Naval Ordnance Laboratory, White Oak, Md.
(NOL technical report 63-47)
STATIC AND DYNAMIC STABILITY STUDIES ON SEVERAL LAZY DOG CONFIGURATIONS AT SUBSONIC AND TRANSONIC SPEEDS (U), by J. B. Eades, jr. and C. Powers. 18 May 1964. 78p. illus., tables. (Aerodynamics research report 191) BuWeps task RMMO-42-005/212-1/F008-09-01.

CONFIDENTIAL

A summary is presented of the investigations conducted in the Naval Ordnance Laboratory's supersonic tunnel no. 1 on several of the Navy's Lazy Dog weapon configurations. Lazy Dog is a free-fall missile employing a 50 caliber bullet or its core as the basic aerodynamic body.

1. Missile - Aerodynamics
2. Missiles - Lazy Dog
I. Title
II. Eades, James B., jr.
III. Powers, Charlotte W., jt. author
IV. Series
V. Project

Abstract card is unclassified.

Naval Ordnance Laboratory, White Oak, Md.
(NOL technical report 63-47)
STATIC AND DYNAMIC STABILITY STUDIES ON SEVERAL LAZY DOG CONFIGURATIONS AT SUBSONIC AND TRANSONIC SPEEDS (U), by J. B. Eades, jr. and C. Powers. 18 May 1964. 78p. illus., tables. (Aerodynamics research report 191) BuWeps task RMMO-42-005/212-1/F008-09-01.

CONFIDENTIAL

A summary is presented of the investigations conducted in the Naval Ordnance Laboratory's supersonic tunnel no. 1 on several of the Navy's Lazy Dog weapon configurations. Lazy Dog is a free-fall missile employing a 50 caliber bullet or its core as the basic aerodynamic body.

1. Missile - Aerodynamics
2. Missiles - Lazy Dog
I. Title
II. Eades, James B., jr.
III. Powers, Charlotte W., jt. author
IV. Series
V. Project

Abstract card is unclassified.

Naval Ordnance Laboratory, White Oak, Md.
(NOL technical report 63-47)
STATIC AND DYNAMIC STABILITY STUDIES ON SEVERAL LAZY DOG CONFIGURATIONS AT SUBSONIC AND TRANSONIC SPEEDS (U), by J. B. Eades, jr. and C. Powers. 18 May 1964. 78p. illus., tables. (Aerodynamics research report 191) BuWeps task RMMO-42-005/212-1/F008-09-01.

CONFIDENTIAL

A summary is presented of the investigations conducted in the Naval Ordnance Laboratory's supersonic tunnel no. 1 on several of the Navy's Lazy Dog weapon configurations. Lazy Dog is a free-fall missile employing a 50 caliber bullet or its core as the basic aerodynamic body.

1. Missile - Aerodynamics
2. Missiles - Lazy Dog
I. Title
II. Eades, James B., jr.
III. Powers, Charlotte W., jt. author
IV. Series
V. Project

Abstract card is unclassified.

Naval Ordnance Laboratory, White Oak, Md.
(NOL technical report 63-47)
STATIC AND DYNAMIC STABILITY STUDIES ON SEVERAL LAZY DOG CONFIGURATIONS AT SUBSONIC AND TRANSONIC SPEEDS (U), by J. B. Eades, jr. and C. Powers. 18 May 1964. 78p. illus., tables. (Aerodynamics research report 191) BuWeps task RMMO-42-005/212-1/F008-09-01.

CONFIDENTIAL

A summary is presented of the investigations conducted in the Naval Ordnance Laboratory's supersonic tunnel no. 1 on several of the Navy's Lazy Dog weapon configurations. Lazy Dog is a free-fall missile employing a 50 caliber bullet or its core as the basic aerodynamic body.

1. Missile - Aerodynamics
2. Missiles - Lazy Dog
I. Title
II. Eades, James B., jr.
III. Powers, Charlotte W., jt. author
IV. Series
V. Project

Abstract card is unclassified.